Acta Morphologica et Anthropologica 31 (3–4)

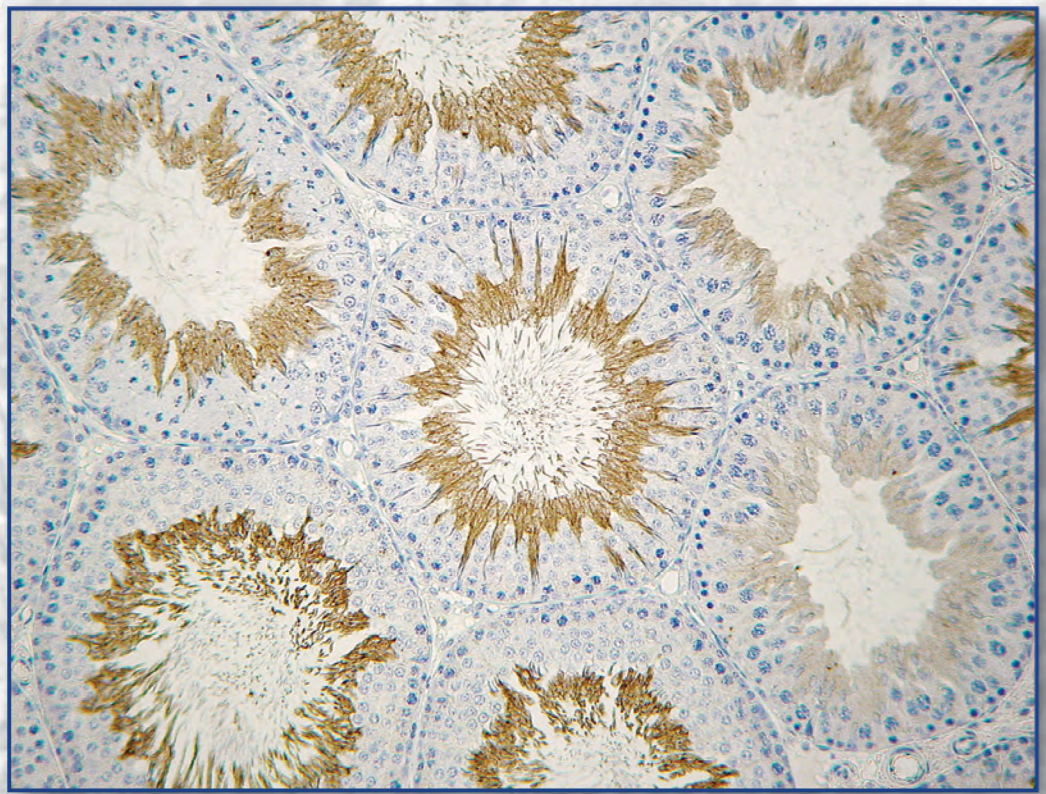

Prof. Marin Drinov Publishing House
of Bulgarian Academy of Sciences

Acta Morphologica et Anthropologica
is the continuation of Acta cytobiologica et morphologica

Indexed in:

BIOSIS databases
Life sciences and biomedical literature on Web of Science

WEB OF SCIENCE

WorldCat®

NCBI NLM Catalog

ISSN INTERNATIONAL STANDARD SERIAL NUMBER INTERNATIONAL CENTRE

ZDB ZEITSCHRIFTEN DATENBANK

Editorial Correspondence
Institute of Experimental Morphology, Pathology and Anthropology with Museum
Bulgarian Academy of Sciences
Acta Morphologica et Anthropologica
Acad. Georgi Bonchev Str., Bl. 25
1113 Sofia, Bulgaria

E-mail: ama.journal@iempam.bas.bg; yordanka.gluhcheva@iempam.bas.bg; ygluhcheva@hotmail.com
Tel.: +359 2 979 2344

Издаването на настоящия том 31, книжки 3 и 4 е осъществено с финансовата подкрепа на Фонд „Научни изследвания“, Договор КП-06-НП5/78 от 08.12.2023 г. Фонд „Научни изследвания“ не носи отговорност за съдържанието на материалите.

Prof. Marin Drinov Publishing House of Bulgarian Academy of Sciences
Bulgaria, 1113 Sofia, Acad. Georgi Bonchev Str., Bl. 6

Graphic designer .Veronika Tomcheva.
Format 70×100/16 Printed sheets 8,00

Printing Office of Prof. Marin Drinov Publishing House of Bulgarian Academy of Sciences
Bulgaria, 1113 Sofia, Acad. Georgi Bonchev Str., Bl. 5

Acta Morphologica et Anthropologica

ISSN 1311-8773 (print)
ISSN 2535-0811 (online)

Acta Morphologica et Anthropologica

31
(3-4)

31 (3-4) ● Sofia ● 2024
Institute of Experimental Morphology, Pathology and Anthropology with Museum
Bulgarian Anatomical Society

Contents

MORPHOLOGY 31 (3)

Original Articles

Review Articles

Original Articles

Review Articles

Institute of Experimental Morphology, Pathology and Anthropology with Museum
Bulgarian Anatomical Society

Acta Morphologica et Anthropologica, 31 (3-4)
Sofia ● 2024

Original Articles

Differentiation of Adult Leydig Cells in Relation to Spermatogenesis in Experimental Conditions of Androgen Deprivation: Scientific Contribution by Prof. Michail Davidoff to Development of Our Knowledge on Adult Leydig Cell Population

Nina Atanassova[1], Yvetta Koeva[2], Mariana Bakalska[1]*

[1] Institute of Experimental Morphology, Pathology and Anthropology with Museum, Bulgarian Academy of Sciences, Sofia, Bulgaria
[2] Department of Anatomy, Histology and Embryology, Faculty of Medicine, Medical University – Plovdiv, Bulgaria

*Corresponding author e-mail: ninaatanassova@yahoo.com

The present paper provides an overview of our long collaborative studies with Prof. Michael Davidoff on the EDS (Ethane Dimethanesulfonate) experimental model for androgen deprivation and to evaluate our contribution for new knowledge about protein expression of cellular markers for differentiation of adult Leydig cells in relation to spermatogenesis. Degenerative and regenerative events in spermatogenesis and time specific changes in androgen receptor expression in Sertoli cells occur in tandem with development of new adult Leydig cell population after EDS indicating close functional relationship between Sertoli cells, Leydig cells and germ cells. By comparison of long term EDS model with short term EDS plus testosterone model we provided new understanding about regulation of androgen receptor by its own ligand testosterone.

Key words: Leydig cells, Sertoli cells, spermatogenesis, androgen receptor, testis

Introduction

Our studies on the development of adult Leydig cell population in relation to spermatogenesis started in the late nineties of the past century under the supervision by Prof. Michail Davidoff. Together with studies on neuroendocrine nature of adult Leydig

cells carried out in the Institute of Experimental Morphology and Anthropology, Prof. Davidoff prompted our studies on consecutive stages of differentiation of adult Leydig cells. He started application of long term experimental model in rat for treatment with ethane dimethanesulfonate (EDS) which is a toxin that selectively and temporally eliminates adult Leydig cells within the first 48 hours [9]. This is followed by severe androgen deficiency due to drop in testosterone levels below 0.1 ng/ml. Thus, the EDS long term model is unique tool to study development of the regenerating adult Leydig cell population that occurred within 7 weeks. The EDS experimental model is a useful tool to investigate androgen dependent events in spermatogenesis, as well. We compare our findings with data generated by a short term EDS experimental model with testosterone administration provided by Prof. Richard Sharpe from the Centre for Reproductive Health, Edinburgh, UK [13].

The aim of the present paper was to provide an overview of our long collaborative studies with Prof. Davidoff on the EDS experimental model and to evaluate our contribution for new knowledge about cellular markers for stages of differentiation of regeneration adult Leydig cell population in relation to spermatogenesis. By comparison of long term EDS model with short term EDS plus testosterone we provided new knowledge about the regulation of androgen receptor (AR) by its own ligand testosterone.

Materials and Methods

Leydig cell ablation followed by testosterone withdrawal in adult rats was induced by single intraperitoneal injection of EDS at a dose of 75 mg/kg body weight dissolved in dimethylsulfoxide and water (1:3, v/v). EDS is not commercially available and was synthesized in our laboratory from ethylene glycol and methane sulfonylchloride as described by Jackson and Jackson [8]. The testes were removed at 7, 14, 21, 35 and 49 days after treatment followed by fixation in Bouin's fluid for 24 hours. Short term EDS treatment with testosterone administration was used to assess the effect of acute testosterone manipulation. Thus, 6 days after EDS-induced testosterone withdrawal a single subcutaneous injection of testosterone ester (25 mg) was applied and testicular samples were taken 4 h later [13]. ABC-HRP immunohistochemistry was performed on 5 μm thick paraffin cross sections for visualization of different testicular cellular markers. For Leydig cells they were 3β-hydroxysteroid dehydrogenase (HSD) [1, 4]; 11β-HSD [10]; Insulin-like 3 peptide (INSL3) and its receptor LGR8 [12], receptors for T3 thyroid hormone (c-erbAα and c-erbAβ [7]). For Sertoli cells – AR [1] and cyclin D2 [13]; for germ cells – testicular angiotensin converting enzyme (tACE) [2]. Apoptotic germ cells were visualized by TUNEL method [5]. Ultrastructural studies were performed by routine TEM [3]. Plasma samples were stored at -20°C until used for hormonal analysis of testosterone and LH by RIA [5]. Statistical analysis was performed by unpaired Student T-test.

Results and Discussion

Our studies started with development of regenerating new Leydig cell population after EDS treatment. Leydig cells were visualised by specific cytoplasm marker 3β-HSD that is a key enzyme in androgen biosynthesis indicative for acquirement of steroidogenic competence of Leydig cells (**Fig. 1A**). Complete loss of Leydig cells

was evident on day 7 after EDS injection (**Fig. 1B**). On the 14th day after EDS, first steroidogenic Leydig cells, that are newly-formed adult Leydig cells, appeared in testicular interstitium between seminiferous tubules. Later, on day 21st and day 35th numerous Leydig cells were seen (**Fig. 1C**) [1].

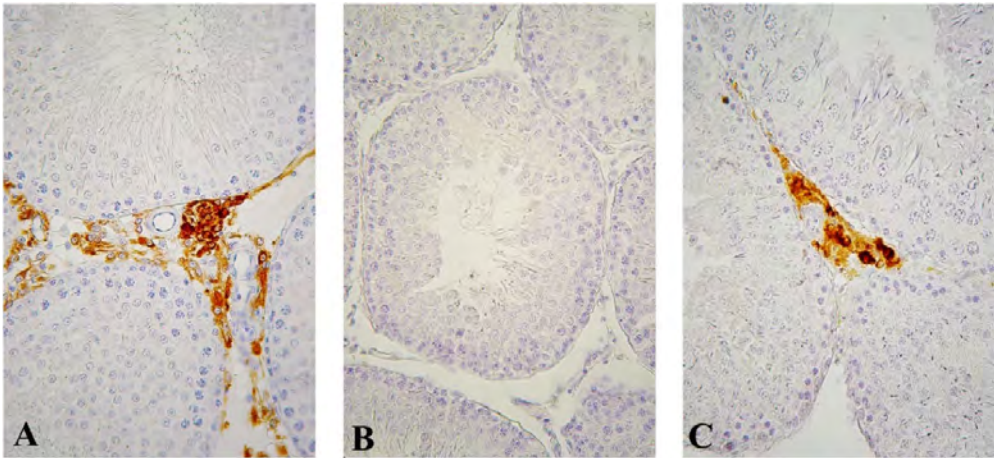

Fig. 1. Immunoexpression of 3β-HSD in control and EDS-treated adult rat testis. **A** – Control; **B** – 7th day after EDS; **C** – 21st day after EDS. ×400

Electron microscopy observation on day 7 after EDS revealed presence of spindle-shaped cells with elongated nucleus and little cytoplasm that were situated in the interstitium. These cells were supposed as presumptive progenitor cells for Leydig cells that were negative for 3β-HSD. Three weeks after EDS treatment the ultrastructure of Leydig cells revealed oval shape with round nucleus and numerous lipid inclusions that were characteristic for the next two steps for Leydig cell differentiation – newly-formed and immature adult Leydig cells. These cells corresponded to 3β-HSD positive cells [4]. Five weeks post EDS mature adult Leydig cells appeared as evident by their morphological characteristics – round nucleus with prominent nucleolus, abundant smooth endoplasmic reticulum and mitochondria with tubular crists [3].

Together with acquirement with steroidogenic competence newly-formed Leydig cells start expression of neuronal markers as glial fibrillary acidic protein (GFAP), tyrosine kinase A, glial cell line–derived neurotrophic factor (GDNF), neuron-specific enolase, neural cell adhesion molecule [7].

In later studies we followed the expression of cell markers specific for differentiating Leydig cells – 11β-HSD [10], Insulin like 3 peptide and its receptor LGR8 [12], T3 thyroid hormone receptors c-erbAα and c-erbAβ [11].

11β-HSD is enzyme that catalyzes the reversible conversion of physiologically active corticosterone to the biologically inert 11β-dehydrocorticosterone and thus protects the Leydig cells against the suppressive effect of glucocorticoids. The developmental pathway of adult Leydig cell population is accompanied with increase in the 11β-HDS activity. Therefore, 11β-HDS can be used as a marker for their functional maturity. First immune-positive for 11β-HSD cells appeared on day 14 after EDS that supposed to be progenitor cells transforming into newly-formed Leydig cells. Progressive increase in the 11β-HSD2 reaction intensity and the number of positive

cells occurred later than day 21st post EDS with maximum on day 35 [10]. Our data suggested that the changes in 11β-HSD2 expression can be used for evaluation of adult Leydig cell differentiation in rat testis.

INSL3 localized predominantly in the gonadal tissues. During fetal life INSL3 is produced by fetal Leydig cell population (different from adult Leydig cells) being critical for testicular descent before birth. In postnatal life regulation of INSL3 gene is independent of that for steroidogenic enzymes. INSL3 is a useful marker of Leydig cell differentiation status. INSL3 is a specific ligand for LGR8 receptor. Pattern of INSL3 and LGR8 receptor protein expression were similar with that of 11β-HSD [12]. It was obvious that INSL3/LGR8 ligand-receptor system, in auto-paracrine fashion, has influence on adult type Leydig cell differentiation.

The pattern of protein expression of T3 thyroid hormone receptors (c-erbAα and c-erbAβ) was similar to that of other Leydig cell differentiation markers mentioned above (11β-HDS, INSL3/LGR8). Data were in support for regulatory role of thyroid hormones in the differentiation of adult Leydig cell population in postnatal life [11].

Together with our studies on the development of regenerating Leydig cell population after EDS treatment, we focused our interest on spermatogenesis in condition of testosterone deprivation, as well. It is well known that germ cell development is strongly dependent on proper androgen levels [14]. Spermatogenesis is a complex process involving many consecutive steps of germ cell differentiation that occurs in stage specific manner called stages of seminiferous epithelium. In rat there are 14 stages that differ by association in germ cell types and subtypes – spermatogonia, spermatocytes and spermatids. Different stages have specific requirement of testosterone and FSH levels. Middle stages (VII–VIII) require maximal testosterone levels and they are considered as androgen-dependent stages.

To identify specific changes in seminiferous epithelium in condition of testosterone insufficiency we applied immunostaining for tACE – specific marker for elongating spermatids. Testicular ACE is expressed in a stage specific manner. The enzyme is localized in the cytoplasm of elongating spermatids from step 8 to step 19 of spermiogenesis. Weak immunoreactivity was seen in elongating spermatids step 9 (stage IX of spermatogenic cycle) followed by progressive increase in elongating

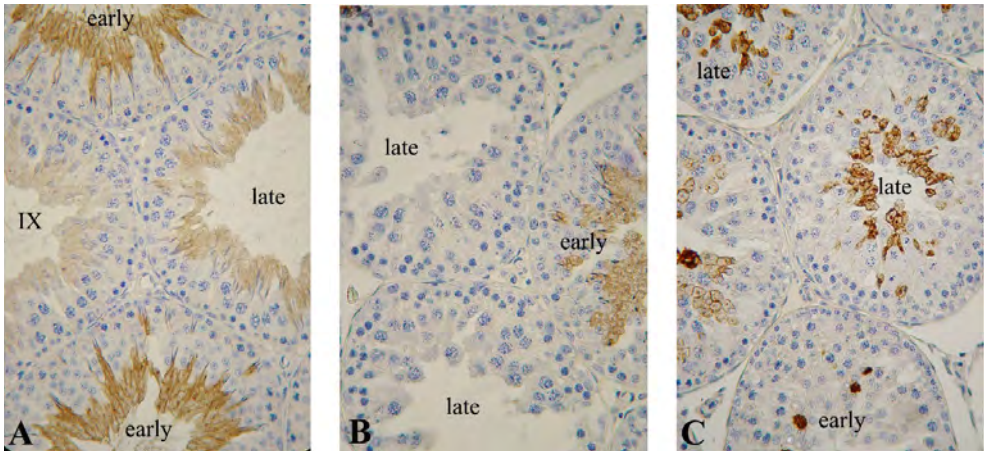

Fig. 2. Immunoexpression of testicular ACE in control and EDS-treated adult rat testis. **A** – Control; **B** – 7th day after EDS; **C** – 21st day after EDS. ×400

spermatids step 12-14 at late stages (XII-XIV) and in elongating spermatids step 15-18 at early stages form the next cycle (I-VI). Maximal intensity was reached in mature spermatozoa step 19 (stage VIII) (**Fig. 2A)**. We found on 7th day after EDS that late stages (IX-XIV) were depleted from elongated spermatids (step 9-14) whereas early stages (I-VI) remained intact (**Fig. 2B**). On day 14th post EDS elongating spermatids were completely lost from the seminiferous tubules. On day 21st, first sign of recovery of spermatogenesis was seen with the appearance of elongated spermatids in late stages (step 9-14), but early stages were still depleted from elongated spermatids (step 15-19) (**Fig. 2C**). On day 35 spermatogenesis is fully recovered [2]. Therefore our data indicated that depletion and recovery of elongating spermatids after EDS treatment occurred in stage-specific pattern. It can be concluded that degenerative and regenerative events in germ cell (spermatid) population occur in tandem with development of new adult Leydig cell population after EDS treatment.

Having in mind that apoptosis is a hormonally-induced process, we enumerated apoptotic cell visualized by TUNNEL method. Data were presented as number of apoptotic cell per tubule; percent of seminiferous tubules containing apoptotic cells and apoptotic index after multiplying of first two parameters. There was a similar trend in the three apoptotic parameters. Maximal germ cell apoptosis was established on day 7 when testosterone levels dropped to lowest value. Apoptotic cells decreased in number in the course of recovery of Leydig cell population as evident by gradual increase in testosterone levels but still under control range (**Table 1**). LH levels were elevated as a result of lack of testosterone feedback control on pituitary gland. Our results indicated that quantitative pattern of germ cell death after testosterone deprivation revealed in advance the kinetic of germ cell depletion and regeneration in a long period after EDS [5].

Table 1. Summary of EDS–induced changes in germ cell apoptosis, testosterone levels and LH plasma levels in adult rats. Data represent mean ± SD (n=4; *** p< 0.001, ** p< 0.01, * p< 0.05, ns – non significant, in comparison with control value)

Day after treatment	Number of apoptotic cells per ST	% of ST with apoptotic cells	Apoptotic Index	Testosterone levels (ng/ml)	LH levels (ng/ml)
Control	1.61 ± 0.18	6.81 ± 2.03	11.00 ± 3.57	2.14 ± 0.39	0.86 ± 0.18
7	3.55 ± 0.07 ***	40.80 ± 8.91 ***	144.14 ± 21.40 ***	< 0.1	3.66 ± 1.76 **
14	1.58 ± 0.14 ns	18.43 ± 1.59 ***	29.27 ± 4.90 ***	0.51 ± 0.25 ***	3.97 ± 1.18 ***
21	1.84 ± 0.15 ns	15.61 ± 6.02 *	29.20 ± 13.32 *	1.27 ± 0.3 **	not measured
35	1.34 ± 0.26 ns	18.22 ± 1.12 ***	24.46 ± 5.88 **	not measured	not measured

ST – seminiferous tubule

Androgen support for spermatogenesis is mediated by AR that is expressed in the nuclei of Leydig cells, peritubular cells and Sertoli cells but not in germ cells indicating that androgen support for developing germ cells is dependent on Sertoli cells. [6] There

is a state-specific pattern of expression of AR within the spermatogenic cycle. Low levels are seen at late stages (IX-XI) followed by increase in early stages (I-VI) and maximal levels are reached at VII-VIII stages (androgen dependent when spermatozoa are released into the tubular lumen) (**Fig. 3A**).

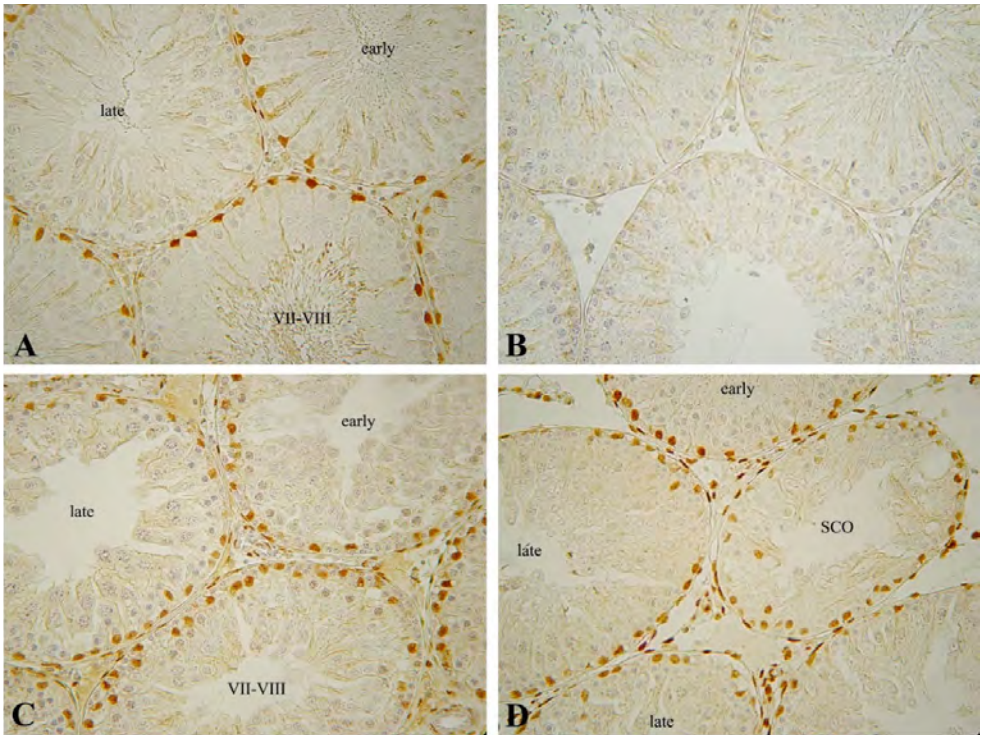

Fig. 3. Immunoexpression of Androgen receptor in control and EDS-treated adult rat testis. **A** – Control; **B** – 7th day after EDS; **C** – 14th day after EDS; **D** – 21st day after EDS. ×400

On day 7 after EDS we found complete loss in AR protein expression in Sertoli cells nuclei (**Fig. 3B**). Two and three weeks after EDS androgen receptor appeared with uniform strong intensity in all stages and stage-specific manner was not seen (**Fig. 3C**). Stage specificity was restored 5 weeks after EDS. Relating these findings to hormonal profile it seems that strong uniform AR expression could be considered as compensatory mechanism of unappropriate testosterone levels. There was no change in AR expression in Leydig cells. The specific changes in AR after EDS including its loss and recovery in Sertoli cells paralleled with degenerative and regenerative events in Leydig and germ cell populations confirming close functional relationship between Sertoli cells, Leydig cells and germ cells [1].

Short term EDS models with testosterone administration provided important data about regulatory mechanism of AR by its own ligand testosterone. Immune-staining for 3β-HSD was used to validate the model and lack of Leydig cells on day 6 after EDS and in testosterone administration conditions, as well (**Fig. 4B, C**).

On day 6 after EDS injection AR protein expression was completely lost in Sertoli cells nuclei (**Fig. 5B**). When testosterone was applied on the day of EDS injection

the spermatogenesis was maintained as well stage specific manner of AR protein expression (**Fig. 5C**). Moreovere, AR expression was restored when testosterone was applied for 4 days after 6 days of EDS condition. Our data suggested that maintenance of stage-specific AR expression in Sertoli cells after EDS requires acute administration of high amount of testosterone but not gradual increase in androgen production during long-term recovery of Leydig cell population after EDS.

A possible candidate involved in the regulation of stage-specific expression of AR was considered Cyclin D2 that play a role different from that in the cell cycle [13]. In control conditions Sertoli cells do not express

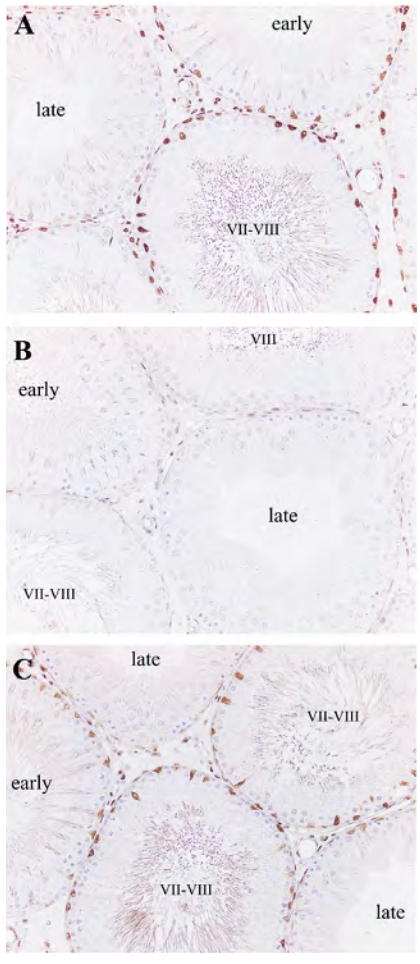

Fig. 4. Immunoexpression of 3β-HSD in adult rat testis: Control (**A**), 6th day after EDS-injection (**B**); 6th day after EDS with testosterone administration (**C**). ×400

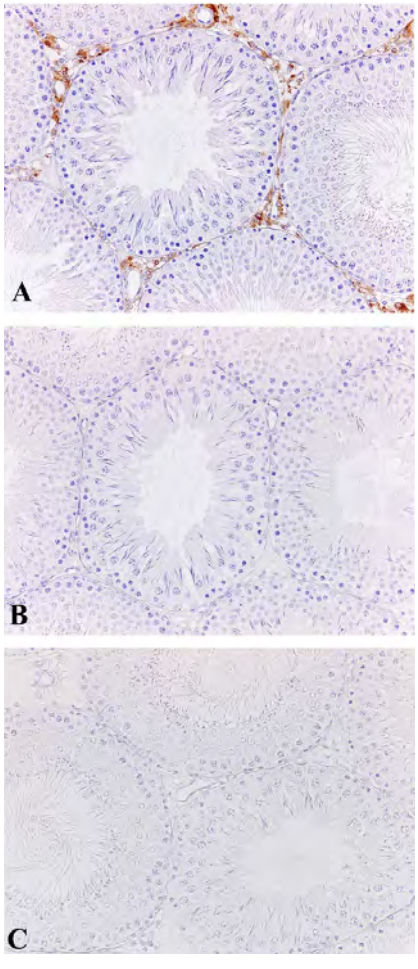

Fig. 5. Immunoexpression of Androgen receptor in adult rat testis: Control (**A**), 6th day after EDS-injection (**B**); 6th day after EDS with testosterone administration (**C**). ×400

Cyclin D2. After 6 days EDS Cyclin D2 protein expression appeared in Sertoli cell nuclei at late stages and testosterone administration recovered control pattern. It seems that Cyclin D2 is a negative regulator of AR expression in Sertoli cells.

Conclusion

The current overview of our data from collaborative studies with Prof. Davidoff on the EDS experimental model for androgen deprivation provided new knowledge about protein expression of cellular markers for differentiation of adult Leydig cells in relation to spermatogenesis. The morphology and protein expression of Leydig cell markers suggested that development of new adult Leydig cell population after EDS repeats the normal dynamics of differentiation of postnatal Leydig cells within a similar time range. Degenerative and regenerative events in spermatogenesis and time specific changes in androgen receptor expression in Sertoli cells occur in tandem with development of new adult Leydig cell population after EDS indicating close functional relationship between Sertoli cells, Leydig cells and germ cells. By comparison of long term EDS with short term EDS plus testosterone model we provided new understanding about regulation of androgen receptor by its own ligand testosterone.

References

1. **Atanassova, N., Y. Koeva, M. Bakalska, E. Pavlova, B. Nikolov, M. Davidoff**. Loss and recovery of androgen receptor protein expression in the adult rat testis following androgen withdrawal by ethane dimethanesulfonate. – *Folia Histochemica et Cytobiologica,* **44** (2), 2006, 81-86.
2. **Atanassova, N., E. Lakova, E. Pavlova, D. Dimova, Y. Koeva.** Expression of testicular Angiotensin Converting Enzyme (tACE) in experimental condition of androgen deficiency in rat. – *Comp. rend. Acad. bulg. Sci.*, **69**(11), 2016, 1437-1442.
3. **Bakalska, M., N. Atanassova, P. Angelova, Y. Koeva, B. Nikolov, M. Davidoff.** Degeneration and restoration of spermatogenesis in relation to the changes in Leydig cell population following ethane dimethanesulfonate (EDS) treatment in adult rats. - *Endocrine Regulations,* **35**, 2001, 211-217.
4. **Bakalska, M., Y. Koeva, N. Atanassova, P. Angelova, , B. Nikolov, M. Davidoff.** Steroidogenic and structural differentiation of new Leydig cell population following exposure of adult rats to Ethane Dimethanesulfonate. – *Folia Biologica (Praha*), **48**, 2002, 205-209.
5. **Bakalska, M., N. Atanassova, Y. Koeva, B. Nikolov, M. Davidoff.** Induction of male germ cell apoptosis by testosterone withdrawal after EDS treatment in adult rats. – *Endocrine Regulations*, **38**, 2004, 103-110.
6. **Bremner, W. J., M. R. Millar, R. M. Sharpe, P. T. K. Saunders.** Immunohistochemical localization of androgen receptor in the rat testis: Evidence for stage-dependent expression and regulation by androgens. - *Endocrinology*, **135**, 1994, 1227-1234.
7. **Davidoff, M. S., R. Middendorff, G. Enikolopov, D. Riethmacher, A. F. Holstein, D. Müller.** Progenitor cells of the testosterone-producing Leydig cells revealed. – *The Journal of Cell Biology*, **167**(5), 2004, 935-944.
8. **Jackson, C. M., H. Jackson.** Comparative protective actions of gonadotrophins and testosterone against the antispermatogenic action of ethane dimethanesulphonate. – *J. Reproduction and Fertility,* **71,** 1984, 393-401.

9. Kerr, J. B., K. Donachie, F. F. G. Rommerts. Selective destruction and regeneration of rat Leydig cells in vivo. A new method for the study of seminiferous tubular-interstitial tissue interaction. – *Cell Tissue Res.,* **242**, 1985, 145-156.

10. Koeva, Y., M. Bakalska, N. Atanassova, K. Georgieva, M. Davidoff. 11β-Hydroxysteroid dehydrogenase type 2 expression in the newly formed Leydig cells after ethane dimethanesulphonate treatment of adult rats. – *Folia Histochemica et Cytobiologica,* **45**(4), 2007, 1-8.

11. Koeva, Y., M. Bakalska, N. Atanassova, M. Davidoff. C-erbAα and c-erbAβ in the Leydig cell repopulation by ethane-1,2 dimethanesulphonate model of mature rats. – *Folia Medica (Plovdiv),* **L(2)**, 2008, 53-57.

12. Koeva, Y., M. Bakalska, N. Atanassova, M. Davidoff. INSLF3-LGR8 ligand-receptor system in testis of mature rats after exposure with ethane dimethanesulphonate (short communication). – *Folia Medica (Plovdiv),* **L(3)**, 2008, 37-42.

13. Tan, K. A. L., K. J. Turner, P. T. K. Saunders, G. Verhoeven, K. De Gendt, N. Atanassova, R. M. Sharpe. Androgen regulation of stage-dependent cyclin D2 expression in Sertoli cells suggests a role in modulating androgen action on spermatogenesis. – *Biology of Reproduction,* **72**, 2005, 1151-1160.

14. Sharpe, R. M. Regulation of spermatogenesis. In: *The Physiology of Reproduction* (Eds. E. Knobil, J. D Neill), 2nd ed., New York, Raven Press, 1994, 1363-1433

Institute of Experimental Morphology, Pathology and Anthropology with Museum
Bulgarian Anatomical Society

Acta Morphologica et Anthropologica, 31 (3-4)
Sofia ● 2024

Exploring the Possibility of a Synergistic Effect of the Extracts from Two Medicinal Plants in a Mouse Model of Ehrlich's Breast Carcinoma

Mashenka Dimitrova[1], Katerina Dimitrova[1], Inna Sulikovska[1], Ludmil Kirazov[1], Ivaylo Ivanov[2]*

[1] *Institute of Experimental Morphology, Pathology and Anthropology with Museum, Bulgarian Academy of Sciences, Sofia, Bulgaria*
[2] *Department of Bioorganic Chemistry and Biochemistry, Medical University, Sofia, Bulgaria*

*Corresponding author e-mail: mashadim@abv.bg

A combination of two extracts: ethyl acetate /water from the leaves of *Cotinus coggygria* Scop. and 80 % aqueous ethanol from the roots of *Geranium sanguineum* L., was tested for a possible synergistic antitumor effect in a mouse model of the solid form of Ehrlich's breast carcinoma. The effects of the combined extracts were compared to those of the chemotherapeutic 5-fluorouracil applied in the same *in vivo* model. Histopathological and blood analyses were performed. The obtained results showed similar activity of the two preparations (combined extracts and 5-fluorouracil). They both provoked apoptosis in tumor masses thus decreasing the degree of tumor aggression. However, they also caused a severe chronic inflammation probably due to the intra-peritoneal way of administration. We concluded that the combined extracts can act as a substitute of the standard chemotherapeutic 5-fluorouracil however, applied in a more suitable way.

Key words: plant extracts, *Cotinus coggygria* Scop., *Geranium sanguineum* L., 5-fluorouracil, Ehrlich's carcinoma

Introduction

With the development of personalized medicine, it becomes increasingly clear that the use of the same drugs in different patients not only might not lead to a cure, but could also cause undesirable side effects in some cases. Therefore, the search for a variety of antitumor drugs is essential to improve the efficiency of treatment. It is well known that plant-based preparations are suitable for use as adjuncts in a number of diseases, including cancer, due to their better biological tolerance, easy digestibility and biodegradability, and above all, because of their lower toxicity compared to synthetic drugs.

Recently, we obtained extracts from a number of medicinal plants endemic to Bulgaria using both mono- and biphasic organic solvent systems. The resulting extracts were tested for antitumor activity on a panel of human tumor cell lines of different origin compared to a non-tumorigenic human cell line [4, 11]. As expected, each of the tested extracts showed a positive selective action in different types of tumor diseases. Some preliminary studies have shown that the antitumor effects of individual preparations are based on different mechanisms such as high antioxidant potential, marked genotoxicity to tumor cells, proapoptotic activity, cell cycle arrest or several of those effects (unpublished results). Thus, the question arises whether a combination of two extracts with different mechanisms of antitumor action could lead to an enhancement of the beneficial effect. On the other hand, it is necessary to establish whether administration other than oral (as with standard chemotherapeutics) would be safe. For the present study, we chose two preparations – ethyl acetate / water (pH 3.0) extract from the leaves of *Cotinus coggygria* Scop. (smoke tree) and 80 % ethanol extract from the roots of *Geranium sanguineum* L. (bloody geranium). Bloody geranium is known as one of the best antioxidants in nature [1, 10] whereas smoke tree has a widely used anti-inflammatory action [8, 9]. Since both inflammation and oxidative stress are prerequisites of cancer, it is motivating to investigate the effect of such combination *in vivo*.

The aim of the present study is to explore the possibility of a synergistic effect of a combination of the above two extracts in a mouse model of Ehrlich's breast carcinoma.

Materials and Methods

Leaves from *C. coggygria* and roots from *G. sanguineum* in the form of dried crashed materials were purchased from Dikrasin Ltd (Bulgaria) which is specialized in cultivation and distribution of medicinal plants in accordance with international legislation and the Law on the Protection of Biological Diversity in Bulgaria.

Extracts. The two extracts were obtained exactly as described before [2, 5].

G. sanguineum extract (GSE). In brief, dried and crushed roots of *G. sanguineum* were subjected to solid-liquid extraction in 80 % aqueous ethanol at a ratio of 1g : 10 mL initially for 3 hours, after which the solid residue was re-extracted for 3 hours and finally, overnight. The combined filtrates were concentrated *in vacuo*, acetonitrile was added and then evaporated. Then, the residue was treated with diisopropyl ether, filtered and dried *in vacuo* [2].

C. coggygria extract (CCA). Briefly, dried and powdered leaves of *C. coggygria* were extracted with the biphasic system ethyl acetate / water, acidified to pH 3.0 using hydrochloric acid, (at a ratio 1g herb : 8 mL solvent system) with stirring for 2 hours at room temperature. After that, the solid residue was re-extracted with the same biphasic system. The collected filtrates were concentrated on a vacuum evaporator, filtered, the precipitates were washed with diisopropyl ether and dried under vacuum [5].

In vivo experiment. Sixteen mature albino mice (20g b.w.) of the ICR breed were used in the experiment. The animals were kept in plastic cages (each group in a single cage) in the licensed vivarium of the Institute of Experimental Morphology, Pathology and Anthropology with Museum - Bulgarian Academy of Sciences (Permition Nr 11 30

127) in accordance with the national regulation Nr 20/01.11.2012 regarding laboratory animals and animal welfare and European directive 2010/63/EU of the European Parliament. Before the experiment they were fed and watered *ad libitum*. The animals were inoculated with Ehrlich's ascites carcinoma cells (EAC cell line) by a single subcutaneous (*s.c.*) injection of 0.2 mL suspension of 1.10^6 cells/mL into the hind leg to develop a solid form of Ehrlich's mammary gland carcinoma. The test started after a palpation of a tumour masses. Then, the animals were randomly divided into three groups, as follows:

Group 1: 4 animals bearing solid form of Ehrlich's mammary gland carcinoma (positive controls).

Group 2: 8 mice, treated daily for six days by *i.p.* injections with a combination of GSE and CCA. The single dose was composed of 15 mg/kg b.w. from each extract, dissolved together in 0.2 mL PBS (the CCA was pre-dissolved in a minimal amount of DMSO).

Group 3: 4 animals, treated daily for six days with 0.2 ml solution of 15 mg/kg b.w. 5-fluorouracil (5FU – a standard therapeutic) in PBS.

Two days after the end of experiment, the animals were euthanized by decapitation under sedation with 2% xylazine. Blood for testing was collected from the neck. During the autopsy, tissue samples of the tumour mass, liver, kidney and other organs were collected. The tissue pieces were fixed in 10% neutral buffered formalin (Diapath, Italy) and processed according to the standard procedure. The sections were stained with H&E (haematoxylin-eosin). Histopathological observations were made under a microscope Leica DM 5000B (Germany). Blood counts were performed on a Mindray BC 2800 Vet analyzer (Mindray, China) and included the following hematological parameters: leukocytes (WBC), erythrocytes (RBC), hemoglobin (HGB), platelets (PLT) and leucocyte cell counts.

Statistical analyses. The results of the blood tests were expressed as mean values ± SD of the experiments from the four animals. Statistical analyses were performed by the one-way analysis of variance (ANOVA) test using GraphPad Prism 8.0 software; results were denoted as $*p<0.05$, $**p<0.01$ and $***p<0.001$ depending on the statistical significance.

Results and Discussion

Chemical compositions of the two extracts used in the present study were preliminary analyzed by LC-HRMS (Liquid Chromatography – High Resolution Mass Spectrometry) in negative ion mode. Compounds were identified by MS and MS/MS data analysis and in comparison to data from previous studies. It was shown that the ethyl acetate / water extract from the leaves of *C. coggygria* (CCA) contains mainly hydrolysable gallotannins in the form of oligo-O-galloylglucoses with a number of galloyl residues from 5 to 9. Additionally, small amounts of glycosylated flavonols such as quercetin-O-glucoside and myricetin-O-rhamnoside were also found [5]. Those substances all contain a large number of hydroxyl groups, which makes the extract a good antioxidant. On the other hand, the anti-inflammatory properties of aqueous solutions

and different extracts of this herb were well known and widely used in both traditional and modern medicine [8, 9]. The 80 % ethanol extract from the roots of *G. sanguineum* was analyzed similarly to show that the main components are flavan-3-ols (catechin, epicatechin, ellagocatechin and epiellagocatechin), as well as condensed tannins based on them – proanthocyanidins (unpublished results). These compounds also possess a large quantity of hydroxyl groups, which explains the powerful antioxidant activity of the herb reported previously by other authors [1. 10].

Furthermore, the two extracts were tested separately by us in the same *in vivo* model of Ehrlich's breast carcinoma in mice for their antitumor activity [2, 12]. However, in the previous study [12], CCA was administered *per os*. Obviously, the oral application does not preserve the main compounds of the extracts and the noticed mild antitumor and pronounced organ-protective activities may not be due to the extracts' compounds but to their metabolites. In confirmation of this assumption, a previous study [6] showed a high diversity of hydrolytic processes taking place in gut both by the enzymes of intestinal enterocyte and the microbiota, which brake down gallotanins and other plants' secondary metabolites. On the other hand, the *in vitro* experiments on tumor cell lines, which usually precede the *in vivo* tests, involve the herbs' compounds as preserved molecules. That is why we decided to administer the extracts *i.p.* and test the effect of the whole conserved active compounds. The *i.p.* application of GSE [2] did not show any changes in mice behavior, appetite, water consumption, etc. and so, it was considered to be harmless. Also, we performed a pilot study to test the *i.p.* administration of CCA extract in a couple of healthy mice for possible adverse effects. Unfortunately, this led to a mild dysfunction of the hind legs and we decided to lower the dose. In the present study, no visible harmful effects of the combined preparation were noticed during the six days application.

In this study, we used two types of controls – a positive control of mice bearing solid carcinomas, not-treated with any preparation and negative controls of mice with solid tumor, treated with the standard therapeutic 5-fluorouracil (5FU), which can be used in breast carcinoma including in mouse models [3].

The histopathological results from the present experiment are given in **Fig. 1.**

It should be noted that we took pieces of other organs as well (spleen, pancreas, lung and small intestine), but no differences between the groups were noticed. So, we show here only the livers, kidneys and tumor masses.

In the solid tumor mass of non-treated (positive) controls (**Fig. 1A**), liquefactive necrotic masses with cellular debris were observed, as well as a small number of apoptotic cells, surrounded by cellular debris. Additionally, neoplastic multinucleation of many giant tumor cells, mitotic figures and cells with prominent nucleoli could also be seen. All of these findings are in agreement with the usual progression of solid tumors in the Ehrlich's model of breast carcinoma observed by us and in previous experiments. Solid tumors of mice, treated with the extracts preparation (**Fig. 1B**) also showed necrotic masses and cellular debris. In addition, a number of neutrophil granulocytes were seen, as well as abundance of tumor cells with pyknotic nuclei, pointing out to a development of apoptotic processes. Similar results were observed in mice, treated with 5FU (negative controls), in which the number of apoptotic cells was even larger (**Fig. 1C**). It should be pointed out that the solid tumors of several animals infiltrated the nearby subcutaneous adipose tissue and focal islets of adipocytes in the tumor periphery were seen. Such contact between breast cancer cells and fatty tissue is

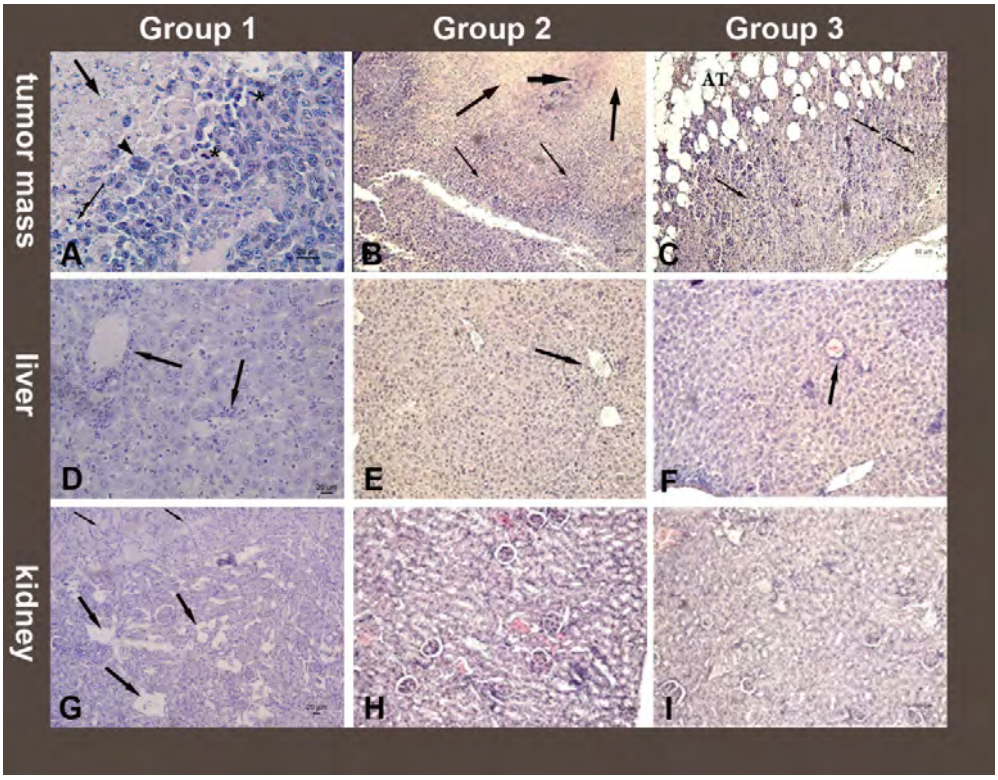

Fig. 1. Histopathological findings (H&E). Left column: Group 1 (positive control, non-treated); middle column: Group 2 (treated with CCA and GSE); right column: Group 3 (treated with 5FU). Upper row: *tumor tissues*: liquifactive necrotic masses (thick arrows), neoplastic multinucliation (arrowhead), apoptotic cells and cell debris (thin arrows), mitotic figures (asterisk), neutrophil granulocytes (short arrow), AT – adipose tissue. Middle row: *liver*: active immune cells (thick arrows). Bottom row: *kidney*: hyaline casts in tubules (thin arrows), dilatation and wall rupture of renal tubules (thick arrows). 200×, Bar = 20 μm.

of a great risk of prompting the tumor growth, due to the stimulation of the proliferation and invasion by secreted proteases, pro-inflammatory cytokines and by modulating cancer cell metabolism [7]. It can be concluded that both 5FU and combined extracts intensify visually the apoptosis of tumor cells.

The liver tissues of all the groups of animals did not show substantial pathological changes except for the elevated number of activated immune cells (mainly leukocytes – some granulocytes and macrophages) observed around the central vein and also, within the blood vessels (**Fig. 1D, E, F**). This effect was more pronounced in non-treated controls (**Fig. 1D**). The kidneys of the positive (non-treated) controls however, showed hyaline casts in tubules and the walls of some renal tubules were ruptured (**Fig. 1G**). The kidney morphology of all the treated animals from groups 2 and 3 was normal (**Fig. 1H, I**). Thus, a mild protective effect of the two types of drugs was assumed.

Results from the blood analyses are given in **Table 1**.

Table 1. Results from the blood analysis. Results are given as mean ± SD from 4 independent counts of four animals. Statistical significance was: *p<0.05, **p<0.01 and ***p<0.001 in comparison to the referent values.

Treatment	Parameters						
	WBC (10^9/L)	RBC (10^{12}/L)	HGB (g/L)	PLT (10^9/L)	Leucocyte cell count (%)		
					Lym.	Mon.	Gran.
Referent values	0.8 - 6.8	6.36 – 9.42	110 – 143	450 – 1590	55.8 – 90.6	1.8 – 6.0	8.6 – 38.9
Tumor control (Group 1)	19.4 ± 0.14***	8.64 ± 0.7	117 ± 1.03	1060 ± 6.7	50.1 ± 0.7	5.8 ± 0.7	44.1 ± 0.2**
CCA+GSA (Group 2)	41.5 ± 0.9***	8.9 ± 0.3	108 ± 1.4*	1317 ± 1.8	12.6 ± 0.2***	3.7 ± 0.3	83.7 ± 0.5***
5FU (Group 3)	27.8 ± 2.29***	7.97 ± 1.63	110 ± 9	1548±28.7	18.9 ± 6.2***	3.0 ± 1.5	78.1 ± 7.5***

From the table, a pronounced leukocytosis is seen in all the experimental animals, which is high in 5FU-treated animals, but especially prominent in the mice treated with the combined extracts. From leukocyte cell count it becomes clear that the leukocytosis is due to the very big number of granulocytes, again especially high in the extracts-treated animals. This result coincides with the morphological findings of a substantial number of neutrophils in the tumor tissue (Fig.1B). On the other hand, the number of lymphocytes in the two treated groups is lower than the one in tumor controls and the referent values. Both results of high granulocytes and low lymphocytes can be a sign of a chronic inflammation. Obviously, both 5FU and plant extracts increase the inflammation to a higher extent than the tumor itself. This result most probably is due to the *i.p.* application of those substances. Of course, this is not the common way to apply a chemotherapeutic of any kind. However, in a mouse model it would be very difficult to perform an intravenous application. On the other hand, RBC remains within the reference ranges. The HGB of extract treated animals is slightly lower than the reference and tumor values but not enough to consider anemia. Thus, the results from the blood analysis can be considered as ambiguous.

Conclusions

From the above studies it becomes obvious that *i.p.* application is not proper neither for combined extracts nor for the standard chemotherapeutic 5FU. Since from our previous studies such application mode proved to be safe for GSE, we rationalized

that the hydrolysable gallotannins in CCA may cause a local irritation, and the dose of 5FU most probably is higher than the safety one. We can also conclude that CCA and GSE have not a detectable synergistic effect. On the other hand, the combined preparation has the same effect in the solid Ehrlich's breast carcinoma as 5FU which is proved from both the blood and morphological analyses. Thus, it would be reasonable to assume that the extracts can be usable instead of 5FU however, by a more suitable way of application.

Acknowledgement. This work is financially supported by the National Science Fund of the Bulgarian Ministry of Education and Science, Grant Nr KP-06-N31/1.

References

1. Ávila, M. B., J. A. Gayosso de Lúcio, N. V. Mendoza, C. V. González, M. De la O Arciniega, G. A. V. *Geranium species* as antioxidants. In: *Oxidative stress and chronic degenerative diseases – a role for antioxidants* (Ed. J. A. Morales-González), 2013, IntechOpen, Rijeka, Available at https://doi.org/10.5772/45722.

2. Dimitrova, M., K. Todorova, I. Iliev, I. Sulikovska, L. Kirazov, I. Ivanov. Effects of *Geranium sanguineum* ethanol extract after *i.p.* application in a mouse model of Ehrlich's breast cancer. – *Acta Morphol. Anthropol.*, **29**(3-4), 2022, 29-32.

3. Hashemi-Moghaddam, H., S. Kazemi-Bagsangani, M. Jamili, S. Zavareh. Evaluation of magnetic nanoparticles coated by 5-fluorouracil imprinted polymer for controlled drug delivery in mouse breast cancer model. – *Int. Journal. Pharm.*, **497**, 2016, 228-238.

4. Iliev, I., I. Ivanov, K. Todorova, D. Tasheva, M. Dimitrova. Cotinus coggygria non-volatile fraction affects the survival of human cultured cells. – *Acta Morphol. Anthropol.,* **28**(1-2), 2021, 19-27.

5. Ivanov, I., A. Vasileva, D. M. Tasheva, Dimitrova. Isolation and characterization of natural inhibitors of post-proline specific peptidases from the leaves of *Cotinus coggygria* Scop. – *J. Ethnopharmacology,* **314**, 2023, 116508.

6. Kiss, A. K., J. P. Piwowarski. Ellagitannins, gallotannins and their metabolites – the contribution to the anti-inflammatory effect of food products and medicinal plants. – *Curr. Med. Chem.,* 25, 2018, 4946 – 4967.

7. Kothari, C., C. Diorio, F. Durocher. The importance of breast adipose tissue in breast cancer. – *Int. J. Mol. Sci.,* **21**, 2020, 5760.

8. Lu, K., C.-Y. Yang, Z.-H. Yan. Analgesic and anti-inflammatory activity of *Cotinus coggygria* Scop. extracts in vivo. – *Asian Pacific Journal of Tropical Biomedicine*, **14**, 2024, 225-235.

9. Marčetić, M., D. Božić, M. Milenković, N. Malešević, S. Radulović, N. Kovačević. Antimicrobial, antioxidant and anti-inflammatory activity of young shoots of the smoke tree, *Cotinus coggygria* Scop. – *Phytother. Res*., **27**, 2013, 1658-1663.

10. Pavlova, E., L. Simeonova, J. Serkedjieva. Antioxidant activities of *Geranium sanguineum* L. polyphenolic extract in chemiluminescent model systems. – *Inorg. Chem. Commun.*, **108**, 2019, 107518.

11. Sulikovska, I., E. Ivanova, I. Ivanov, D. Tasheva, M. Dimitrova, B. Nikolova, I. Iliev. Study on the phototoxicity and antitumor activity of plant extracts from *Tanacetum vulgare* L., *Epilobium parviflorum* and *Geranium sanguineum* L. – *Int. J. BIOautomation*, **27**(1), 2023, 39-50.

12. Todorova, K., I. Ivanov, I. Iliev, L. Kirazov, M. Dimitrova. Biological activity of orally given ethyl acetate extract from *Cotinus coggygria* in albino mice with solid and ascites forms of Ehrlich's tumor. – *Acta Morphol. Anthropol.,* **28**(3-4), 2021, 3-9.

Institute of Experimental Morphology, Pathology and Anthropology with Museum
Bulgarian Anatomical Society

Acta Morphologica et Anthropologica, 31 (3-4)
Sofia ● 2024

Morphometric Analysis of the Rat Spinal Trigeminal Nucleus

Andrey Ivanov[1,2] , Dimitrinka Atanasova[1,3], Nikolai Lazarov[1,2]*

[1] *Institute of Neurobiology, Bulgarian Academy of Sciences, Sofia, Bulgaria*
[2] *Department of Anatomy, Histology and Embryology, Medical University of Sofia, Sofia, Bulgaria*
[3] *Department of Anatomy, Faculty of Medicine, Trakia University, Stara Zagora, Bulgaria*

* Corresponding author e-mail: aivanov@medfac.mu-sofia.bg

This study presents a morphometric analysis of neuronal size within the oral (SpVo), interpolar (SpVi), and caudal (SpVc) subnuclei of the spinal trigeminal nucleus (SpV) in rats. Using classical staining and morphometric techniques, we found distinct distributions of small-, medium-, and large-sized neuronal cell bodies across the subnuclei. In general, the SpV consists of over 80% of neurons within the 5–15 micrometer range of their perikarya, with 15% classified as medium-sized (15-20 micrometer range), and 5% as large (above 25 micrometers in diameter). Moreover, the three subnuclei exhibited differing proportions of neuronal soma sizes, suggesting functional specialization within the SpV. This morphometric analysis underscores the heterogeneity of neuronal populations within the spinal trigeminal nucleus and provides insights into its role in somatosensory processing. Understanding neuronal soma size distributions in the SpV enhances our knowledge of its functional organization and may inform future studies investigating sensory integration and pain modulation within the trigeminal sensory system.

Key words: spinal trigeminal nucleus, neuronal size, morphometric analysis, rat

Introduction

A crucial node in the somatosensory pathway, the spinal trigeminal nucleus (SpV) is involved in the transmission and processing of sensory data from the face and mouth cavity [14]. The nucleus is positioned to process thermal and nociceptive impulses within the medulla oblongata. The SpV is separated anatomically into three distinct subnuclei: subnucleus caudalis (SpVc), subnucleus interpolaris (SpVi), and subnucleus oralis (SpVo) [10]. These subnuclei have different cytoarchitectural characteristics

with some of the features being neuronal size, shape, and distribution pattern [14]. The neurons' size, shape, and complexity vary widely based on the underlying function. Hence, the objective of this work is to clarify the neuronal size properties of the SpV subnuclei, offering important insights into their contributions to somatosensory perception.

Materials and Methods

The study was conducted on mature Wistar rats, using a total of 12 male rats with body weights ranging from 180 to 300 g. Adherence to ethical guidelines for experimental animal research in Bulgaria was ensured, following protocols approved by the Ethics Committee of the Institute of Neurobiology, Bulgarian Academy of Sciences (registration FWA 00003059 with the US Department of Health and Human Services), and the Research Ethics Committee at the Medical University of Sofia, as per Directive 2010/63/EU on the protection of animals used for scientific purposes. Initially, the experimental animals were briefly anesthetized with ether, followed by intraperitoneal administration of thiopental (Sigma-Aldrich) at a dose of 40 mg/kg to maintain anesthesia. Cannulation of the ascending aorta via the left ventricle was conducted for perfusion. The circulatory system was washed with 0.05 M phosphate-buffered saline (PBS), pH 7.36, and fixed using 4% paraformaldehyde (Merck) in 0.1 M phosphate buffer for approximately 20 minutes. Following brain removal, the region of interest spanning from the midbrain to the upper spinal cord was dissected. Tissue blocks were postfixed overnight at 4°C in the same fixative, washed thoroughly with tap water, and subsequently processed for embedding in paraffin. Conventionally, 7 μm thick tissue sections were cut and mounted on chrome-gelatinized slides, stained with toluidine blue (500 mg of dye to 100 ml of distilled water) for 5-10 min. Following dehydration, sections were embedded in Entellan (Merck). Observations and photography of the specimens were conducted using an Olympus VS120-L100 Virtual Slide System light microscope. The scanned images were saved in TIF format, and subsequent morphometric analysis of the digital images was undertaken. Over one hundred and seventy images were taken from all three parts of the SpV and we measured the size of over 1000 neurons with the Fiji image processing package [12].

Results

Our morphometric analysis using the Fiji program identified three distinct subgroups of neurons within the SpV based on the sizes of their cell bodies, as shown in **Figure 1.** Neurons classified as small had somatic diameters ranging from 5 to 15 μm, with a mean diameter of 9.89 μm ± 2.16 (n = 798). These neurons represent approximately 79.7% of the total population of neurons within the SpV (Fig. 1). On average, medium-sized neurons possess perikarya with a mean diameter of 16.66 μm ± 1.51 (n = 151), falling within the range of 15 to 20 μm. These neurons make up approximately 15% of the total population of neurons in the nucleus. Neurons categorized as large had a somatic diameter of greater than 25 μm, with a mean diameter of 26.68 μm ± 4.58 (n = 50). In

addition, one very large (giant) neuron was observed with dimensions exceeding 40 μm in somatic diameter (n = 1). Large-sized neurons collectively represent approximately 5% of the total population of neurons within the rat SpV.

Further analysis revealed different distributions of neuronal soma sizes within individual SpV subnuclei (**Figs. 2, 3, and 4**). Specifically, in the SpVc, small cells constituted the majority of neurons (almost 85%), medium-sized neurons represented 14.93%, followed by large-sized neurons, which accounted for less than 1% of all neurons in the nucleus (**Fig. 2**). The SpVi was dominated by small neurons (86%), followed by medium-sized neurons (7.46%), large neurons (6.47%), and sporadic giant neurons (less than one percent) (**Fig. 3**). Specifically, the largest cell body diameter per neuron was measured in the SpVi at 43.93 μm. It is in this subnucleus that the large in size neurons scattered among smaller ones make an impression. In the SpVo, small neurons are almost three times more numerous than medium-sized cells, making up 70% and about 23%, respectively, while large neurons account for almost 7% of all cells in it (**Fig. 4**).

The average diameter of small neurons in the rat SpV ranged from 8.84 to 10.52 μm, that of medium neurons was 16.39 to 16.80 μm, and that of large neurons ranged from 25.45 to 27.82 μm in all subnuclei.

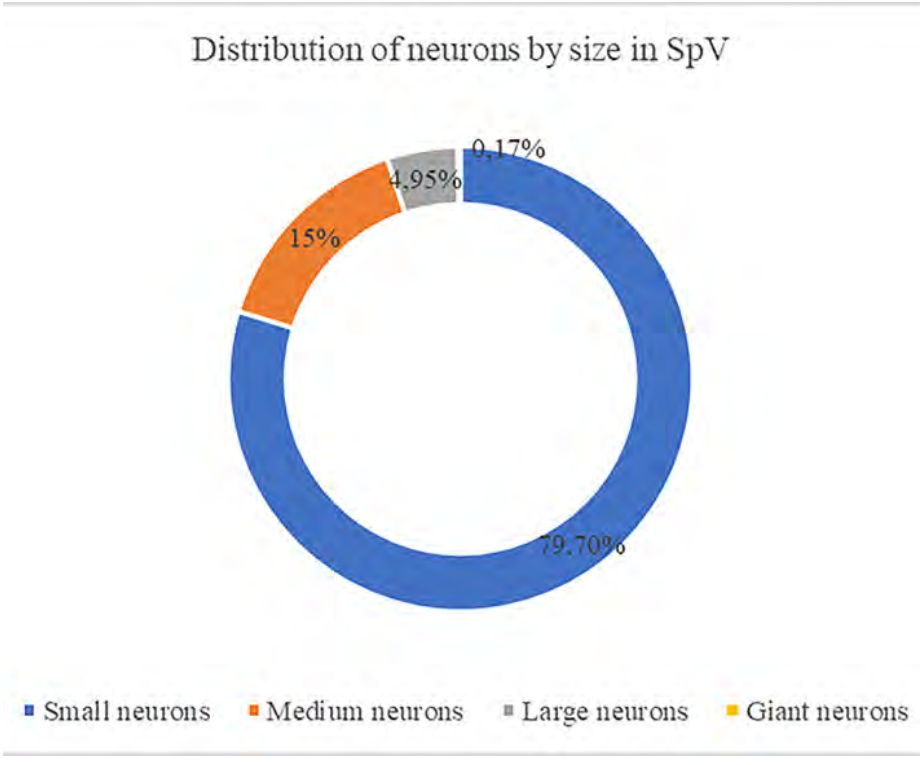

Fig. 1. Percentage distribution of different-sized neurons in the spinal trigeminal nucleus (SpV). Small-sized neurons make up almost 80% of the total neuronal population in the SpV, followed by medium-sized with 15%, and neurons large in size that constitute up 5% of the population. Giant neurons are less than 1%.

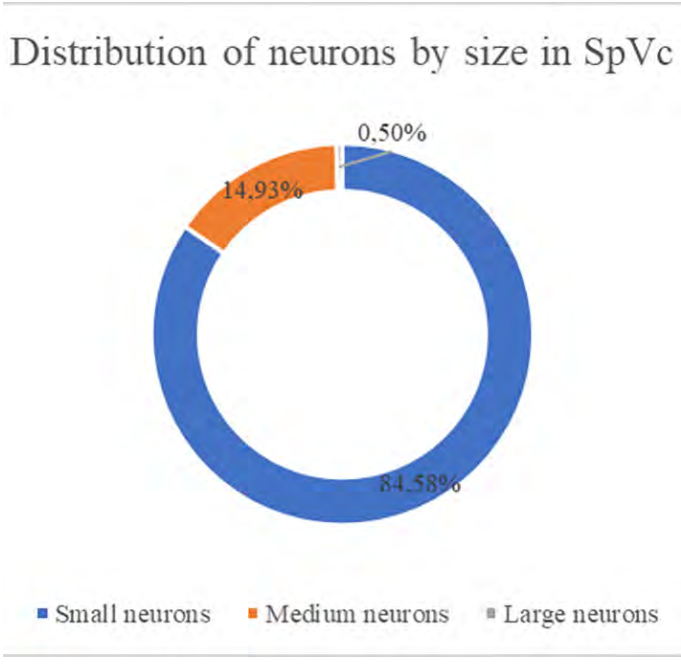

Fig. 2. Percentage distribution of different-sized neurons in the caudal spinal trigeminal subnucleus (SpVc). The predominant neuronal population consists of small cells, comprising nearly 85% of all neurons. Medium-sized neurons constituted approximately 14.93%, with large-sized neurons making up less than 1% of the total neuronal count.

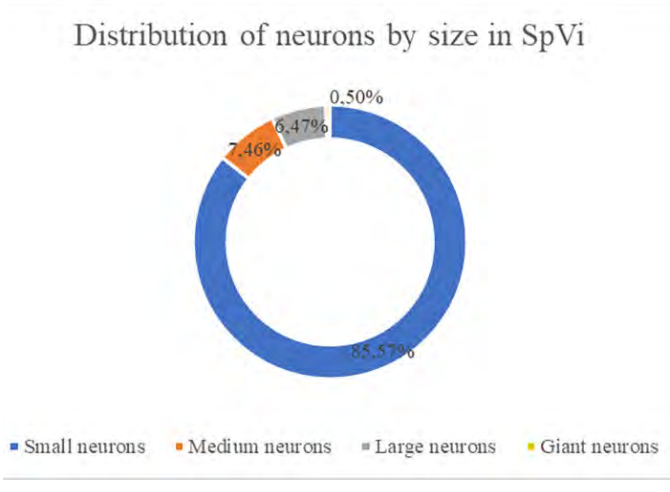

Fig. 3. Percentage distribution of different-sized neurons in the interpolar spinal trigeminal subnucleus (SpVi). Small neurons are the predominant type, accounting for 86% of the total neuronal population, followed by medium-sized neurons at 7.46%, large neurons at 6.47%, and occasional giant neurons, constituting less than one percent of the total neuronal population.

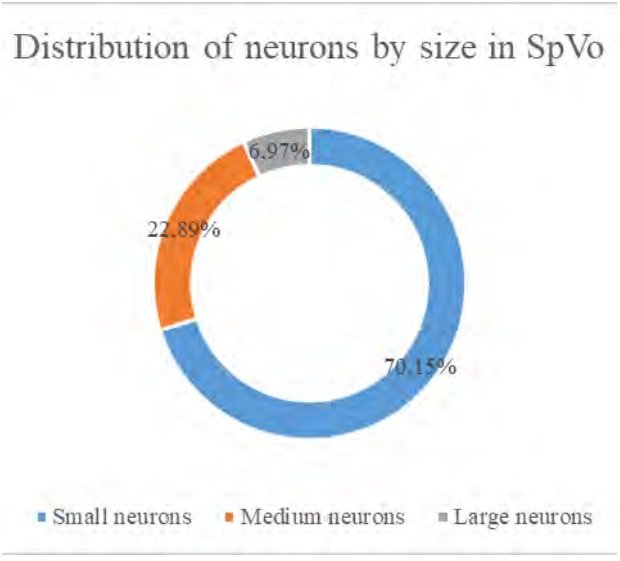

Fig. 4. Percentage distribution of different-sized neurons in the oral spinal trigeminal subnucleus (SpVo). Small neurons outnumber medium-sized cells by nearly threefold, comprising approximately 70% of the total, whereas medium-sized neurons represent about 23%. Large neurons constitute nearly 7% of all cells within this region.

Discussion

The SpV is a critical component of the trigeminal sensory system that is responsible for processing sensory information from the face and head [14]. Understanding the structural characteristics, specifically the size and morphology of neurons in these subnuclei is essential for unraveling the functional organization of the trigeminal sensory system. Supporting the descriptions already made with statistical analysis, our results show that this part of the nucleus contains unique neurons that can be divided into three groups according to the size of their cell bodies.

In the study of the SpV, understanding the size, shape, and distribution of its neuronal population is crucial for elucidating its functional organization and potential implications in sensory processing. We have examined the diverse morphologies of neurons within the rat SpV, encompassing bipolar, pyramidal, pear-shaped, boat-like neurons, among others, identifying at least 7 different neurons types (unpublished data). While the shape of neurons has been explored, the relationship between neuronal soma size and shape, and how these factors collectively contribute to sensory processing, remains an open question.

Certainly, building upon our prior investigations into the cytoarchitectonics of the SpV, this study endeavors to deepen our understanding of its organizational principles by examining the size characteristics of its constituent neurons. Our previous work has provided invaluable insights into the laminar organization, cellular composition,

and structural arrangements within the nucleus [7]. By leveraging this foundational knowledge, we tried to extend our inquiry to elucidate the size-related features of neurons within the SpV.

The size of neurons within the SpV can vary significantly, indicating potential functional diversity and specialization. Neuronal size is often correlated with various physiological properties such as firing rate, synaptic connectivity, and neurotransmitter phenotype [1]. Investigating neuronal soma size can provide insights into the metabolic demands, dendritic arborization, and integration of synaptic inputs within the spinal trigeminal circuitry. Several studies using various histological techniques and immunohistochemistry [4, 5, 6, 8, 13] have consistently reported differences in neuronal soma size among SpVo, SpVi, and SpVc. Previous studies of the morphology of neurons in the SpV categorized neurons in this nucleus based primarily on the size and shape of their cell bodies [6, 8, 9].

Studies on the human oral subnucleus have delineated two major categories of neurons [11, 13]. The first category consists of small rounded or fusiform cells (8-10 μm in diameter) clustered in small clusters or evenly spaced. The second category comprises large neurons (22 μm in diameter) with various morphology. Two of the subnuclei of the SpV have been extensively studied in different species. In the feline interpolar subnucleus, for example, one study has revealed the presence of five different cell types [9]. These types exhibit different morphologies and the diameters of these neurons vary widely from 6-12 μm to 15-25 μm. On the other hand, three major types of neurons are present in the rat oral subnucleus based on their shape and size [2, 3]. The sizes of the neuronal bodies range from 5-15 μm to 25-50 μm in diameter. Focusing on the size of neurons within the subnuclei of the SpV represents a logical progression in our understanding of its functional organization and sensory processing mechanisms.

Conclusion

In conclusion, the structural heterogeneity of neurons within the three subnuclei of the SpV has been well described in the literature, and there are mixed reports regarding the size of neurons within them. Moreover, the discrepancies in the external morphology of spinal trigeminal neurons observed in different studies highlight the complexity of this brain structure. Hence, by complementing previous investigations on neuronal shape and cytoarchitectonics, this study reveals the intricate relationships between neuronal morphology, size, and distribution, ultimately advancing our comprehension of somatosensory integration and relay within the trigeminal sensory pathway.

References

1. Brown, K. M., T. A. Gillette, G. A. Ascoli. Quantifying neuronal size: Summing up trees and splitting the branch difference. – *Semin. Cell Dev. Biol.*, **19**(6), 2008, 485-493.

2. Falls, W. M. A Golgi type II neuron in trigeminal nucleus oralis: A Golgi study in the rat. – *Neurosci Lett*, **41**(1–2), 1983, 1-7.

3. Falls, W. M., R. E. Rice, J. P. Vanwagner. The dorsomedial portion of trigeminal nucleus oralis (vo) in the rat: Cytology and projections to the cerebellum. – *Somatosens. Mot. Res.*, **3**(2), 1985, 89-118.
4. Gobel, S. Golgi studies of the neurons in layer I of the dorsal horn of the medulla (trigeminal nucleus caudalis). – *J. Comp. Neurol.*, **180**(2), 1978, 375-394.
5. Gobel, S. Golgi studies of the neurons in layer II of the dorsal horn of the medulla (trigeminal nucleus caudalis). – *Pain*, **6**(3), 1979, 386.
6. Gobel, S. Golgi studies of the substantia gelationsa neurons in the spinal trigeminal nucleus. – *J. Comp. Neurol.*, **162**(3), 1975, 397-415.
7. Ivanov, A., D. Atanasova, N. Lazarov. Cytoachitecture of the spinal trigeminal nucleus in rats. – *Acta Morphol. Anthropol.*, **26**(3–4), 2019, 46–50.
8. Li, Y. Q., H. Li, T. Kaneko, N. Mizuno. Substantia gelatinosa neurons in the medullary dorsal horn: An intracellular labeling study in the rat. – *J. Comp. Neurol.*, **411**(3), 1999, 399-412.
9. Matthews, M. A., T. V. Hernandez, A. I. Romanska, K. D. Hoffman. Golgi and immunocytochemical analysis of neurons in trigeminal subnucleus interpolaris: Correlations with cellular localization of enkephalin. – *Neuroscience*, **32**(2), 1989, 463-480.
10. Olszewski, J. On the anatomical and functional organization of the spinal trigeminal nucleus. – *J. Comp. Neurol.,* **92**(3), 1950, 401-413
11. Rusu, M. C. The spinal trigeminal nucleus - Considerations on the structure of the nucleus caudalis. – *Folia Morphol. (Warsz)*, **63**(3), 2004, 325-328.
12. Schindelin, J. I. Arganda-Carreras, E. Frise, V. Kaynig, M. Longair, et al. Fiji: An open-source platform for biological-image analysis. – *Nature Methods*, **9**(7), 2012, 676-682.
13. Schoenen, J. The dendritic organization of the human spinal cord: The dorsal horn. – *Neuroscience*, **7**(9), 1982, 2057-2087.
14. Usunoff, K. G., E. Marani, J. H. Schoen. The trigeminal system in man. – *Adv. Anat. Embryol. Cell Biol.*, **136**, 1997.

Institute of Experimental Morphology, Pathology and Anthropology with Museum
Bulgarian Anatomical Society

Acta Morphologica et Anthropologica, 31 (3-4)
Sofia ● 2024

Details of Sperm Tail Fibrous Sheath Revealed by Chemical Dissection and Unembedded Electron Microscopy

Maya Markova

Department of Biology, Medical Faculty, Medical University of Sofia, Sofia, Bulgaria

*Corresponding author e-mail: mayamarkov@gmail.com

The fibrous sheath is a cytoskeletal structure in the sperm tail principal piece composed of two longitudinal columns and multiple transverse ribs. To study details of its structure, we subjected mouse and human spermatozoa to extraction for fibrous sheath, a chemical dissection procedure which removes all other tail components. Extracted fibrous sheaths were observed by unembedded whole-mount transmission electron microscopy. In the distal part, the ribs tended to show a paired arrangement. It apparently reflected the paired structure of the anlagen during spermiogenesis, though this peculiarity was thought to be lost in the mature spermatozoon. Our data suggest that the original paired spines persist in a hidden form in the definitive ribs. Another observation was an apparent widening of distal fibrous sheath up to two times. We suppose that the spacial arrangement of ribs during spermiogenesis is achieved by intercalation, and the process is reversed by the chemical dissection.

Key words: Sperm tail, fibrous sheath, cytoskeleton, whole-mount, ultrastructure

Introduction

The fibrous sheath is a periaxonemal cytoskeletal structure specific for the sperm tail principal piece of therian mammals. It overlies the axoneme and outer dense fibers and consists of two longitudinal columns associated with microtubular doublets 3 and 8, and numerous transverse semicircular ribs interconnecting them. Despite having no motor activity of its own, the fibrous sheath contributes to sperm progressive motility by influencing tail flexibility [4]. It also serves as an attachment scaffold for various proteins, such as glycolytic enzymes [3]. Spermatozoa of some infertile men show fibrous sheath defects, either with a specific phenotype called dysplasia of the fibrous sheath, or in a broader category known as non-specific flagellar anomalies [2]. These defects are associated with loss of motility that may require treatment by

intracytoplasmic sperm injection (ICSI) [1]. At least in some cases, fibrous sheath abnormalities are the root cause of infertility, as shown in patients and mouse models with mutations affecting its components [10]. Because of this functional importance, numerous studies on fibrous sheath structure and biogenesis have been carried out. It has been reported to assemble in distal-to-proximal direction during spermiogenesis, first the angagen of the longitudinal columns and then the rib anlagen. The latter is initially a series of evenly spaced double spines which then attach to the longitudinal columns, thicken, group and coalesce by deposition of additional electron-dense material to form the mature ribs. The deposition and coalescence is more pronounced in the proximal principal piece [5]. The complexity and high electron density of the definitive fibrous sheath poses challenges to investigations of its structure. We used chemical dissection and whole-mount electron microscopy of mouse and human fibrous sheath to find details that are not revealed by conventional protocols.

Materials and Methods

Mouse spermatozoa were obtained from the vas deferens and cauda epididymidis of adult Swiss males, and human ejaculates were donated by healthy normozoospermic volunteers. The study conformed to EU and Bulgarian legislature and ethical guidelines for research.

The sperm cells were extracted for fibrous sheath according to Kim et al. [6, 7]. After washing with phosphate-buffered saline (PBS), pH 7.2, with 0.2 mM phenylmethylsulfonyl fluoride (PMSF), they were incubated twice for 15 min at 4°C with shaking in 50 mM Tris-Cl (pH 8.8) with 2% Triton X-100 and 5 mM dithiothreitol (DTT). Then the spermatozoa were washed in 50 mM Tris-Cl (pH 8.8) with 0.2 mM PMSF. After that, they were incubated for 5 hours at 4°C with shaking in 25 mM Tris-Cl (pH 7.5) with 4.5 M urea and 25 mM DTT, followed by washing first in 25 mM Tris-Cl (pH 7.5) and then in PBS (pH 7.2).

The extracted sperm cell remnants were spread on formvar-coated grids, fixed with 2.5% glutaraldehyde in PBS for 30 min at 4°C, washed with PBS and postfixed with 1% OsO_4 in PBS for 5 min at 4°C. Then they were washed twice with water for 5 minutes each, stained with 1% or 2% uranyl acetate and observed by a transmission electron microscope.

Results and Discussion

Whole-mount electron microscopy after removal of most sperm tail components by chemical dissection allowed us to observe the fibrous sheath in its entirety and to trace structural details. The applied extraction procedure produced similar results in human and mouse spermatozoa, leaving the fibrous sheath as the only visibly preserved tail structure (**Fig. 1**). While the thick and robust proximal fibrous sheath looked largely intact, damage to the longitudinal columns and stretching of the ribs was commonly observed in the distal fibrous sheath.

More details could be observed in distal than in proximal fibrous sheath regions, due to the lower electron density. Ribs tended to show a paired arrangement. These

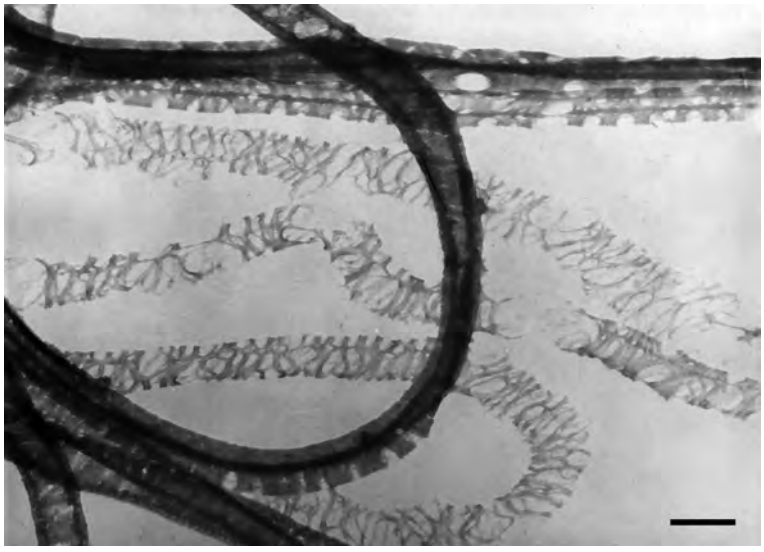

Fig. 1. A representative view of a human fibrous sheath preparation. Bar = 500 nm.

pairs, visible in some of the tail remnants in **Fig. 1**, were most apparent in fibrous sheaths that had been stretched during the processing (**Fig. 2**).

Towards the distal end of the fibrous sheath, its apparent width often increased up to two times. The easiest explanation was two-dimensional spreading after disintegration of one of the longitudinal columns. This could be the case for some fibrous sheaths

Fig. 2. Streched, visibly damaged mouse distal fibrous sheath. Ribs are apparently arranged in pairs, some of which are indicated by arrows. Bar = 500 nm.

such as the one in **Fig. 2**, but detailed view of others suggested pulling apart of ribs still attached with one of their ends to opposite longitudinal columns (**Fig. 3**).

We have previously observed interesting ultrastructural details in mouse and human sperm cells by whole-mount electron microscopy after another type of chemical dissection – extraction for nuclear matrix and intermediate filaments [8, 9]. Now, we applied a similar approach specifically to the sperm tail fibrous sheath, a tissue-specific cytoskeletal component that is still poorly understood because of inherent technical difficulties associated with its study. Chemical dissection facilitates observation by removing fractions of the cellular content to expose the structure of interest, and whole-mount unembedded electron microscopy circumvents the difficulties in interpreting images of a three-dimensional structure on ultrathin sections.

Extraction for fibrous sheath uses non-ionic detergent, DTT and urea to dissolve all other sperm tail components [6, 7]. Our observations showed that ribs of extracted fibrous sheaths tended to occur in pairs. This apparently corresponded to the paired anlagen described in [5] during spermiogenesis, but we have not found in the literature observations of paired fibrous sheath ribs in mature spermatozoa. We could hypothesize that the original double spines persist in the definitive ribs and are only masked by overlaying material that is partly removed or relaxed by the chemical dissection and mechanical stress applied during the preparation for microscopy. Another interesting observation was the apparent widening of distal fibrous sheath, even when both longitudinal columns still had ribs attached to them. We suppose that the spacial arrangement of ribs during spermiogenesis is achieved by intercalation, and the process is partly reversed by the chemical dissection.

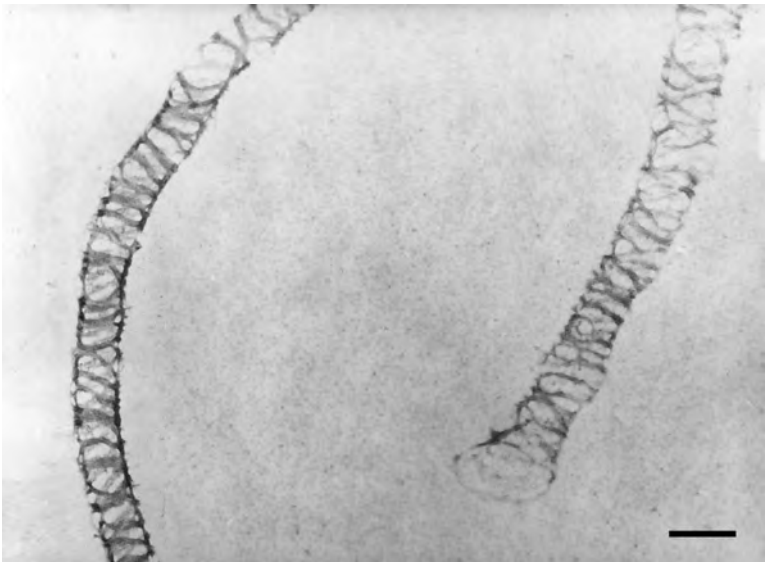

Fig. 3. Two regions of the fibrous sheath of the same mouse sperm tail. At the distal end (bottom right), the diameter increases twice, and ribs attached to opposite columns are seen pulled apart. Bar = 500 nm.

Conclusions

Our observations of sperm tail whole-mounts after extraction for fibrous sheath show that the paired structure of the rib anlagen persists in a hidden form in the definitive ribs, and suggest that their positioning during fibrous sheath formation is a result of intercalation.

Acknowledgements: This work was supported by Grants No. D-97/24.06.2020 and D-137/14.06.2022 of the Medical University of Sofia.

References

1. Boursier, A., A. Boudry, V. Mitchell, A. Loyens, N. Rives, A. Moerman, L. Thomas, E. Escudier, A. Toure, M. Whitfield, C. Coutton, G. Martinez, R. F. Ray, Z. E. Kherraf, S. Viville, M. Legendre, T. Smol, G. Robin, A. L. Barbotin. Results and perinatal outcomes from 189 ICSI cycles of couples with asthenozoospermic men and flagellar defects assessed by transmission electron microscopy. – *Reprod. Biomed. Online*, **47**, 2023, 103328.

2. Chemes, H. E. Phenotypic varieties of sperm pathology: Genetic abnormalities or environmental influences can result in different patterns of abnormal spermatozoa. – *Anim. Reprod. Sci*., **194**, 2018, 41-56.

3. Eddy, E. M. The scaffold role of the fibrous sheath. – *Soc. Reprod. Fertil. Suppl*., **65**, 2007, 45-62.

4. Eddy, E. M., K. Toshimori, D. A. O'Brien. Fibrous sheath of mammalian spermatozoa. – *Microsc. Res. Tech*., **61**, 2003, 103-115.

5. Irons, M. J., Y. Clermont. Kinetics of fibrous sheath formation in the rat spermatid. – *Am. J. Anat*., **165**, 1982, 121-130.

6. Kim, Y. H., J. R. McFarlane, G. Almahbobi, P. G. Stanton, P. D. Temple-Smith, D. M. de Kretser. Isolation and partial characterization of rat sperm tail fibrous sheath proteins and comparison with rabbit and human spermatozoa using a polyclonal antiserum. – *J. Reprod. Fertil.*, **104**, 1995, 107-114.

7. Kim, Y. H., D. M. de Kretser, P. D. Temple-Smith, M. T. Hearn, J. R. McFarlane. Isolation and characterization of human and rabbit sperm tail fibrous sheath. – *Mol. Hum. Reprod.*, **3**, 1997, 307-313.

8. Markova, M. D. Electron microscopic observations of mouse sperm whole mounts after extraction for nuclear matrix and intermediate filaments. – *Arch. Androl*., **47**, 2001, 37-45.

9. Markova, M. D. Electron microscopic observations of human sperm whole-mounts after extraction for nuclear matrix and intermediate filaments (NM-IF). – *Int. J. Androl.*, **27**, 2004, 291-295.

10. Zhang, G., D. Li, C. Tu, L. Meng, Y. Tan, Z. Ji, J. Cheng, G. Lu, G. Lin, H. Zhang, J. Sun, M. Wang, J. Du, W. Xu. Loss-of-function missense variant of AKAP4 induced male infertility through reduced interaction with QRICH2 during sperm flagella development. – *Hum. Mol. Genet*., **31**, 2021, 219-231.

Institute of Experimental Morphology, Pathology and Anthropology with Museum
Bulgarian Anatomical Society

Acta Morphologica et Anthropologica, 31 (3-4)
Sofia ● 2024

Review Articles

Renal Iron Metabolism and Its Role in the Kidney

Yavor Tabakov, Yordanka Gluhcheva*

Institute of Experimental Morphology, Pathology and Anthropology with Museum, Bulgarian Academy of Sciences, Sofia, Bulgaria

*Corresponding author e-mail: yavor.tabakov@iempam.bas.bg

For a long time iron transport and utilization in the kidney have been underestimated. The aim of the present review is to discuss the available research data about kidney iron and its role in some renal pathologies resulting from disturbed iron metabolism. The complex dynamics between systemic and local cellular iron regulation reveal kidney's key role in iron homeostasis. This has been shown by the presence of several major iron transports in the nephrons and by the fact that the kidney synthesises erythropoietin (EPO), master regulator of erythropoiesis. Furthermore, renal pathologies have a wide-reaching negative effect on iron homeostasis and like any of the canonical organs involved in iron metabolism, the kidney is very susceptible to iron disorders. Iron metabolism has become a focus for novel therapeutic strategies for several renal pathological conditions.

Key words: iron metabolism, regulation, kidney, kidney pathologies

Introduction

Iron (Fe) is the fourth most abundant element on Earth; therefore, it is not surprising that almost all organisms have evolved to include this unique element and its properties in various cellular process. Iron primarily exists in either ferrous (Fe^{2+}) or ferric (Fe^{3+}) oxidation state in biological systems. In a healthy, non-malnourished human there are approximately 3-5 g of iron; 60-75% of which is bound to haem, forming haemoglobin and around 10% is incorporated in myoglobin. The remaining amount forms complexes with various other enzymes and proteins. Most of the inorganic iron (non-haem) is stored as ferritin (Ft) or haemosiderin in macrophages and hepatocytes and only a very small amount is bound to the circulating serum protein transferrin (Tf). Approximately

1-2 mg of iron is lost daily through sweat, blood loss, sloughing of intestinal epithelial cells, and desquamation. To compensate, the body absorbs an equal amount in the same time period. Additionally, iron must be recycled and tightly regulated within the system to support haemoglobin synthesis and other metabolic processes. In summary, iron is an essential trace element involved in oxidation-reduction reactions, oxygen transport and storage, and energy metabolism. In excess it can have a pathological effect on cells, since it is involved in reactive oxygen species (ROS) production and pathogenic microbes require it for survival [7].

The kidneys are paired bean-shaped organs, located retroperitoneally in the posterior abdomen at the level of the 12th thoracic rib. The main function of the kidneys is to maintain homeostasis by reabsorbing essential nutrients and elements from the blood, whilst excreting metabolic waste and xenobiotics via urine. For a long time, researchers overlooked the kidneys as a major contributor to systemic iron homeostasis. This was due to the widely accepted fact that any "free" iron in the blood is bound to transferrin and that the complex is too big to be filtered by the glomerulus. Nevertheless, several articles published in the past few years have brought up the presence of various metal transporters in the kidneys and have established their involvement in systemic iron homeostasis [21, 24].

The aim of the present review is to discuss the research data regarding iron homeostasis in the kidney and some renal pathologies resulting from disturbed iron metabolism.

Iron Metabolism

Inorganic dietary iron is absorbed at the brush border of the duodenal enterocytes via divalent metal transporter 1 (DMT1). Dietary iron is usually in the oxidized ferric state (Fe^{3+}), and it must be reduced before entry into the cell. This is done by the membrane-associated ferrireductase – duodenal cytochrome b (Dcytb) [26]. Haem iron is absorbed through a different manner that so far remains unconfirmed, but animal models have identified haem carrier protein 1 (HCP1) and/or haem transporter HRG1 (SLC48A1) as potential transporters. Haem iron is released intracellularly by the inducible haemoxygenase 1 (HOX1/HO-1) [11, 22]. Intracellular iron is used for multiple processes and most of it is transferred to the mitochondria for haem and Fe-S clusters production by mitoferrin [19]. Haem is indispensable for haemoglobin, cytochromes, and enzyme activity. Fe-S clusters are essential to proteins involved in genome maintenance, energy conversion, iron regulation and protein translation [3, 6]. Excess intracellular iron is stored in the storage protein ferritin; this is done to maintain the labile iron pool (LIP) in specific limits and to avoid toxicity. Ferritin oxidizes and sequesters excess ferrous iron into a ferrihydrite mineral core. Iron sequestered in the Ft of enterocytes is lost after a few days through the sloughing of intestinal epithelial cells [1, 26]. Dietary cytosolic iron is exported into the plasma by ferroportin (Fpn). Exported Fe^{2+} iron is oxidized to Fe^{3+} by the ferroxidase hephaestin (Heph) and ceruloplasmin (Cp) **(Fig. 1)**. In the plasma, Fe^{3+} circulates bound to Tf, a glycoprotein that has two binding sites for ferric iron and maintains iron in a soluble form. Transferrin-bound iron (TBI) can be then recognised by TFR1 and delivered to cells via an endosomal cycle **(Fig. 2)** [26].

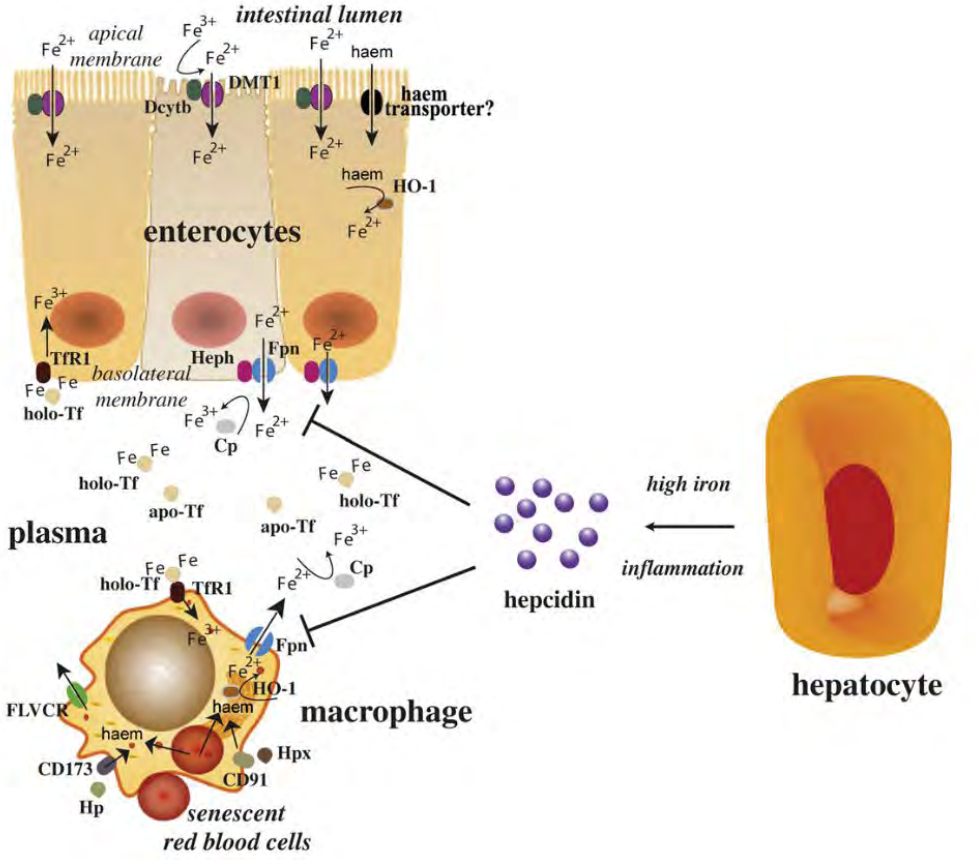

Fig. 1. Iron metabolism and systemic control by hepcidin. Enterocytes absorb inorganic or haem iron from the diet and macrophages phagocytose iron-loaded senescent red blood cells. Both types of cells release Fe^{2+} into the plasma via ferroportin (Fpn), which is incorporated into apo-Tf following oxidation to Fe^{3+} via hephaestin (Heph) or ceruloplasmin (Cp). Hepatocytes generate hepcidin in response to high iron or inflammatory signals, which inhibits the efflux of iron via Fpn and promotes its retention within enterocytes and macrophages [26].

Regulation of Iron Metabolism

Iron metabolism is tightly controlled on two levels, cellular and systemic. The cellular control of iron is done by the iron responsive element (IRE) – iron regulatory protein (IRP) system. The system exerts a post-transcriptional control on proteins associated with storage and transport. In an iron-deficient state, IRP1/2 stabilize TFR1 mRNA, which leads to increase in iron uptake. Additionally, iron storage and export are blocked due to ferritin and ferroportin translation being suppressed. When iron levels are repleted, Fe-S clusters convert IRP1 to cytosolic aconitase and IRP2 undergoes proteasomal degradation **(Fig. 2)** [4].

The systemic control of iron is regulated by the hormone hepcidin, which is produced by the liver. After secretion into the blood stream, hepcidin binds to its target – Fpn, and leads to its internalization and subsequent lysosomal degradation. Fpn degradation prevents the uptake of iron by the gut and prevents macrophages

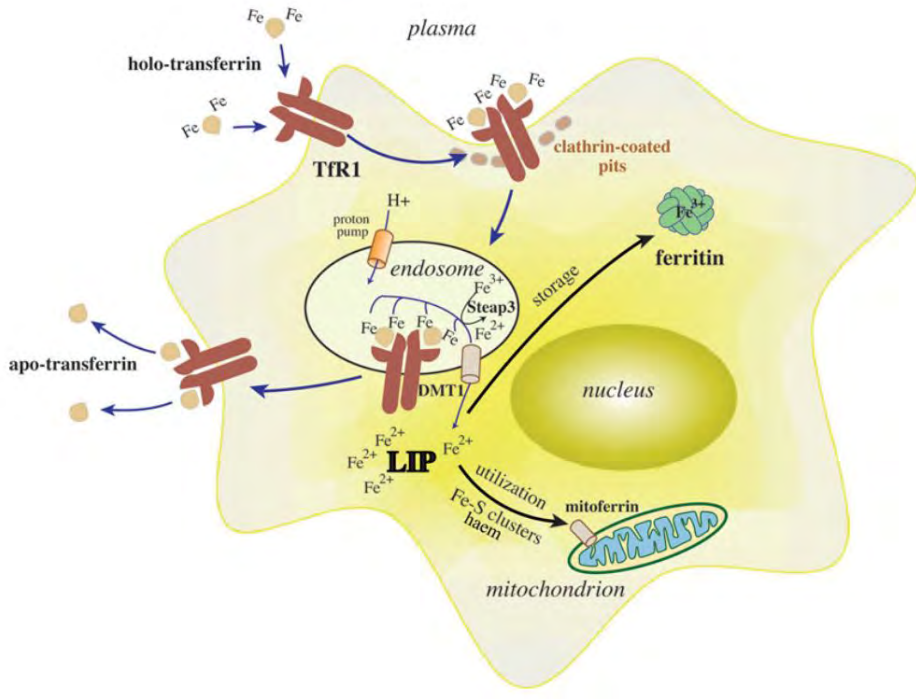

Fig. 2. Cellular iron uptake via the Tf cycle. Iron-loaded holo-Tf binds to TfR1 and is endocytosed via clathrin-coated pits. A proton pump acidifies the endosome, releasing Fe^{3+}, which is then reduced to Fe^{2+} by Steap3 and transported to the cytosol by DMT1. Fe^{2+} is directed to mitochondria via mitoferrin for metabolic utilization and excess iron is stored in ferritin. A cytosolic fraction of Fe^{2+} constitutes the LIP. The apo-Tf–TfR1 complex is recycled to the cell surface, where apo-Tf is released to capture plasma Fe^{3+} [26].

from releasing their iron stores. Circulating and tissue iron are positive regulators of hepcidin production. Endothelial cells in the liver sense an iron increase and produce bone morphogenic proteins 6 and 2 (BMP6/2), which induce hepcidin production by the hepatocytes. BMP6 production is dependent on iron concentrations, and it is believed that is the dominant ligand in high iron conditions. Whereas BMP2 is less iron sensitive and has higher concentrations in normal conditions, leading to the conclusion that it is the main regulator in normal physiology. Hepcidin levels can also be upregulated by inflammatory cytokines, interleukin 6 (IL-6) and macrophages. This crosstalk can potentiate iron sequestration during inflammation. Potent inhibitors of hepcidin production, which leads to increase in plasma iron, are iron deficiency, erythropoiesis, anaemia, and hypoxia **(Fig. 1)** [2, 4, 15].

Renal Function and Iron Metabolism

Nephrons are the functional units of the kidney, they are epithelial tubular structures, with specific interconnected morphological regions. Each region possesses specific functional properties that ensure the primary function of the kidneys. The regions are glomerulus, proximal tubule, loop of Henle, distal tubule, connecting tubule and finally collecting duct **(Fig. 3)**.

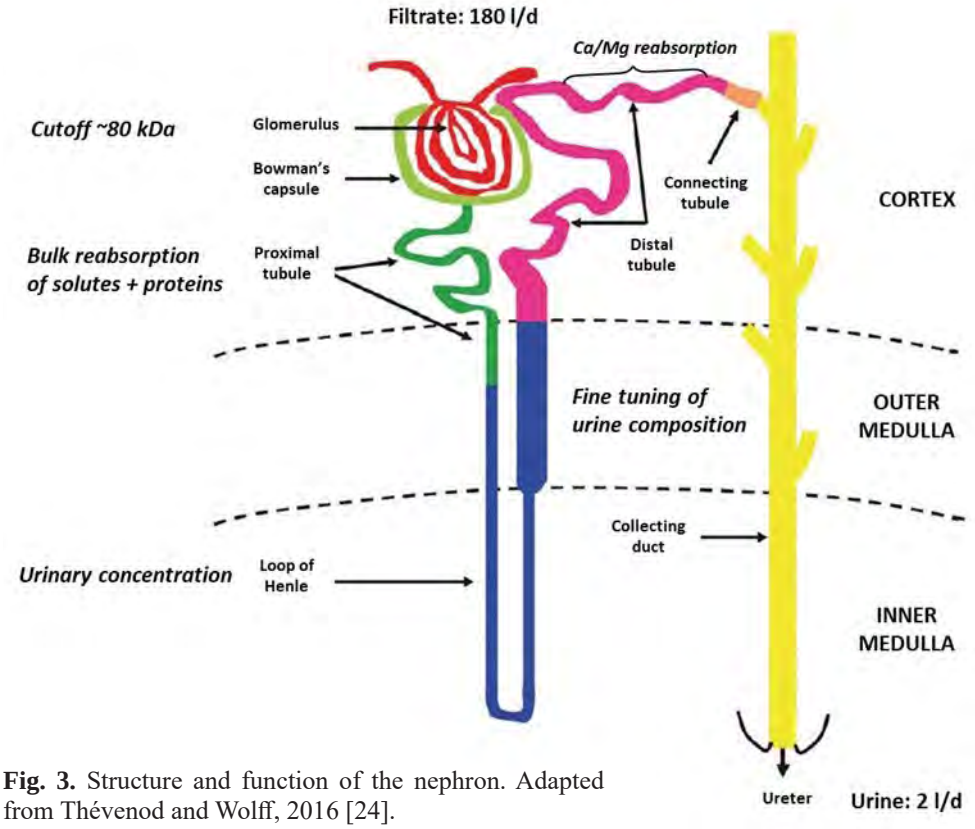

Fig. 3. Structure and function of the nephron. Adapted from Thévenod and Wolff, 2016 [24].

As mentioned previously, the kidney was often overlooked as a major contributor to systemic iron homeostasis, due to TBI exceeding the molecular mass limit of the glomerulus of ~80 kDa [21]. Some of the first indications that this belief was erroneous began with research in Faconi's syndrome, a pathology affecting the reabsorption potential of the proximal tubule (PT) [9]. Patients with this syndrome have an increased urinary excretion of proteins up to 160 kDa and subsequently have higher levels of urinary Tf than healthy individuals [16]. The general presence of Tf in the urine and the fact that in certain pathologies its levels increased led researchers to the conclusion that TBI can pass through the glomerulus. This was further substantiated by the presence of several iron transporters in the PT, such as cubilin, DMT1, TfR1 [29]. Cubilin was originally considered a receptor only for apoliprotein A1 and albumin in the kidney, but Kozyraki et al. 2001, discovered that it is a novel ligand for TBI located at the apical pole of polarized epithelial cells [10]. Due to lacking a transmembrane region, cubilin is dependent on megalin to carry out its functions. Megalin itself, colocalizes and binds to cubilin and the two receptors work together for ligand uptake. Megalin-dependent cubilin-mediated endocytosis is considered one of the main ways by which filtered TBI is reabsorbed and its proposed role is to rescue iron and supply the iron-dependent enzymes in the renal proximal tubules [10]. DMT1 is another iron transporter located in the PT, which further hints towards the importance of the kidneys

in iron homeostasis. In fact in one of the first studies on DMT1, some of the highest levels of DMT1 mRNA were identified in renal tissue [5]. Ultimately, findings like this inspired Smith and Thévenod, 2009 to propose a hypothetical model of renal iron transport **(Fig. 4)** [21].

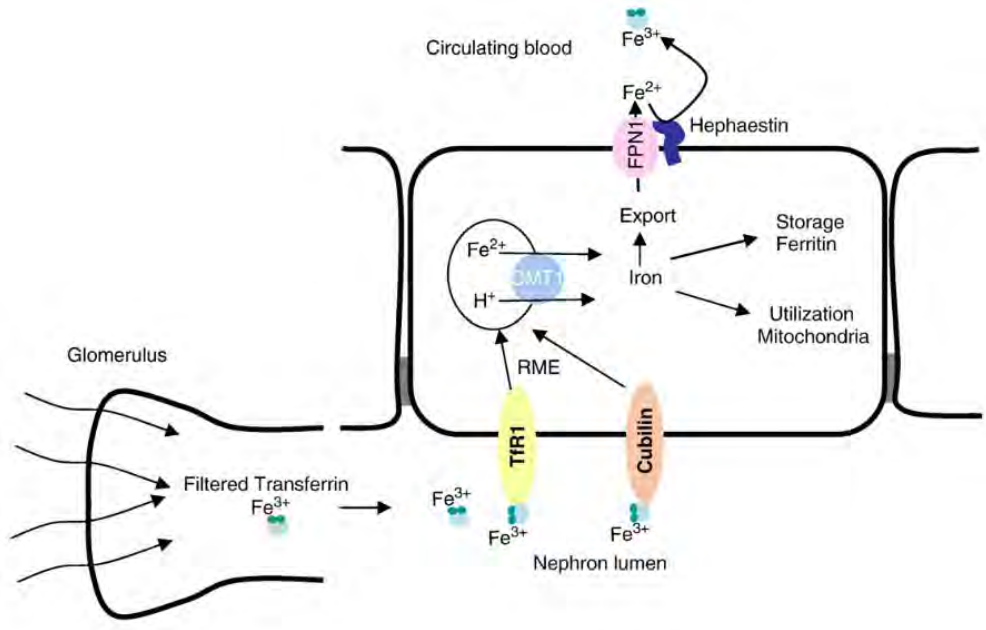

Fig. 4. Hypothetical model of renal iron transport. TBI is filtered and reabsorbed by proximal tubule cells by receptor mediated endocytosis (RME) bound to either to TfR1 or cubilin. TBI is transited to late endosomes/lysosomes where iron dissociates from Tf. Fe^{2+} (potential Dcytb activity) is translocated to the cell cytosol. Smith and Thévenod are not sure of Fe^{2+}'s ultimate fate and so propose three possible outcomes: (1) Fe^{2+} is utilized by PT mitochondria or iron requiring processes; (2) Fe^{2+} is stored in ferritin; (3) Fe^{2+} is exported back into the circulation via FPN1 aided by hephaestin. According to the authors, the three potential fates are not mutually exclusive [21].

Iron, The Kidney and Disease

With the growing interest in the kidney's role in systemic iron homeostasis, researchers have additionally enquired about the effect of renal pathologies on iron homeostasis and vice versa, the pathological effect of iron on the kidney. Kidney diseases do not escape the toxic effects of iron, and ferroptosis is identified as a pathophysiological mechanism that could be a therapeutic target to avoid damage or progression of kidney disease. Various animal models have been developed to study iron overload [18].

Renal Pathologies and Fe metabolism

The body can experience direct loss of iron with urine as a result of proteinuria caused by glomerulopathy. Tf and iron excretion with urine is increased with patients with focal segmental glomerulosclerosis (FSGS), focal glomerulonephritis, mesangioproliferative glomerulonephritis and diabetic nephropathy. These diseases are associated with systemic absolute iron deficiency and iron deficiency anaemia (IDA) [25]. Renal disorders may also affect systemic iron homeostasis indirectly by negatively affecting the production of erythropoietin. EPO is a glycoprotein hormone synthesised by the peritubular cells of the kidney and it stimulates red blood cell production. Renal cell loss and inflammation in chronic kidney disease (CKD) cause low levels of circulating EPO that correlates with the degree of anaemia and decreased erythropoietic activity [13, 27]. In patients with proteinuria, loss of EPO with urine is increased and may lead to lower systemic levels of the hormone, which has been observed in animal and human studies [8, 28].

Kidney pathologies and specifically CKD can affect iron metabolism in another way, by elevating hepcidin levels. Patients with CKD present with chronic inflammation, receive intravenous (IV) iron which raises iron stores and have low glomerular filtration rate (GFR). All of this leads to increase of Hep and decrease in its excretion. The increase in serum Hep impairs absorption of dietary iron and promotes iron sequestration by the reticuloendothelial system. Therefore, patients also present with functional iron deficiency (FID), characterized with impaired release of iron from stores and not meeting the needs of erythropoiesis, low serum Tf saturation (TSAT) levels and normal or high Ft levels [25].

Systemic Fe disorders and the kidney

Disruption of iron homeostasis, iron overload, has been known to exert a negative effect on organs that are heavy iron users and/or involved in iron recycling. Iron overload is primarily caused by hereditary haemochromatosis (HH), a genetical condition, caused by resistance or general deficiency of hepcidin. The causes are inherited genetical defects that affect proteins involved in the production, function, or regulation of hepcidin. This results in an unregulated uptake of iron by the duodenum which eventually leads to systemic iron overload [17]. Systemic iron overload can also be caused as a secondary pathological feature of thalassaemia disorders. They are characterized with reduced production of α-globin or β-globin chains, structural units of haemoglobin. Based on which chain production is disturbed, the disorders are classified as α-thalassaemia or β-thalassaemia. Nevertheless, both syndromes have dysfunctional haemoglobin production and impaired erythropoiesis. Patients with β-thalassaemia are classified as either intermediate or major, based on globin production levels, anaemia severity and clinical presentation. Both have an ineffective and increased erythropoiesis which results in a reduced hepcidin production. Additionally, patients with β-thalassaemia major require life-long, lifesaving blood transfusions, which could further exacerbate any systemic iron overload [14, 23]. Iron overload leads to elevated levels of Ft and TBI, increased iron saturation of Tf and increase in non-Tf bound iron (NTBI) and catalytic iron in the LIP. The LIP is a pool of NTBI, that in normal conditions participates in redox cycling, it does so by converting hydrogen peroxide to free-radical ions (Fenton reactions). Catalytic iron can cause oxidative damage to cell membranes, proteins and DNA [12, 20].

Conclusion

The kidney is potentially one of the biggest contributors to systemic iron homeostasis. This has been shown by the presence of several major iron transports in the nephrons and also by the fact that the kidney synthesises EPO, master regulator of erythropoiesis. Furthermore, renal pathologies have a wide-reaching negative effect on iron homeostasis and like any of the canonical organs involved in iron metabolism, the kidney is very susceptible to iron disorders.

Acknowledgements: This work was supported by the Bulgarian Ministry of Education and Science under the National Research Programme "Young scientists and postdoctoral students-2" approved by DCM 206/07.04.2022.

References

1. Arosio, P., F. Carmona, R. Gozzelino, F. Maccarinelli, M. Poli. The importance of eukaryotic ferritins in iron handling and cytoprotection. – *Biochem. J.,* **472**, 2015, 1-15.

2. Aschemeyer, S., B. Qiao, D. Stefanova, E. V. Valore, A. C. Sek, T. A. Ruwe, K. R. Vieth, G. Jung, C. Casu, S. Rivella, M. Jormakka, B. Mackenzie, T. Ganz, E. Nemeth. Structure-function analysis of ferroportin defines the binding site and an alternative mechanism of action of hepcidin. – *Blood,* **131**, 2018, 899-910.

3. Braymer, J. J., R. Lill. Iron-sulfur cluster biogenesis and trafficking in mitochondria. – J. *Biol. Chem.*, **292**, 2017, 12754-12763.

4. Camaschella, C., A. Nai, L. Silvestri. Iron metabolism and iron disorders revisited in the hepcidin era. – *Haematologica,* **105**, 2020, 260-272.

5. Gunshin, H., B. Mackenzie, U. V. Berger, Y. Gunshin, M. F. Romero, W. F. Boron, S. Nussberger, J. L. Gollan, M. A. Hediger. Cloning and characterization of a mammalian proton-coupled metal-ion transporter. – *Nature,* **388**, 1997, 482-488.

6. Hamza, I., H. A. Dailey. One ring to rule them all: Trafficking of heme and heme synthesis intermediates in the metazoans. – *Biochim. Biophys. Acta (BBA) – Molecular Cell Research*, **1823**, 2012, 1617-1632.

7. Hider, R. C., X. Kong. Iron: Effect of overload and deficiency. – *Met. Ions Life Sci.*, **13,** 2013, 229-295.

8. Inoue, A., T. Babazono, K. Suzuki, Y. Iwamoto. Albuminuria is an independent predictor of decreased serum erythropoietin levels in type 2 diabetic patients. – *Nephrol. Dial. Transplant.*, **22**, 2007, 287-288.

9. Klootwijk, E. D., M. Reichold, R. J. Unwin, R. Kleta, R. Warth, D. Bockenhauer. Renal Fanconi syndrome: taking a proximal look at the nephron. – *Nephrol. Dial. Transplant.,* **30**, 2015, 1456-1460.

10. Kozyraki, R., J. Fyfe, P. J. Verroust, C. Jacobsen, A. Dautry-Varsat, J. Gburek, T. E. Willnow, E. I. Christensen, S. K. Moestrup. Megalin-dependent cubilin-mediated endocytosis is a major pathway for the apical uptake of transferrin in polarized epithelia. – *Proc. Natl. Acad. Sci.,* **98**, 2001, 12491-12496.

11. Le Blanc, S., M. D. Garrick, M. Arredondo. Heme carrier protein 1 transports heme and is involved in heme-Fe metabolism. – *Am. J. Physiol.-Cell Physiol.*, **302**, 2012, C1780-1785.

12. Leaf, D. E., D. W. Swinkels. Catalytic iron and acute kidney injury. – *Am. J. Physiol. – Ren. Physiol.,* **311**, 2016, F871-876.

13. McGonigle, R. J., J. D. Wallin, R. K. Shadduck, J. W. Fisher. Erythropoietin deficiency and inhibition of erythropoiesis in renal insufficiency. – *Kidney Int.,* **25**, 1984, 437-444.

14. Nemeth, E. Hepcidin in β-thalassemia. – *Ann. N. Y. Acad. Sci.,* **1202**, 2010, 31–35.
15. Nemeth, E., M. S. Tuttle, J. Powelson, M. B. Vaughn, A. Donovan, D. M. Ward, T. Ganz, J. Kaplan. Hepcidin regulates cellular iron efflux by binding to ferroportin and inducing its internalization. – *Science,* **306**, 2004, 2090-2093.
16. Norden, A. G. W., M. Lapsley, P. J. Lee, C. D. Pusey, S. J. Scheinman, F. W. K. Tam, R. V. Thakker, R. J. Unwin, O. Wrong. Glomerular protein sieving and implications for renal failure in Fanconi syndrome. – *Kidney Int.*, **60**, 2001, 1885-1892.
17. Powell, L. W., R. C. Seckington, Y. Deugnier. Haemochromatosis. – *The Lancet,* **388**, 2016, 706-716.
18. Ríos-Silva, M., Y. Cárdenas, A. G. Ortega-Macías, X. Trujillo, E. Murillo-Zamora, O. Mendoza-Cano, J. A. Bricio-Barrios, I. Ibarra, M. Huerta. Animal models of kidney iron overload and ferroptosis: a review of the literature. – *BioMetals,* **36**, 2023, 1173-1187.
19. Shaw, G. C., J. J. Cope, L. Li, K. Corson, C. Hersey, G. E. Ackermann, B. Gwynn, A. J. Lambert, R. A. Wingert, D. Traver, N. S. Trede, B. A. Barut, Y. Zhou, E. Minet, A. Donovan, A. Brownlie, R. Balzan, M. J. Weiss, L. L. Peters, J. Kaplan, L. I. Zon, B. H. Paw. Mitoferrin is essential for erythroid iron assimilation. - *Nature,* **440**, 2006, 96-100.
20. Slotki, I., Z. I. Cabantchik. The Labile side of iron supplementation in CKD. – *J. Am. Soc. Nephrol.*, **26**, 2015, 2612-2619.
21. Smith, C. P., F. Thévenod. Iron transport and the kidney. - *Biochim. Biophys. Acta BBA – Gen. Subj.,* **1790**, 2009, 724-730.
22. Staroń, R., P. Lipiński, M. Lenartowicz, A. Bednarz, A. Gajowiak, E. Smuda, W. Krzeptowski, M. Pieszka, T. Korolonek, I. Hamza, D. W. Swinkels, R. P. L. V. Swelm, R. R. Starzyński. Dietary hemoglobin rescues young piglets from severe iron deficiency anemia: Duodenal expression profile of genes involved in heme iron absorption. – *PLOS One*, **12**, 2017, e0181117.
23. Taher, A. T., D. J. Weatherall, M. D. Cappellini. Thalassaemia. – *Lancet Lond. Engl.,* **391**, 2018, 155-167.
24. Thévenod, F., N. A. Wolff. Iron transport in the kidney: implications for physiology and cadmium nephrotoxicity. – *Metallomics,* **8**, 2016, 17-42.
25. van Swelm, R. P. L., J. F. M. Wetzels, D. W. Swinkels. The multifaceted role of iron in renal health and disease. – *Nat. Rev. Nephrol.*, **16**, 2020, 77-98.
26. Wang, J., K. Pantopoulos. Regulation of cellular iron metabolism. – *Biochem. J.*, **434**, 2011, 365-381.
27. Weiss, G., L. T. Goodnough. Anemia of chronic disease. – *New Engl. J. Med.,* **352**, 2005, 1011-1123.
28. Yamaguchi-Yamada, M., N. Manabe, K. Uchio-Yamada, N. Akashi, Y. Goto, Y. Miyamoto, M. Nagao, Y. Yamamoto, A. Ogura, H. Miyamoto. Anemia with chronic renal disorder and disrupted metabolism of erythropoietin in ICR-derived glomerulonephritis (ICGN) mice. – *J. Vet. Med. Sci.,* **66**, 2004, 423-431.
29. Zhang, D., E. Meyron-Holtz, T. A. Rouault. Renal iron metabolism: Transferrin iron delivery and the role of iron regulatory proteins. – *J. Am. Soc. Nephrol.,* **18**, 2007, 401.

Institute of Experimental Morphology, Pathology and Anthropology with Museum
Bulgarian Anatomical Society

Acta Morphologica et Anthropologica, 31 (3-4)
Sofia ● 2024

Mixed Pathology and Alzheimer's Disease

Ludmil Kirazov[1], Mashenka Dimitrova[1]*

[1]*Institute of Experimental Morphology, Pathology and Anthropology with Museum, Bulgarian Academy of Sciences, Sofia, Bulgaria*

*Corresponding author e-mail: lkirazov@yahoo.com

In elderly individuals with dementia, it is increasingly established that mixed brain pathologies are the cause. Pathological changes typical of Alzheimer's disease have been observed to coexist with vascular problems associated with vascular dementia. Coexistence with Lewy bodies is also frequently observed. In some cases, brain changes associated with all three conditions coexist – Alzheimer's disease, vascular dementia and dementia with Lewy bodies. Here, we review the co-morbidities of Alzheimer's disease, their relevance to disease progression, and the presence of certain risk factors that also appear to influence disease progression.

Key words: Alzheimer's disease, mixed pathology

Introduction

The National Institute on Aging-Alzheimer's Association Task Force on Alzheimer's Disease (AD) diagnoses AD based on brain pathology at autopsy or in vivo with the use of biomarkers rather than clinical presentation [13]. They view the disease as a sequence with a long preclinical phase along with cognitive impairment developing over many years, accompanied by an accumulation of AD markers that begins decades before the manifestation of clinical signs.

Although AD is the most common cause of dementia, it can be accompanied by a number of other pathologies. AD-pathology increases with age, but at the same time, many other brain diseases that affect cognitive functions develop as well. Examples are cerebrovascular changes such as heart attacks, atherosclerosis and arteriosclerosis, changes in the white matter of the brain, Lewy body disease and hippocampal sclerosis [18]. Although each of these dementia-causing pathologies develop differently, they are not mutually exclusive. Several studies show that a large percentage of elderly people, regardless of whether they have symptoms of dementia or not, are carriers of different pathologies in the brain – the so-called mixed pathology [27]. Autopsy brains of patients diagnosed with AD often show mixed pathology. In very few of

the cases in which AD is indicated as the main diagnosis, solely neuropathological findings characteristic of AD are found at autopsy [28]. In patients diagnosed with AD, where autopsy results show the presence of AD-pathology, vascular and other types of pathologies are very often found as well [25, 29].

Role of the cerebrovascular dysfunction

A number of studies demonstrate the role of cerebrovascular dysfunction as an important risk factor in the development of AD. Cerebrovascular dysfunction is found earlier than cognitive decline and before the formation of Aβ-deposits [9]. Cerebrovascular morphological changes, blood-brain barrier dysfunction and reduced cerebral blood flow are associated with the development of AD [12]. Another pathological hallmark of AD that also contributes to vascular dysfunction is the presence of Aβ deposits in the walls of cerebral blood vessels, referred to as cerebral amyloid angiopathy, which is also involved in the development of the pathology [23].

Electron microscopic studies show that degenerated small blood vessels, including capillaries, are closely associated with amyloid deposits in senile plaques. There are suggestions that it is amyloid angiopathy of small blood vessels and degeneration of capillaries that leads to a lack of energy of the surrounding nerve cells and their degeneration. The results of very early studies by several working groups give them reason to assume that blood vessels play a major role in the formation of senile plaques. In examining the brains of a large number of patients who died with a diagnosis of AD, Joachim et al. (1988) [16] observed that "at least a minimal degree of amyloid angiopathy is found in any brain that has the histopathological changes characteristic of AD". According to Miyakawa (2010) [22], these results strongly support the hypothesis that one of the main reasons for the development of AD pathology are changes in the blood-brain barrier.

Age-related and individual risks

Any pathology that accompanies AD is an additional burden on the brain, which increases the risk of developing dementia [2, 11]. The probability of developing different pathologies increases with age, and therefore, in the oldest people, mixed pathology is the most common cause of developing dementia [14]. Matthews et al. (2009) [21] show that co-morbidities may be the cause of half and more dementias compared to AD-pathology. With advancing age, AD- and non-AD-type pathologies accumulate, so the proportion of mixed pathology grows, as does the risk of developing dementia. Combinations of different pathologies may be most diverse and the contribution of each to the development of dementia may be different in different individuals [7].

Understanding the role of different pathologies is important for assessing the risk factors leading to the development of AD. In their study, Boyle et al. (2013) [6] show that known types of neurodegenerative pathologies can explain less than half of the observed cognitive impairment in old age. This may be due to as yet unexplained pathological processes, but it may also be due to individual differences in the ability of the brain to protect itself from the development of pathologies [3].

It is known that the morphological signs of AD, as well as other known pathologies, are not clearly interrelated with the impairment of cognitive functions. In clinicopathological studies and with the use of biomarkers, it has been shown that at the same degree of manifestation of pathological changes, some individuals have clinical symptoms, while others have no deterioration [4]. This likely means that some individuals can develop resilience and respond flexibly to pathological processes,

allowing them to compensate for a greater degree of pathological changes than others. This has been termed cognitive or neuronal reserve capacity [3]. The biological basis of neuronal reserve includes cellular, synaptic, and biochemical pathways [1]. These may involve synaptic and particularly presynaptic proteins, neuronal or nuclear hypertrophy, changes in neuronal density and brain microstructure and others.

Risk factor for developing AD

In light of the role that mixed pathologies have, as well as the persistence of pathologies in the development of AD, it is important to consider the risk factors involved in these processes. In principle, risk factors may affect AD-pathology, vascular or other pathologies, modulate the interaction between them or be related to yet unknown pathologies.

We will list some factors other than genetics that also seem to influence the development of AD.

One such group is sociodemographic and behavioral factors. Education belongs to them. It has long been assumed that higher education slows the development of cognitive deficits. Multiple studies have shown the relationship between education and the degree of cognitive deficit independent of the degree of AD-pathology [8, 10, 26]. None of these studies show a direct relationship between education and the development of AD-pathology. It is believed that its positive role is carried out by improving the resistance of the brain against pathologies and building neuronal reserve capacity. This capacity may be expressed in the greater plasticity of the brain and the ability to more easily build compensatory connections at the site of the affected ones.

The group of sociodemographic and behavioural factors also includes physical, cognitive and social activities. Maintaining these activities is associated with a reduced risk of developing dementia [31, 32]. They can exert their positive effect through mechanisms such as improving the cardiovascular condition, as well as building reserve capacity by stimulating cognitive functions. Reading, solving crosswords, and participating in various games reduce the risk of dementia of the Alzheimer's type [30] and help preserve the plasticity of the brain. This is probably done through the same mechanisms that are influenced by education.

Increasing attention is being paid to the influence of nutrition and different diets on the risk of developing dementia. There is also a relationship between sleep and circadian rhythm with the dynamics of Aβ accumulation, and here the relationship is probably bidirectional – sleep helps to eliminate Aβ, and Aβ accumulation can lead to sleep disorders [17].

There are also psychological risk factors. According to Boyle et al. (2012) [5], people who have a purpose in life show fewer cognitive deficits, while depressive symptomatology contributes to cognitive impairment [32].

There are, of course, medical risk factors as well. Among them, the primary ones are cardiovascular, and their relationship with the risk of developing cerebrovascular disease and vascular dementia is well documented. Trauma of the head can be placed second. There are numerous studies on the relationship between traumatic brain injury and the increased risk of dementia [15]. There is no clear evidence whether AD is a direct pathological consequence or whether other neurodegenerative processes, such as chronic traumatic encephalopathy, are involved. Research results on the relationship between traumatic brain injury and Aβ deposition are conflicting.

Conclusions

It is clear from the above that dementias can have complex causes and their treatment must be complex [24]. In addition, AD is a multifunctional disease and the counteraction against it cannot be limited in only one direction. More and more systems in the brain are being discovered that are affected by the occurrence of AD. Many model systems have been used to study AD [19] but they have a number of limitations [20]. Due to its asymptomatic development for perhaps tens of years, it is particularly important to look for early markers to detect the pathological processes. The lack of clarity about the exact mechanisms causing AD as well as its long course means that therapy should also be very long-term and continue into old age. This, on one hand, places a heavy burden on public resources. On the other hand, medical treatment of the elderly can be problematic due to age-related changes in the kidneys and liver. Therefore, the main goal of research and the fight against AD should be its prevention. This can start now with improved control of cardiovascular risk factors, improved education and increased public information about the major risk factors.

At the same time, in-depth studies of the biochemical basis of Alzheimer's disease must continue in order to clarify its etiology in detail.

References

1. **Arnold, S. E., N. Louneva, K. Cao, L. S. Wang, L. Y. Han, D. A. Wolk, S. Negash, S. E. Leurgans, J. A. Schneider, A. S. Buchman, R. S. Wilson, D. A. Bennett**. Cellular, synaptic, and biochemical features of resilient cognition in Alzheimer's disease. – *Neurobiol. Aging*, **34**(1), 2013, 157-168.
2. **Azarpazhooh, M. R., A. Avan, L. E. Cipriano, D. G. Munoz, L. A. Sposato, V. Hachinski.** Concomitant vascular and neurodegenerative pathologies double the risk of dementia. – *Alzheimer's Dement.*, **14**, 2018, 148-156.
3. **Bennett, D. A.** Mixed pathologies and neural reserve: implications of complexity for Alzheimer disease drug discovery. – *PLOS Med***., 14,** 2017, e1002256.
4. **Bennett, D. A., R. S. Wilson, P. A. Boyle, A. S. Buchman, J. A. Schneider.** Relation of neuropathology to cognition in persons without cognitive impairment**.** – *Ann. Neurol***., 72,** 2012, 599-609.
5. **Boyle, P. A., A. S. Buchman, R. S. Wilson, L. Yu, J. A. Schneider, D. A. Bennett.** Effect of purpose in life on the relation between Alzheimer disease pathologic changes on cognitive function in advanced age. – *Arch. Gen. Psychiatry*, **69**, 2012, 499-504.
6. **Boyle, P. A., R. S. Wilson, L.Yu, A. M. Barr, W. G. Honer, J. A. Schneider, D. A. Bennett.** Much of late life cognitive decline is not due to common neurodegenerative pathologies. – *Ann. Neurol*., **74**, 2013, 478-489.
7. **Boyle, P. A., L. Yu, R. S. Wilson, S. E. Leurgans, J. A. Schneider, D. A. Bennett**. Person-specific contribution of neuropathologies to cognitive loss in old age. – *Ann. Neurol*., **83**, 2018, 74-83.
8. **Brayne, C., P. G. Ince, H. A. Keage, I. G. McKeith, F. E. Matthews, T. Polvikoski T., R. Sulkava**. Education, the brain and dementia: neuroprotection or compensation? – *Brain*, **133**(Pt 8), 2010, 2210-2216.
9. **Brown, W. R., C. R. Thore**. Review: Cerebral microvascular pathology in ageing and neurodegeneration. – *Neuropathol. Appl. Neurobiol.,* **37**, 2012, 56-74.
10. **Farfel, J. M., R. Nitrini, C. K. Suemoto, L. T. Grinberg, R. E. Ferretti, R. E. Leite, E. Tampellini, L. Lima, D. S. Farias, R. C. Neves, R. D. Rodriguez, P. R. Menezes, F.**

Fregni, D. A. Bennett, C. A. Pasqualucci, W. Jacob Filho. Brazilian Aging Brain Study Group. Very low levels of education and cognitive reserve: a clinicopathologic study. – *Neurology*, **81**(7), 2013, 650-657.

11. Forrest, S. L., G. G. Kovacs. Current Concepts of Mixed Pathologies in Neurodegenerative Diseases. – *Canadian J. Neurological Sci*., **50**(3), 2023, 329-345,

12. Iturria-Medina, Y., R. C. Sotero, P. J. Toussaint, J. M. Mateos-Pérez, A. C. Evans. The Alzheimer's disease neuroimaging initiative. Early role of vascular dysregulation on late-onset Alzheimer's disease based on multifactorial data-driven analysis. – *Nat. Commun*., **7**, 2016, 11934

13. Jack, C. R. Jr., D. A. Bennett, K. Blennow, M. C. Carrillo, B. Dunn, S. B. Haeberlein, D. M. Holtzman, W. Jagust, F. Jessen, J. Karlawish, E. Liu, J. L. Molinuevo, T. Montine, C. Phelps, K. P. Rankin, C. C. Rowe, P. Scheltens, E. Siemers, H. M. Snyder, R. Sperling, Contributors. NIA-AA Research Framework: Toward a biological definition of Alzheimer's disease. – *Alzheimer's Dement.*, **14**, 2018, 535-562.

14. James, B. D., D. A. Bennett, P. A. Boyle, S. Leurgans, J. A. Schneider. Dementia from Alzheimer disease and mixed pathologies in the oldest old. – *JAMA*, **307**, 2012, 1798-1800.

15. Jellinger, K. A. Head injury and dementia. – *Curr. Opin. Neurol.,* **17**, 2004, 719-723.

16. Joachim, C. L., J. H. Morris, D. J. Selkoe. Clinically diagnosed Alzheimer's disease: autopsy results in 150 cases. – *Ann. Neurol.,* **24**(1), 1988, 50-56.

17. Ju, Y.-E., B. P. Lucey, D. M. Holtzman. Sleep and Alzheimer disease pathology—a bidirectional relationship. – *Nat. Rev. Neurol.*, **10**, 2014, 115-119.

18. Kapasi, A., C. DeCarli, J. A. Schneider. Impact of multiple pathologies on the threshold for clinically overt dementia. – *Acta Neuropathol.,* **134**, 2017, 171-186.

19. Kirazov, L., E. Kirazov, C. Naydenov, V. Mitev. Model systems and approaches to the study of the metabolism of Alzheimer's amyloid precursor protein. – *Acta Morphol. Anthropol.,* **21**, 2015, 55-61.

20. Korczyn, A. D. The amyloid cascade hypothesis. – *Alzheimers Dement*., **4**(3)**,** 2008, 176-178.

21. Matthews, F. E., C. Brayne, J. Lowe, I. McKeith, S. B. Wharton, P. Ince. Epidemiological pathology of dementia: attributable-risks at death in the Medical Research Council Cognitive Function and Ageing Study. – *PLOS Med.*, **6**, 2009, e1000180.

22. Miyakawa, T. Vascular pathology in Alzheimer's disease. – *Psychogeriatrics,* **10**(1), 2010, 39-44.

23. Morrone, C . D., J. Bishay, J. A. McLaurin J. A. Potential role of venular amyloid in Alzheimer's disease pathogenesis. – *Int. J. Mol. Sci*., **21**(6), 2020, 1985.

24. Nichols, E., R. Merrick, H. I. Simon, D. Himali, J. J. Himali, S. Hunter, H. A. D. Keage, C. S. Latimer, M. R. Scott, J. D. Steinmetz, J. M. Walker, S. B. Wharton, C. D. Wiedner, P. K. Crane, C. D. Keene, L. J. Launer, F. E. Matthews, J. Schneider, S. Seshadri, L. White, C. Brayne, T. Vos. The prevalence, correlation, and co-occurrence of neuropathology in old age: harmonisation of 12 measures across six community-based autopsy studies of dementia. – *The Lancet,* **4**(3), 2023, E115-E125.

25. Robinson, J. L., X. X. Sharon, D. R. Baer, E.-R. Suh, V. M. Van Deerlin, N. J. Loh, D. J. Irwin, C. T. McMillan, D. A. Wolk, A. C. Plotkin, D. Weintraub, T. Schuck, V. M. Y. Lee, J. Q. Trojanowski, E. B. Lee. Pathological combinations in neurodegenerative disease are heterogeneous and disease-associated. – *Brain*, **146**(6), 2023, 2557–2569.

26. Roe, C .M., C. Xiong, J. P. Miller, N. J. Cairns, J. C. Morris. Interaction of neuritic plaques and education predicts dementia. – *Alzheimer Dis. Assoc. Disord*., **22**, 2008, 188-193.

27. Schneider, J. A., Z. Arvanitakis, W. Bang, D. A. Bennett. Mixed brain pathologies account for most dementia cases in community-dwelling older persons. – *Neurology*, **69**, 2007, 2197-2204.

28. Tosun, D., O. Yardibi, T. L. S. Benzinger, W. A. Kukull, C. L. Masters, R. J. Perrin, M. W. Weiner, A. Simen, A. J. Schwarz. Identifying individuals with non-Alzheimer's disease co-pathologies: A precision medicine approach to clinical trials in sporadic Alzheimer's disease. – *Alzheimer's and Dementia*, **20**(1), 2024, 421-436.

29. Twait, L. E., L. Gerritsen, J. E. F. Moonen, I. M. W. Verberk,; C. E. Teunissen, P. J. Visser, W. M. van der Flier, M. I. Geerlings, UCC SMART Study Group, the NCDC Consortium. Plasma markers of Alzheimer's disease pathology, neuronal injury, and astrocytic activation and MRI load of vascular pathology and neurodegeneration: The SMART-MR study. – *Journal of the American Heart Association,* **13**(4), 2024

30. Valenzuela, M., C. Brayne, P. Sachdev, G. Wilcock, F. Matthews. Medical Research Council. Cognitive function and ageing study. Cognitive lifestyle and long-term risk of dementia and survival after diagnosis in a multicenter population-based cohort. – *Am. J. Epidemiol.* , **173(9)**, 2011, 1004-1012.

31. van der Flier, W. M., M. E. de Vugt, E. M. A. Smets et al. Towards a future where Alzheimer's disease pathology is stopped before the onset of dementia. – *Nat. Aging*, **3**, 2023, 494–505.

32. Wilson, R. S., A. W. Capuano, P. A. Boyle, G. M. Hoganson, L. P. Hizel, R. C. Shah, S. Nag, J. A. Schneider, S. E. Arnold, D. A. Bennett. Clinical-pathologic study of depressive symptoms and cognitive decline in old age. – *Neurology*, **83**(8)**,** 2014, 702-709.

Institute of Experimental Morphology, Pathology and Anthropology with Museum
Bulgarian Anatomical Society

Acta Morphologica et Anthropologica, 31 (3-4)
Sofia ● 2024

ANTHROPOLOGY AND ANATOMY 31 (4)

Original Articles

Quantitative Assessment of Structural Complexity in Human Cerebellum through Analysis of Skeletonized MR Images: Anatomical Correlations, Sex Differences, and Age-Related Changes

Nataliia Maryenko, Oleksandr Stepanenko*

Department of Histology, Cytology and Embryology, Kharkiv National Medical University, Kharkiv, Ukraine

*Corresponding author e-mail: maryenko.n@gmail.com, ni.marienko@knmu.edu.ua

The present study provides a quantitative assessment of the human cerebellum structural complexity using analysis of skeletonized images. Magnetic resonance images from 100 apparently healthy individuals (aged 18-86 years) were examined. Following segmentation, the images were skeletonized, and quantitative analysis of the digital skeletons was conducted. The following parameters were determined: number of branches and their junctions, end-point, slab and junction pixels, average and maximum branch length, triple and quadruple points. Sex differences were assessed. Correlation analysis included determining the relationships between the studied parameters and age, morphometric parameters derived from Euclidean and fractal geometries, as well as the same parameters of the digital skeletons identified in the cerebral hemispheres. In conclusion, quantitative analysis of digital cerebellar skeletons offers advantages for assessing the structural complexity of the cerebellum. This method and the results of the present study can be applied in diagnosing cerebellar malformations and distinguishing between malformations and atrophic alterations.

Key words: age, cerebellum, morphometry, tomography, sex differences

Introduction

The human cerebellum possesses a complex tree-like structure characterized by the branching of its white matter. Changes in cerebellar structure, typically simplification, occur in malformations, often resembling those observed in atrophic alterations [12]. Therefore, the development of methods for quantitatively assessing cerebellar structural complexity is particularly important. Commonly used methods for quantitative characterization of the cerebellum are derived from Euclidean geometry, involving measurements of linear dimensions [4], sectional area [4, 13], and volume [15]. In recent decades, due to the fractal properties of the cerebellum (self-affinity and scale invariance), fractal analysis derived from fractal geometry has been employed to characterize cerebellar structural complexity [1, 6, 8, 16].

An alternative method used to analyze complex, tree-like structures is quantitative analysis of skeletonized images. This technique involves skeletonization of silhouette images followed by automated counting of branches, junctions, endpoints, and related parameters. It has been utilized to characterize the arborization of neuronal dendritic trees [3, 11] and glial cell processes [17]. Skeletonization can also serve as a preprocessing step for fractal analysis, including studies of neurons [5, 10], the cerebellum [6], and the white matter of the cerebral hemispheres [2, 18].

Given the tree-like nature of the cerebellar white matter and the neuron-like appearance of the cerebellum on sagittal sections, we aimed to apply quantitative analysis of skeletonized images to investigate its structural complexity. In our previous preliminary study, we employed this method for magnetic resonance (MR) images of the cerebellum as supportive analysis [8]. In the present study, we expanded the sample size from 30 to 100 and widened the age range from 18-30 years to 18-86 years. Our objective was to investigate sex differences, age-related changes, and determine the anatomical correlations of quantitative parameters of digital cerebellar skeletons.

Material and Methods

In this study, T2-weighted MR images from 100 apparently healthy individuals (44 males and 56 females), aged 18-86 years, were analyzed. The age and sex distribution of the study sample is presented in **Table 1**. Participants underwent diagnostic MR brain scanning using a 1.5 Tesla Siemens Magnetom Symphony magnetic resonance imaging scanner. Individuals with no MR confirmed brain pathology were considered ostensibly healthy and included in the study. Written informed consent was obtained from all participants. The study was approved by the Commission on Ethics and Bioethics of Kharkiv National Medical University (Minutes of Meetings No. 10 dated November 7, 2018, and No. 5 dated February 1, 2023) for research involving human subjects.

Table 1. The age and sex distribution of the participants of the study

Sex group	Age range, years				Total
	18-30	**31-45**	**46-60**	**61-86**	
Both, N	31	29	24	16	100
Males, N	14	14	8	8	44
Females, N	17	15	16	8	56

The midsagittal sections of the cerebellar vermis were selected for analysis (**Fig. 1A**). The image size was 160×160 pixels, with an absolute image scale of 3 pixels = 1 mm. During preprocessing, the background was removed (**Fig. 1B**), followed by segmentation using thresholding with an empirical pixel intensity threshold value of 100. This resulted in a binary silhouette image of the overall cerebellar tissue (**Fig. 1C**). Subsequently, the images underwent skeletonization using the "skeletonize" tool in Image J software [14]. The digital skeleton line thickness was set at 1 pixel (**Fig. 1D**). Skeleton analysis was conducted using the "analyze skeleton" tool in Image J (**Fig. 1E, F**). The following parameters were determined: 1. number of branches; 2. number of junctions; 3. end-point pixels (voxels) – pixels forming the

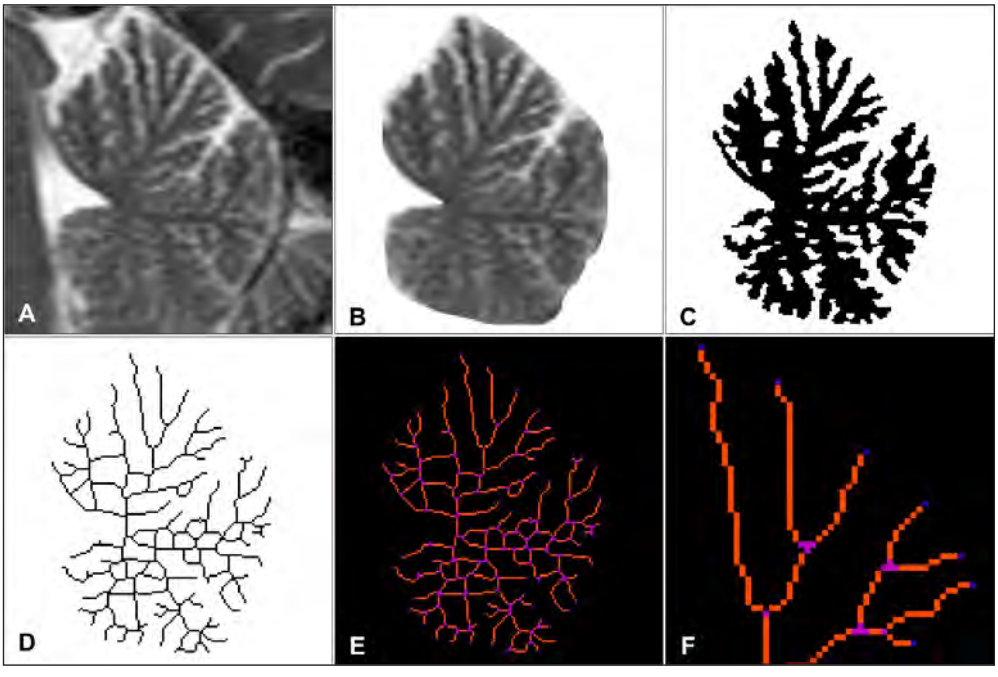

Fig. 1. Cerebellar MR image analysis algorithm (T2-weighted image, midsagittal section of the cerebellar vermis). A – initial image; B – background removal; C – segmentation of the overall cerebellar tissue; D – skeletonization; E, F – quantitative analysis of digital skeleton: slab pixels (forming branches) are shown in orange, junction pixels in purple, and end-point pixels in blue

endpoints of the digital skeleton, corresponding to the number of superficially exposed gyri; 4. junction pixels (voxels) – pixels forming the junctions; 5. slab pixels (voxels) – pixels forming the branches; 6. average branch length; 7. maximum branch length; 8. triple points (number of junctions connecting three branches); 9. quadruple points (number of junctions connecting four branches).

For correlation analysis, we used additional parameters derived from Euclidean and fractal geometries (see [9] for descriptive data and analysis of these parameters). Euclidean geometry-based parameters included: perimeter P1 (length of the visible cerebellar pial surface contour); area A1 (cerebellar tissue area, including fissures and sulci content); perimeter-to-area ratio (P1/A1); shape factor (circularity) SF1; perimeter P2 (length of the entire cerebellar pial surface contour, including hidden surface within fissures and sulci); area A2 (cerebellar tissue area excluding fissures and sulci content); perimeter-to-area ratio (P2/A2); shape factor (circularity) SF2; gyrification index calculated as P2/P1; and area ratio calculated as A2/A1. Fractal geometry-derived parameters included fractal dimensions (FD), such as FD of overall cerebellar tissue, white matter, cortex, granular layer of cortex, molecular layer of cortex, cerebellar digital skeleton, and outer contour [9].

Additionally, we examined correlation relationships between the studied parameters of cerebellar skeletons and those determined in cerebral hemispheres in our previous study (involving the same sample) [7]. The previous study analyzed five sections: four coronal and one axial, where Coronal 1 was located at the anterior poles of the temporal lobes, Coronal 2 at the level of mammillary bodies, Coronal 3 at the level of the quadrigeminal plate, Coronal 4 at the level of the splenium of the corpus callosum, and Axial at the level of the thalamus [7].

Statistical analysis was conducted using Microsoft Excel 2016. Descriptive data are presented as mean (M), standard deviation (SD), minimum value (min), 25th percentile (Q1), median (Me), 75th percentile (Q3), and maximum value (max). The normality of the value distribution was assessed using the Shapiro-Wilk W test. As some parameters exhibited non-normal distribution (**Table 2**), non-parametric statistical methods were chosen for further analysis. The Mann-Whitney U test was used to assess the significance of statistical differences between parameters in males and females. Relationships between the studied morphometric parameters were evaluated using the non-parametric Spearman's rank correlation coefficient (R), with significance determined by the Student t-test. The F-test was applied to compare linear regression equations characterizing the age dynamics of the studied parameters in males and females. The significance level for all results was set at $\alpha = 0.05$.

Results

The descriptive statistical data are presented in **Table 2**. The values of the studied parameters were distributed across a wide range. The mean and median values of most parameters (except for average and maximum branch length and quadruple points) were higher in males compared to females, but a significant difference was observed only for end-point pixels. This suggests a slightly higher branching degree in male cerebella, resulting in more numerous superficial gyri.

Table 2. Descriptive statistics for the cerebellar digital skeleton quantitative parameters

Parameter	*Sex group*	M	SD	min	Q1	Me	Q3	max	*P (normality)*	*P (sex difference)*
Branches	***Both***	114.57	25.58	48	98	114	130	178	*0.211*	*0.394*
	Males	117.27	27.18	48	98	117	131	176		
	Females	112.45	24.29	54	99	111	127	178		
Junctions	***Both***	59.52	14.16	25	51	58	67	97	*0.181*	*0.471*
	Males	60.75	14.73	25	51	62	70	95		
	Females	58.55	13.75	26	52	58	66	97		
End-point pixels	***Both***	43.29	5.36	28	40	44	47	58	*0.815*	*0.049*
	Males	44.48	6.04	28	41	45	48	58		
	Females	42.36	4.61	31	39	43	46	51		
Junction pixels	***Both***	231.74	60.51	85	194	226	262	416	*0.052*	*0.751*
	Males	234.45	62.46	85	194	226	276	379		
	Females	229.61	59.42	93	194	225	257	416		
Slab pixels	***Both***	745.8	99.03	431	679	734	816	956	*0.102*	*0.127*
	Males	758.84	96.68	431	703	762	834	908		
	Females	735.55	100.5	461	665	723	809	956		
Average branch length (pixels)	***Both***	10.77	1.01	8.88	10.11	10.65	11.43	13.44	*0.05*	*0.448*
	Males	10.71	1.17	8.88	9.94	10.37	11.6	13.44		
	Females	10.82	0.87	8.98	10.2	10.67	11.28	12.75		

CONTINUATION OF Table 2. Descriptive statistics for the cerebellar digital skeleton quantitative parameters

Parameter	*Sex group*	M	SD	min	Q1	Me	Q3	max	*P (normality)*	*P (sex difference)*
Maximum branch length (pixels)	***Both***	33.17	5.34	22.31	29.46	32.03	35.86	47.46	*0.008*	*0.767*
	Males	33.22	5.33	22.31	29.92	32.76	35.67	45.45		
	Females	33.13	5.4	24.33	29.29	31.94	36.11	47.46		
Triple points	***Both***	45.83	11.12	19	38.75	45	52	77	*0.542*	*0.464*
	Males	46.93	11.43	23	39	47	52	77		
	Females	44.96	10.9	19	37	45	52	72		
Quadruple points	***Both***	11.08	3.71	2	9	11	14	20	*0.115*	*0.876*
	Males	11.05	3.89	2	8	10	15	19		
	Females	11.11	3.6	5	9	11	13	20		

Most of the studied parameters exhibited positive correlations with each other (**Table 3**), except for average and maximum branch length, which showed negative correlations with other parameters but positive correlations with each other. This suggests that cerebella with a greater number of branches have shorter branches compared to less branched cerebella.

Table 3. Correlations of the cerebellar digital skeleton quantitative parameters

Parameter	1	2	3	4	5	6	7	8	9
	Branches	Junctions	End-point pixels	Junction pixels	Slab pixels	Average branch length	Maximum branch length	Triple points	Quadruple points
Branches	-	0.987*	0.634*	0.957*	0.805*	-0.831*	-0.291*	0.910*	0.710*
Junctions	0.987*	-	0.552*	0.938*	0.812*	-0.815*	-0.254*	0.952*	0.672*
End-point pixels	0.634*	0.552*	-	0.558*	0.475*	-0.626*	-0.236*	0.516*	0.395*
Junction pixels	0.957*	0.938*	0.558*	-	0.771*	-0.763*	-0.301*	0.827*	0.736*
Slab pixels	0.805*	0.812*	0.475*	0.771*	-	-0.390*	-0.065	0.780*	0.490*
Average branch length	-0.831*	-0.815*	-0.626*	-0.763*	-0.390*	-	0.391*	-0.765*	-0.641*
Maximum branch length	-0.291*	-0.254*	-0.236*	-0.301*	-0.065	0.391*	-	-0.178	-0.285*
Triple points	0.910*	0.952*	0.516*	0.827*	0.780*	-0.765*	-0.178	-	0.467*
Quadruple points	0.710*	0.672*	0.395*	0.736*	0.490*	-0.641*	-0.285*	0.467*	-

Note: * – $P < 0.05$

The correlation analysis with parameters derived from Euclidean geometry has shown weak to moderate correlations (**Table 4**). Specifically, most of the studied parameters characterizing branching degree (branches, junctions, end-point pixels, junction pixels, slab pixels) demonstrated positive correlations with perimeter and area values, suggesting that an increase in cerebellar vermis size results in an increase in branching degree. Additionally, the gyrification index (indirectly characterizing the number and complexity of gyri) has demonstrated positive correlations with the studied parameters, especially end-point pixels characterizing the number of superficial gyri.

Most of the studied parameters (except for maximum branch length) have shown moderate to strong correlation relationships with the parameters derived from fractal geometry (**Table 5**). The strongest correlations with quantitative parameters of the cerebellar digital skeleton were demonstrated by FD of the overall cerebellar cortex and its layers, FD of the digital skeleton, and cerebellar contour. FD of the overall

cerebellar tissue was less correlated with the studied parameters, and FD of white matter showed no significant correlations. FD is a parameter that characterizes the degree of spatial and structural complexity of the irregular figures. This explains the stronger correlations of the studied parameters with parameters of fractal geometry compared to those derived from Euclidean geometry, which best characterize structures with simple configurations.

Table 4. Correlations of the cerebellar digital skeleton quantitative parameters and Euclidean geometry derived parameters

Parameter	1	2	3	4	5	6	7	8	9
	Branches	**Junctions**	**End-point pixels**	**Junction pixels**	**Slab pixels**	**Average branch length**	**Maximum branch length**	**Triple points**	**Quadruple points**
Perimeter P1	0.383*	0.386*	0.366*	0.327*	0.644*	-0.084	0.030	0.408*	0.128
Area A1	0.338*	0.341*	0.359*	0.294*	0.626*	-0.016	0.087	0.380*	0.105
Perimeter-to-area ratio P1/A1	-0.217*	-0.215*	-0.274*	-0.194	-0.430*	-0.019	-0.079	-0.254*	-0.081
Shape factor SF1	0.002	0.004	0.033	0.024	-0.021	0.008	-0.058	0.024	0.040
Perimeter P2	0.385*	0.344*	0.612*	0.327*	0.495*	-0.238*	-0.054	0.342*	0.153
Area A2	0.355*	0.397*	0.115	0.353*	0.697*	0.048	0.106	0.465*	0.025
Perimeter-to-area ratio P2/A2	0.012	-0.053	0.387*	-0.030	-0.181	-0.211*	-0.103	-0.109	0.092
Shape factor SF2	-0.204*	-0.143	-0.557*	-0.153	-0.146	0.255*	0.110	-0.110	-0.135
Gyrification index P2/P1	0.279*	0.228*	0.558*	0.241*	0.272*	-0.253*	-0.089	0.209*	0.148
Area ratio A2/A1	0.153	0.209*	-0.225*	0.190	0.349*	0.082	0.032	0.259*	-0.064

Note: * – $P < 0.05$

Table 5. Correlations of the cerebellar digital skeleton quantitative parameters and fractal geometry derived parameters

Parameter	1	2	3	4	5	6	7	8	9
	Branches	Junctions	End-point pixels	Junction pixels	Slab pixels	Average branch length	Maximum branch length	Triple points	Quadruple points
FD(overall tissue)	0.448*	0.442*	0.266*	0.438*	0.480*	-0.287*	-0.094	0.414*	0.266*
FD (white matter)	-0.079	-0.066	-0.045	-0.069	-0.059	0.037	-0.010	-0.055	-0.073
FD (overall cortex)	0.642*	0.617*	0.455*	0.608*	0.565*	-0.494*	-0.151	0.572*	0.441*
FD (granular layer of cortex)	0.651*	0.634*	0.384*	0.633*	0.633*	-0.463*	-0.142	0.591*	0.465*
FD (molecular layer of cortex)	0.620*	0.595*	0.435*	0.571*	0.536*	-0.502*	-0.179	0.552*	0.443*
FD (skeleton)	0.801*	0.772*	0.494*	0.775*	0.681*	-0.615*	-0.240*	0.693*	0.563*
FD (contour)	0.553*	0.540*	0.402*	0.488*	0.587*	-0.376*	-0.104	0.518*	0.313*

Note: * – $P < 0.05$

The parameters of the cerebellar skeletons have shown mostly weak correlations with the same parameters determined in the cerebral hemispheres (**Table 6**). Moderate significant correlations were shown by slab pixels and end-point pixels, which characterize the number of gyri in both the cerebellum and cerebrum. It can be assumed that there are common factors leading to the complication of the configuration of both brain regions.

Table 6. Correlations of the cerebellar digital skeleton quantitative parameters with the same parameters determined in cerebral hemispheres

Parameter	1	2	3	4	5	6	7	8	9
Section of cerebral hemispheres	**Branches**	**Junctions**	**End-point pixels**	**Junction pixels**	**Slab pixels**	**Average branch length**	**Maximum branch length**	**Triple points**	**Quadruple points**
Coronal 1	0.236*	0.266*	0.075	0.162	0.350*	-0.144	-0.161	0.083	0.161
Coronal 2	0.249*	0.230*	0.225*	0.185	0.268*	-0.292*	-0.056	0.052	-0.160
Coronal 3	0.228*	0.210*	0.324*	0.129	0.351*	-0.195	0.020	-0.164	-0.052
Coronal 4	0.233*	0.226*	0.201*	0.203*	0.219*	-0.238*	0.103	-0.041	-0.088
Axial	-0.001	-0.006	0.124	-0.017	0.123	-0.075	0.031	0.022	0.061
Average value (all sections)	0.268*	0.239*	0.309*	0.203*	0.345*	-0.276*	0.007	-0.019	-0.030

Note: * – $P < 0.05$

The correlations with age were mostly weak (**Table 7**). The parameters characterizing the branching degree showed slight decreases during aging.

Table 7. Correlations of the cerebellar digital skeleton quantitative parameters and age

Sex group	**Parameter**	**1**	**2**	**3**	**4**	**5**	**6**	**7**	**8**	**9**
		Branches	**Junctions**	**End-point pixels**	**Junction pixels**	**Slab pixels**	**Average branch length**	**Maximum branch length**	**Triple points**	**Quadruple points**
Both	**R**	-0.364*	-0.350*	-0.249*	-0.336*	-0.379*	0.227*	0.035	-0.348*	-0.223*
	Rn(A1)	-0.261*	-0.244*	-0.119	-0.247*	-0.170	0.242*	0.078	-0.227*	-0.198*
Males	**R**	-0.390*	-0.394*	-0.282	-0.348*	-0.449*	0.222	0.000	-0.430*	-0.150
	Rn(A1)	-0.282	-0.294	-0.081	-0.240	-0.207	0.228	-0.013	-0.329*	-0.134
Females	**R**	-0.317*	-0.287*	-0.204	-0.307*	-0.307*	0.210	0.082	-0.277*	-0.248
	Rn(A1)	-0.214	-0.172	-0.132	-0.225	-0.110	0.240	0.160	-0.143	-0.207

Note: * – $P < 0.05$; R – regular correlation coefficient; Rn(A1) – correlation coefficient normalized by area A1

Considering the positive correlations of the studied parameters with the absolute sizes of the cerebellum, we computed correlation coefficients normalized by area A1 (**Table 7**). The normalized correlations were weaker, supporting the suggestion of the area's influence. After normalization, the end-point pixels showed no significant correlations with age. The correlations of the studied parameters with age in males were slightly stronger than in females, but after area normalization, only a few correlations remained significant. Comparing linear regression equations characterizing the age dynamics in males and females, no significant differences were observed ($P > 0.05$).

Discussion

The present study employed quantitative analysis of skeletonized images of the cerebellum – a method commonly used for investigating neurons and the branched processes of glial cells [3, 11, 17]. Considering the tree-like configuration of the cerebellum, this method has proven informative not only at the microscopic but also at the macroscopic level of brain organization. Quantitative analysis of the digital skeleton allows for a quantitative and automated characterization of the structural complexity of tree-like structures: the more gyri the cerebellum has and the higher its branching degree, the higher the degree of structural complexity, resulting in a digital skeleton with more branches, junctions, and endpoints.

A prospective application of the results of the present study is in the diagnosis of malformations and their differentiation from atrophic changes. For this purpose, it is necessary to select a parameter that remains unchanged or changes minimally throughout life. Such a parameter can be considered the number of endpoint pixels (the number of gyri remains constant throughout life). It can be assumed that in atrophic alterations, this parameter will remain unchanged, while in malformations, significant changes in all parameters characterizing the structural complexity of the cerebellum may be observed. The FD values, which also characterize the structural complexity, are often affected by age-related changes of brain [2, 9, 18]. Therefore, the parameters of digital skeletons are more appropriate for this purpose.

Conclusions

Quantitative analysis of skeletonized images is an informative method of investigation for complex tree-like structures and can be applied not only at the microscopic but also at the macroscopic level. This method can be used in clinical practice for diagnosing cerebellar malformations and in theoretical neuromorphological studies to characterize the structural complexity of the cerebellum and other brain structures.

References

1. **Akar, E., S. Kara, H. Akdemir, A. Kırış.** 3D structural complexity analysis of cerebellum in Chiari malformation type I. – *Medical & Biological Engineering & Computing*, **55**(12), 2017, 2169-2182.
2. **Farahibozorg, S., M. Hashemi-Golpayegani, J. Ashburner.** Age- and sex-related variations in the brain white matter fractal dimension throughout adulthood: an MRI study. – *Clinical Neuroradiology*, **25**(1), 2015, 19-32.
3. **Greenblum, A., R. Sznitman, P. Fua, E. Arratia, M. Oren, B. Podbilewicz, J. Sznitman.** Dendritic tree extraction from noisy maximum intensity projection images in C. elegans. – *Biomedical Engineering Online,* **13**, 2014, 74.
4. **Hayakawa, K., Y. Konishi, T. Matsuda, M. Kuriyama, K. Konishi, K. Yamashita, R. Okumura, D. Hamanaka.** Development and aging of brain midline structures: assessment with MR imaging. – *Radiology*, **172**(1), 1989, 171–177.
5. **Jelinek, H. F., E. Fernandez.** Neurons and fractals: how reliable and useful are calculations of fractal dimensions? – *Journal of Neuroscience Methods*, **81**(1-2), 1998, 9-18.
6. **Liu, J. Z., L. D. Zhang, G. H. Yue.** Fractal dimension in human cerebellum measured by magnetic resonance imaging. – *Biophysical Journal*, **85**(6), 2003, 4041-4046.
7. **Maryenko, N. I., O. Y. Stepanenko.** Shape of cerebral hemispheres: structural and spatial complexity. Quantitative analysis of skeletonized MR images. – *Reports of Morphology*, **28**(3), 2022, 62-73.
8. **Maryenko, N., O. Stepanenko.** Characterization of white matter branching in human cerebella: quantitative morphological assessment and fractal analysis of skeletonized MR images. – *Biomedical Research and Therapy*, **8**(5), 2021, 4345-4357.
9. **Maryenko, N. I., O. Y. Stepanenko.** Evaluation of cerebellar aging in MRI images: Fractal analysis compared to Euclidean geometry-based morphometry. – *Meta-Radiology*, **2**(3), 2024, 100101(1-12).
10. **Milosević, N. T., D. Ristanović.** Fractality of dendritic arborization of spinal cord neurons. – *Neurosci. Lett*, **396**(3), 2006, 172-176.
11. **Orlowski, D., C. R. Bjarkam.** A simple reproducible and time saving method of semi-automatic dendrite spine density estimation compared to manual spine counting. – *J. Neurosci. Methods*, 208(2), 2012, 128-133.
12. **Poretti, A., E. Boltshauser, D. Doherty.** Cerebellar hypoplasia: Differential diagnosis and diagnostic approach. – *Am. J. Med. Genet. Part C Semin. Med. Genet*., **166**, 2014, 211-226.
13. **Raz, N., I. J. Torres, W. D. Spencer, K. White, J. D. Acker.** Age-related regional differences in cerebellar vermis observed in vivo. – *Archives of Neurology*, **49**(4), 1992, 412–416.
14. **Schneider, C. A., W. S. Rasband, K. W. Eliceiri.** NIH Image to ImageJ: 25 years of image analysis. – *Nature Methods*, **9**(7), 2012, 671-675.
15. **Serati, M., G. Delvecchio, G. Orsenigo, C. Perlini, M. Barillari, M. Ruggeri, A. C. Altamura, M. Bellani, P. Brambilla.** Potential gender-related aging processes occur earlier and faster in the vermis of patients with bipolar disorder: An MRI study. – *Neuropsychobiology*, 75(1), 2017, 32-38.

16. **Wu, Y. T., K. K. Shyu, C. W. Jao, Z. Y. Wang, B. W. Soong, H. M. Wu, P. S. Wang.** Fractal dimension analysis for quantifying cerebellar morphological change of multiple system atrophy of the cerebellar type (MSA-C). – *NeuroImage*, **49**(1), 2010, 539–551.
17. **Young, K., H. Morrison.** Quantifying microglia morphology from photomicrographs of immunohistochemistry prepared tissue using ImageJ. – *Journal of Visualized Experiments*, **136**, 2018, 5764.
18. **Zhang, L., D. Dean, J. Z. Liu, V. Sahgal, X. Wang, X., G. H. Yue.** Quantifying degeneration of white matter in normal aging using fractal dimension. – *Neurobiology of Aging*, **28**(10), 2007, 1543-1555.

Institute of Experimental Morphology, Pathology and Anthropology with Museum
Bulgarian Anatomical Society

Acta Morphologica et Anthropologica, 31 (3-4)
Sofia ● 2024

Association of Serum Secreted Protein Acidic and Rich in Cysteine (SPARC) Levels with the Severity of Coronary Artery Lesion in Type 2 Diabetic Patients with Coronary Heart Disease among South Indian Population

Divia Paul. Aricatt[1], Pradeep Pereira[2], Ranajit Das[3], Ashwini Prabhu[3], Cleeta Rebeiro[4], Rhema Jacob[2]*

[1] *Department of Anatomy, Fr Muller Medical College, Kankanady, Mangalore, Karnataka*
[2] *Department of Cardiology, Fr Muller Medical College, Kankanady, Mangalore, Karnataka*
[3] *Yenepoya Research Centre, Yenepoya (Deemed to be University), Mangalore, Karnataka*
[4] *Fr Muller Research Centre, Fr Muller Medical College, Kankanady, Mangalore, Karnataka*

*Corresponding author e-mail: drdiviaaricatt@gmail.com, divia_manoj@yahoo.com

Type 2 diabetic patients have high plasma secreted protein acidic and rich in cysteine (SPARC) levels. We aimed to find the association between SPARC levels, type 2 diabetes mellitus (T2DM) and incidence of coronary artery disease with the objectives to investigate SPARC levels with the severity of coronary artery lesion in T2DM patients with and without coronary artery disease (CAD). A single center cross sectional study was conducted with 160 samples. All ethical principles were followed. The patients were categorized in to group A (C), group B (T2DM only), group C (CAD with T2DM), D group (CAD only) for SPARC analysis by Elisa. Gensini score was calculated for coronary stenosis. Patients with liver and kidney dysfunctions were excluded. We found a highly significant difference and association between the serum SPARC level and Gensini score between groups. This study identifies the possibility of SPARC as a new early biomarker for diagnosing CAD in diabetic patients.

Key words: Type 2 Diabetes mellitus; SPARC biomarker; Coronary stenosis; Gensini Score; Biochemical indicators

Introduction

Type 2 diabetes mellitus (T2DM) is on the verge of becoming a pandemic in India [30]. Coronary artery disease (CAD) is a major cause of death and disability among people with T2DM [10, 22]. Statistical predictions denote that by the end of year 2025, 80.9 million people will have diabetes in India, with an evidence of increased

prevalence of CAD among T2DM patients [19, 24]. Secreted protein acidic and rich in cysteine (SPARC), also known as BM-40 and osteonectine, is non-collagenous [21] as well as collagen-binding protein [3]. This molecule plays an important non-structural role in extracellular matrix of bone [5], and has three structural domains with active glycoproteins [17], which were initially reported from bones and named as osteonectine [21].This is an extracellular matrix-related glycoprotein with molecule low molecular weight, which is secreted by heart, brain, kidney, pancreas and skeletal muscle. SPARC in human blood is differentiated mainly from the subcutaneous adipose tissue [23]. Importantly, SPARC protein and gene expression or its serum level changes are during a variety of conditions. Based on its participation in angiogenesis and repair of damaged tissues [1], clinical researches should focus on relationship of SPARC with tumor and wound healing [27].

Recent research has shown that SPARC is involved in the pathophysiological processes of obesity [23], insulin resistance [26] and type 2 diabetes [7, 15]. Newly diagnosed T2DM patients also do possess high plasma SPARC levels [7]. T2DM is an independent risk factor for CAD; hence the close relationship between SPARC, T2DM and its complications suggest that there exists certain relevance between SPARC and the incidence of CAD.

Previous studies have shown that SPARC is highly expressed in T2DM and CAD [10, 30], however, the relationship between SPARC and T2DM combined with CAD has not been reported so far. Quantitative coronary angiography reports investigated by Gensini scoring can explore the quantitative analysis of coronary stenosis. The present study was aimed to investigate the association between serum SPARC levels, T2DM and incidence of CAD with the objectives to assess SPARC levels in T2DM patients with and without CAD and to investigate the correlation of serum SPARC levels with the severity of coronary artery lesion in T2DM patients with coronary heart disease.

Materials and Methods

Study population

A single center cross-sectional study was conducted. All ethical principles for human research were followed and ethical approval was obtained from the Institutional Ethics Committee of the hospital from where the data was collected. The age of the study subjects was given a cut-off at 75 years due to marginal benefits marked during the follow-ups. Hence, a conservative approach is proven to be appropriate for the above-mentioned age, which itself indicates a poor prognosis with an average yearly mortality rate of 33%–35% [2]. The sample size was estimated by consulting a statistician and using the statistical software G* Power 3.0.10. One hundred and sixty subjects were selected for the study by systematic sampling strategy. This consists of 40 healthy controls, 40 patients with T2DM, 40 cases with CAD and diabetes, 40 patients with CAD without diabetes. The above patients were named group A (healthy), group B (T2DM only), group C (T2DM with CAD), D group (CAD only).

The inclusion criteria recruited the participants above 18 years of age and either sex. The patients who report for routine health checkups with no relevant medical history were taken as control group A. Group B (T2DM only) followed WHO

diagnostic criteria of 1999 for diagnosis of diabetes assessment. Diagnosis criteria of CAD were defined according to the stenosis involvement percentages in the involved artery. Exclusion criteria included persons with a previous history of coronary artery bypass graft (CABG), and recanalized normal looking coronary arteries with or without in-stent restenosis coronary arteries as well as patients with severe liver and kidney dysfunction, hyperlipidemia and arthritis. Samples with previous history of myocardial infarction, post-trauma and infection, cancer patients treated with chemo/ radiation therapy were also excluded.

Database Pooling

i. SPARC determination: Fasting blood samples (3mL) were collected from all groups into vacutainers. Samples were held on upright position for 30 min before centrifugation. Samples were centrifuged for 3000 rpm at 25°C for 15 min. After collecting the serum, the SPARC levels *(ug/L)* were quantified using enzyme-linked immunosorbent assay (ELISA), as per manufacturer's instructions. Company: Krishgen Biosystems.

ii. Determination of biochemical indicators: Fasting blood samples (3 mL) were collected from all the study participants for biochemical investigations. Fasting blood sugar (FBS) was assessed for group A participants for confirming their blood glucose levels. HbA1c (to assess about active control of diabetes), lipid profile tests (Insulin resistance and T2DM have been constantly associated with high triglyceride and low HDL-cholesterol levels) and C-peptide release test were performed for participants with highly elevated HbA1c using the standard biochemical procedures and tests (Indicative of uncontrolled diabetes) values in groups B and C.

iii. Quantitative analysis of coronary stenosis by Gensini: The Gensini scoring system used an ordinal ranking based on stenosis severity in 11 coronary segments (score range, 0 to 72)[11]. Non-stenosed arteries were recorded with 0 point. 1% to 25% stenosis was recorded with 1 point. 26%-50% stenosis was recorded with 2 points. 51% to 75% stenosis was recorded with 4 points. Patients with 76% to 90% were recorded with 6 points. 91% to 99% stenosis was recorded as 16 points. 100 percent stenosed arteries were recorded with 32 points. LMCA with CVD were recorded as five points. LAD or LCx proximal segment lesion was recorded with 2.5 points. The middle of the LAD artery lesion was recorded with 1.5 points. The LAD artery distal lesions were recorded with 1 point. Lesions from middle and distal sections of LCx after obtuse marginal branch were recorded with 1 score. RCA lesions were recorded 1 score. Small branch lesions of RCA were recorded with 0.5 score. Total score of coronary artery lesions were the sum of each segment.

Clinical end point definitions

WHO diagnostic criteria of 1999 were used for the diagnosis of diabetes: the symptoms of diabetes combined with plasma glucose≥11.1mmol/L (200mg/dL) at any time, or FPG≥7.0mmol/l (126mg/dL),or OGTT 2h PG≥11.1mmol/L (200mg/dL), and it is necessary to be repeated to confirm with diabetes [6]. Diagnosis criteria of CAD were defined according to the stenosis involvement percentages in the involved artery. A stenosis diameter of 50% or >50% in one or more sites of the coronary artery was regarded as CAD. In this system, we observed three major coronary arteries including the left anterior descending (LAD) with its diagonal (DIAG) branch, left circumflex (LCx) with its obtuse marginal (OM) branch and RCA with its PDA and PLB branches [11].

Statistical analysis of the present study was performed using the GraphPad Prism v9. The participants were named group A (healthy), group B (T2DM only), group C (T2DM with CAD), group D (CAD only). Descriptive statistics was used to summarize the data and results were expressed in mean difference. One way ANOVA, followed by Tukey's multiple comparisons was employed to compare the serum SPARC levels among the different groups. The association between the biochemical indices (HbA1C) and serum SPARC level for Group B and C was statistically assessed using Pearson's correlation. Further, the association between the Gensini score and serum SPARC level for Group C and D was statistically assessed using Pearson's correlation. Multiple linear regression analysis was performed to assess the relevance between SPARC levels and T2DM combined with age and gender. $P<0.05$ was considered statistically significant.

Results

The healthy controls- Group A, T2DM- Type 2 diabetic mellitus- Group B, T2DM with CAD- Type 2 diabetic mellitus with coronary artery disease- Group C, CAD-coronary artery disease- Group D differed significantly among each other in terms of SPARC level (ug/L) (One-way ANOVA, $p<0.05$). While comparing the groups pair-wise, we found a highly significant difference in the serum SPARC levels (ug/L) between the A vs C and D groups (Tukey's multiple comparison, $p<0.0001$), and the B vs C and D groups (Tukey's multiple comparison, $p<0.0001$ and $p=0.003$, respectively). Overall, the highest mean serum SPARC level (ug/L) was observed in C group (x=9.94), followed by D group (x=8.3).The mean SPARC level (ug/L) was found to be discernibly low among B (x=4.90) and A (x=3.14) groups (**Table 1, Fig. 1**).

Table 1. Multiple comparison based on Elisa reports among four group of samples (n=160).

Groups	Group 1 (V1)	Group 2 (V2)	Samples			
			Mean V1	**Mean V2**	**MD**	**p-value**
Healthy Controls	A	T2DM (B)	3.141	4.903	-1.762	0.2579
	A	T2DM with CAD (C)	3.141	9.941	-6.799	<0.0001****
	A	CAD (D)	3.141	8.3	-5.159	<0.0001****
Diabetic	T2DM (B)	T2DM with CAD (C)	4.903	9.941	-5.038	<0.0001****
	T2DM(B)	CAD (D)	4.903	8.3	-3.397	0.0028***
	T2DM with CAD (C)	CAD (D)	9.941	8.3	1.64	0.3195

The results based on SPARC Elisa Kit reports expressed in (ug/L) for each group

Statistical test used: *Post Hoc (Tukeys test), $p<0.01^{****}$indicates highly significant difference, $p<0.05^{***}$indicates significant difference, $p>0.05$ indicates non significant difference between dependant variable and comparison variables.*

Abbreviations: *MD-Mean difference, A- Healthy Controls, B-T2DM – Type 2 diabetic mellitus, C-T2DM with CAD – Type 2 diabetic mellitus with coronary artery disease, D- CAD – coronary artery disease*

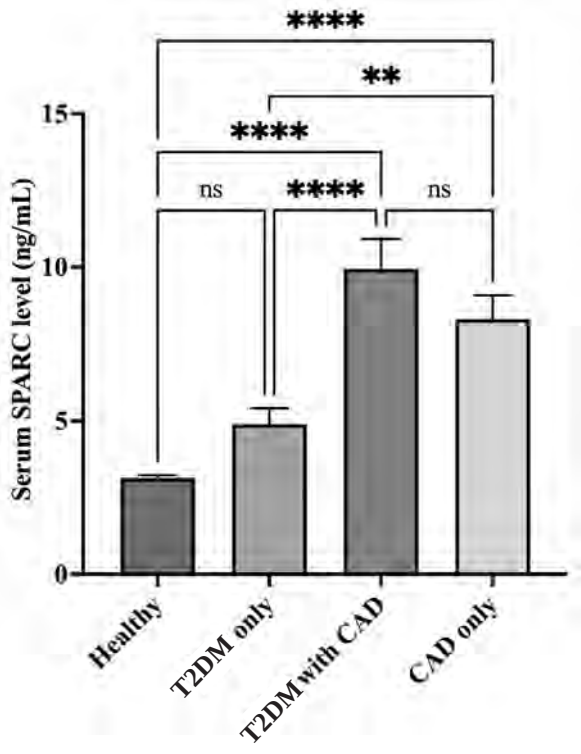

Fig.1 SPARC level in four groups.

We found a significant association between serum SPARC levels (ug/L) and Gensini score for both C (Pearson's correlation, r=0.45, p=0.004) and D (Pearson's correlation, r=0.34, p=0.029) groups (**Table 2**). We also observed a significant correlation between serum SPARC level (ug/L) and HbA1C both in B group (Pearson's correlation, r=0.66, p<0.0001), and C group (Pearson's correlation, r=0.38, p=0.016), the association was found to be discernibly higher in the former (**Table 3, Figs. 2, 3**).

Table 2. Correlation of Elisa reports with Gensini score among group C and D samples (n=80).

	Groups	**Correlation analysis**	
ELISA REPORTS Vs. GENSINI SCORE	T2DM with CAD (C)	r	0.4482
		p-value	0.0037***
	CAD (D)	r	0.344
		p-value	0.0298***

The results based on SPARC Elisa Kit reports expressed in (ug/L) for each group
Statistical test used: *Pearson correlation test. p<0.01**** *indicates highly significant difference, p<0.05*** *indicates significant difference, p>0.05 indicates non significant difference between Elisa and Gensini score among group C and D samples.*
Abbreviations: *C – T2DM with CAD – Type 2 diabetic mellitus with coronary artery disease, D – CAD-coronary artery disease*

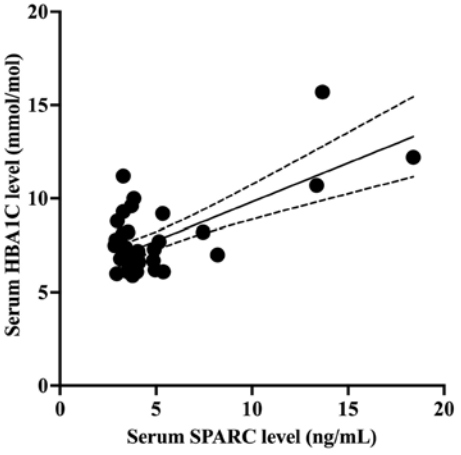

Fig. 2. SPARC levels vs biochemical indices (HbA1C) in T2DM cases.

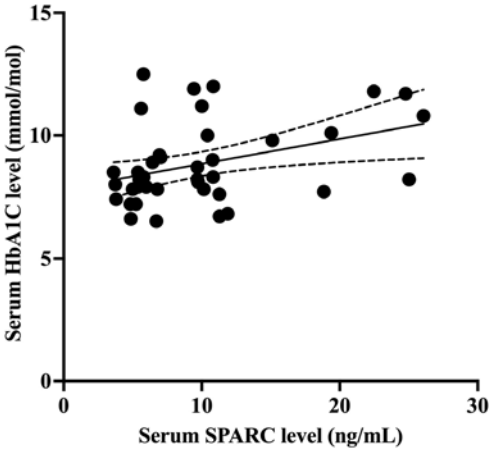

Fig. 3. SPARC levels vs biochemical indices (HbA1C) in T2DM with CAD.

Table 3. Correlation of Elisa reports with HBA1C among group B and C samples (n=80).

	Groups	**Correlation analysis**	
ELISA REPORTS Vs. HBA1C	T2DM (B)	r	0.6603
		p-value	<0.0001****
	T2DM with CAD (C)	r	0.38
		p-value	0.0156***

The results based on SPARC Elisa Kit reports expressed in (ug/L) for each group
*Statistical test used: Pearson correlation test. p<0.01****indicates highly significant difference, p<0.05***indicates significant difference, p>0.05 indicates non significant difference Elisa and HBA1C among group B and C samples*
Abbreviations: B-T2DM- Type 2 diabetic mellitus, C - T2DM with CAD- Type 2 diabetic mellitus with coronary artery disease,

To assess the effect of age and gender on the serum SPARC levels (ug/L), we investigated the association in a multiple linear regression framework. Serum SPARC level (ug/L) was highly elevated among males in the B group (|t|=4.75, p=0.009); but not in C and D groups. Further, older age was found to be significantly associated with higher serum SPARC levels (ug/L) in the B (|t|=7.37, p=0.002) and D (|t|=2.15, p=0.038) groups, but not in the C group. While the length of years being diabetic has significant association with serum SPARC level (ug/L) among patients with C (|t|=2.56, p=0.02), no such association was observed among B group patients (|t|=1.42, p=0.23). Congruent with the correlation analysis, serum HbA1C level was found to be significantly associated with serum SPARC level (ug/L)in both B and C groups (|t|=10.1, p=0.0005, |t|=2.28, p=0.034 respectively). However, as depicted by the correlation analysis, the association was found to be discernibly higher in the former.

Discussion

The healthy controls- Group A, T2DM – Type 2 diabetic mellitus- Group B, T2DM with CAD – Type 2 diabetic mellitus with coronary artery disease- Group C, CAD-coronary artery disease- Group D. Diabetic subjects have higher prevalence as well as increased risk of CAD than the non-diabetic counterparts [19, 24]. Left main coronary artery (LMCA) and its branches were observed as narrower in diabetic patients than in non-diabetics, when the diameters of both were compared using qualitative comparative analysis (QCA). Evidence for the narrowing of lumen diameter of coronary arteries in patients with diabetics and several factors affecting the lumen diameters have been studied previously in different countries on different populations [1, 6-7, 15-16]. The improved awareness and enhanced treatment options can control the cardiovascular risk factors in participants with known diabetes [4].

SPARC is involved in insulin resistance by activating PI3K/AKT pathway, which is the major insulin transduction pathway. SPARC and inflammatory factors during CAD causes severe vascular stress reactions. SPARC can lead to changes in the structure of extracellular matrix by affecting the deposition of fibronectin and laminin [18], can regulate cell migration, and has anti-cell adhesive effect. Studies have shown that SPARC is closely related to inflammatory response factors and adipose factors [13]. In the present study, we observed significant association between serum SPARC levels and HbA1C both in group Band group C, the association was found to be discernibly higher in the former.

The possible mechanism of SPARC is the occurrence and development of insulin resistance. Related research has shown that SPARC can inhibit the proliferation and differentiation of VEGF, PDGF and FGF stimulated fibroblasts, smooth muscle cells and endothelial cells to impede the vascular repair process. This phenomenon can damage the blood vessel barrier to induce atherosclerosis as time advances, and promotes the deposition of smooth muscle cells in the intima to a rapid progression of vascular endothelial atherosclerosis [25]. In our study, while the length of years being diabetic had significant association with serum SPARC levels among patients with group C, no such association was observed among group B patients. We could relate that adiponectin can relieve the inflammation of endothelial cells, protect vascular endothelial and increase insulin sensitivity. When oxidative stress occurs, SPARC secretion increases in the body. SPARC is positively correlated with adiponectin and leptin, which can activate the tyrosine kinase (JAK) signaling system, which are the relative factors to be involved in the formation of atherosclerosis [12].

SPARC damages the vascular barrier and thus participates in the formation of coronary atherosclerosis [14, 28]; thus SPARC levels can be use as predictor of coronary atherosclerosis. In the present study, the mean SPARC level was found to be discernibly low among group A and was increased in group B. The highest mean serum SPARC level was observed in group C followed by group D and group B. Increased SPARC in obese and T2DM subjects suggested that SPARC may play a role in pathogenesis of both obesity and diabetes [31].SPARC can cause fatty fibrosis, increase excessive lipids in circulation by re-locating it from liver, pancreas, blood vessels and other non-adipose tissues [25]. This process causes increased levels of triglycerides in the circulating blood, thereby leading to the development of insulin resistance and is gender specific.

Authors have reported that inhibition of adipose tissue build-up along with the increased consumption of dietary lipids contributes majorly to systemic hyperlipidemia and influx of triglycerides to the vital organs, ultimately leading to insulin resistance [20]. The discovery of a potential novel function for SPARC in the control of insulin secretion relevant to the onset of Type 2 diabetes is described by Harries et al. [8]. By reducing the expression of RGS4, SPARC was able to control insulin secretion, demonstrating that SPARC was important for both G-protein signaling in beta cells as well as insulin secretion physiology [9]. Since inflammatory cytokine itself can cause atherosclerosis, SPARC can promote the occurrence of CAD through this synergistic effect. We could relate these findings to the present study as the association in a multiple linear regression framework with effect of age and gender on the serum SPARC level, the male gender is highly significantly associated with higher serum SPARC level in the group B patients but not in the group C and D patients.

Different "jeopardy scores" were developed to quantitate plaque burden, to predict patient-based clinical outcomes and to identify the risk factors for the presence of atherosclerosis and its progression. Serum SPARC level is elevated in T2DM patients with coronary heart disease, which can be correlated with the severity of coronary artery disease significantly[29].The Gensini scoring system used an ordinal ranking based on stenosis severity in 11 coronary segments (score range, 0 to 72) [11]. In our study, we found significant association between serum SPARC level and Gensini score for participants from both groups C and D. The scoring indices were higher in group C patients compared to group D. Thus, we can correlate that the SPARC values and Gensini scores were interrelated and has higher predictive value.

Conclusion

SPARC levels can be used as predictor of coronary atherosclerosis. It is hypothesized that if we can reduce SPARC content during the onset of T2DM, risk of` CAD could be delayed. This study identifies the possibility of SPARC as a new early biomarker for diagnosing CAD in diabetic patients. This study may enable better life in patients diagnosed with diabetes and to deliver improved outcomes for diabetic patients when combined with clinical diagnostics.

Acknowledgements: All authors appreciate the great effort of Dr. Ranajit Das, Yenepoya Research Centre, Mangalore, Karnataka, India for analysing and verifying the data of this study. We acknowledge Father Muller Medical College, Kakanady, Mangalore, India for the Institutional Grant (Grant Number: FMRC/FMMC/ST/04/2021) towards the smooth execution of the study.

Ethical Approval

All ethical principles for human research were followed and ethical approval was obtained from the Institutional ethics committee of the hospital from where the data was collected [FMMC/FMIEC/l46/2022]. We have obtained informed consents from sample population involved in this study.

References

1. **Adil, M., M. Nadeem, M. Hafizullah, H. Jan.** Comparison of left coronary artery diameter among diabetics and non-diabetics. – *J. Postgrad. Med. Inst*., **26**(4), 2012, 369-376
2. **Azad, N., G. Lemay.** Management of chronic heart failure in the older population. – *JGC*., **11**(4), 2014,329.
3. **Bradshaw, A. D.** The role of secreted protein acidic and rich in cysteine (SPARC) in cardiac repair and fibrosis: Does expression of SPARC by macrophages influence outcomes? – *J. Mol. Cell. Cardiol.,* **93,** 2016,156-161.
4. **Brown, T. M., R. M. Tanner, A. P. Carson, H. Yun, R. S. Rosenson, et al.** Awareness, treatment, and control of LDL cholesterol are lower among US adults with undiagnosed diabetes versus diagnosed diabetes. – *Diabetes Care*, **36**(9), 2013, 2734-2740.
5. **Chlenski, A., L. J. Guerrero, H. R. Salwen, Q. Yang, Y. Tian, et al.** Secreted protein acidic and rich in cysteine is a matrix scavenger chaperone. – *PloS one*, **6**(9), 2011, e23880.
6. **Gabir, M. M., R. L. Hanson, D. Dabelea, G. I. Imperatore, J. A. Roumain, et al.** Plasma glucose and prediction of microvascular disease and mortality: evaluation of 1997 American Diabetes Association and 1999 World Health Organization criteria for diagnosis of diabetes. – *Diabetes care*, **23**(8), 2000, 1113-1118.
7. **Gui, M. H., G. Y. Qin, G. Ning, J. Hong, X. Y. Li, et al.** The comparison of coronary angiographic profiles between diabetic and nondiabetic patients with coronary artery disease in a Chinese population. – *Diabetes Res. Clin. Pract.*, **85**(2), 2009,213-219.
8. **Harries, L. W., L. J. McCulloch, J. E. Holley, T. J. Rawling, H. J. Welters, et al.** A role for SPARC in the moderation of human insulin secretion. – *PloS one*, **8**(6), 2013, e68253.
9. **Hu, L., F. He, M. Huang, Q. Zhao, L. Cheng, et al**. SPARC promotes insulin secretion through down-regulation of RGS4 protein in pancreatic β cells. – *Sci. Rep.*, **10**(1), 2020, 17581.
10. International Diabetes Federation. *IDF Diabetes Atlas,* 7th Edition, Brussels, Belgium, International Diabetes Federation, 2015.
11. **Mann, D. L., D. P. Zipes, P. Libby, R. O. Bonow.** *Braunwald's Heart Disease: A Textbook of Cardiovascular Medicine*, Part 1, vol. 10 (Ed. E. Braunwald), Elsevier Health Sciences, 2017, 392-428.
12. **Kang, Y. J., A. K. Stevenson, P. M. Yau, R. Kollmar.** Sparc protein is required for normal growth of zebrafish otoliths. – *ARO.*, ***9,*** 2008, 436-451.
13. **Kos, K., S. Wong, B. Tan, A. Gummesson, M. Jernas, et al.** Regulation of the fibrosis and angiogenesis promoter SPARC/osteonectin in human adipose tissue by weight change, leptin, insulin, and glucose. – *Diabetes*, **58**(8), 2009, 1780-1788.
14. **Matsuzawa, Y., T. Funahashi, S. Kihara, I. Shimomura.** Adiponectin and metabolic syndrome. – *ATVB.*, **24**(1), 2004, 29-33.
15. **Melidonis, A., V. Dimopoulos, E. Lempidakis, J. Hatzissavas, G. Kouvaras, et. al.** Angiographic study of coronary artery disease in diabetic patients in comparison with nondiabetic patients. – *Angiology*, **50**(12), 1999, 997-1006.

16. **Mosseri, M., M. Nahir, Y. Rozenman, C. Lotan, D. Admon, et al.** Diffuse narrowing of coronary arteries in diabetic patients: the earliest phase of coronary artery disease. – *Cardiol.*, **89**(2), 1998, 103-110.
17. **Motamed, K**. SPARC (osteonectin/BM-40). – *Int. J. Biochem. Cell. Biol.*, **31**(12), 1999, 1363-1366.
18. **Nie, J., E. H. Sage.** SPARC inhibits adipogenesis by its enhancement of β-catenin signaling. – *JBC.*, **284**(2), 2009, 1279-1290.
19. **Reddy, K. S., S. Yusuf.** Emerging epidemic of cardiovascular disease in developing countries. – *Circ.*, **97**(6), 1998, 596-601.
20. **Riboulet-Chavey, A., A. Pierron, I. Durand, J. Murdaca, J. Giudicelli, et al.** Methylglyoxal impairs the insulin signaling pathways independently of the formation of intracellular reactive oxygen species. – *Diabetes*, **55**(5), 2006, 1289-1299.
21. **Rosset, E. M., A.D. Bradshaw.** SPARC/osteonectin in mineralized tissue. – *Matrix Biol.*, ***52***, 2016, 78-87.
22. **Sarwar, N., P. Gao, S. R. Kondapally Seshasai, R. Gobin, S. Kaptoge, et al.** Diabetes mellitus, fasting blood glucose concentration, and risk of vascular disease: a collaborative meta-analysis of 102 prospective studies. – *The Lancet*, **375**(9733), 2010, 2215-2222.
23. **Schwartz, L., K. E. Kip, E. Alderman, J. Lu.** BARI 2D Study Group. Baseline coronary angiographic findings in the bypass angioplasty revascularization investigation 2 Diabetes trial (BARI 2D). – *Am. J. Cardiol.*, **103**(5),2009, 632-638.
24. **Sicree, R.** Diabetes and impaired glucose tolerance. *Diabetes atlas*, **15,** 2006, 109.
25. **Song, H., Y. Guan, L. Zhang, K. Li, C. Dong.** SPARC interacts with AMPK and regulates GLUT4 expression. – *Biochem. Biophys. Res. Commun.,* **396**(4), 2010, 961-966.
26. **Standring, S., N. R. Borley, P. Collins, A. R. Crossman, M. A. Gatzoulis, J. C. Healy.** Gray's Anatomy. 40th*ed. Spain: Churchill Livingstone Elsevier*, **487**, 2008,725-726
27. **Stein, B., W. S. Weintraub, S. S. Gebhart, C. L. Cohen-Bernstein, R. Grosswald, et.al.** Influence of diabetes mellitus on early and late outcome after percutaneous transluminal coronary angioplasty. – *Circulation*, **91**(4), 1995, 979-989.
28. **Valsamakis, G., R. Chetty, P. G. McTernan, N. M. Al-Daghri, A. H. Barnett, et.al**. Fasting serum adiponectin concentration is reduced in Indo-Asian subjects and is related to HDL cholesterol. – *DOM.*, **5**(2), 2003, 131-135.
29. **Wang, Z., H. Y. Song, M. M. An, L. L. Zhu.** Association of serum SPARC level with severity of coronary artery lesion in type 2 diabetic patients with coronary heart disease. – *IJCEM.*, **8**(10), 2015, 19290.
30. **Wild, S., G. Roglic, A. Green, R. Sicree, H. King.** Global prevalence of diabetes: estimates for the year 2000 and projections for 2030. – *Diabetes care*, **27**(5), 2004, 1047-1053.
31. **Wu, D., L. Li, M. Yang, H. Liu, G. Yang.** Elevated plasma levels of SPARC in patients with newly diagnosed type 2 diabetes mellitus. – *Eur. J. Endocrinol.,* **165**(4), 2011, 597-601.

Institute of Experimental Morphology, Pathology and Anthropology with Museum
Bulgarian Anatomical Society

Acta Morphologica et Anthropologica, 31 (3-4)
Sofia ● 2024

Dermatoglyphic features – potential predictors in patients with schizophrenia

Ferihan Ahmed-Popova[1], Zdravka Harizanova[1]*

[1] *Department of Anatomy, Histology and Embryology, Faculty of Medicine, Medical University – Plovdiv, Plovdiv, Bulgaria*

*Corresponding author email: ferihan.popova@mu-plovdiv.bg

A valuable approach to the neurodevelopmental etiology of mental disorders is the assessment of dermatoglyphic patterns in patients with schizophrenia. This study aimed to determine the predictor dermatoglyphic features of independent contribution to the membership status "schizophrenia patient – control subject". The study included 141 patients with schizophrenia and 120 mentally healthy subjects of Bulgarian origin. Fingerprints were obtained using an ink method and were read in accordance with the methods given by Cummins, Midlo. The data were analyzed with SPSS 28.0 using logistic regression. Differences between the patients and control groups were statistically significant for five dermatoglyphic features in males and two in females that made significant contribution to the prediction of the patient-control status in the regression model. The logistics model defines a set of dermatoglyphic features that distinguishes patients with schizophrenia from healthy controls and contributes to the validation of dermatoglyphics as biological markers in schizophrenia development.

Key words: dermatoglyphics, schizophrenia, logistic regression, neurodevelopment, predictor models

Introduction

Over the last years a tendency of using biological markers in mental disorders has been observed, focusing on early prenatal brain damage and caused by the influence of a certain static agent [12, 20]. An important approach to the neurodevelopmental etiology of mental disorders is the assessment of dermatoglyphic patterns in patients with schizophrenia [7, 8, 19].

Dermatoglyphics are individual characteristics with several features, such as stability, personality, regeneration capacity and hereditary determination. Their biological and clinical value is associated with the common ectodermal origin of the brain and dermal patterns and the strictly defined periods of embryonic formation of

papillary ridges (III – IV month of gestation) [21, 23]. In this sense ridge patterns might become reliable biomarkers for neurodevelopmental disorders, which is assumed in the neurodevelopmental hypothesis of mental disorders.

The aim of this study was to determine the predictor dermatoglyphic features of independent contribution to the membership status "schizophrenia patient – control subject".

Material and methods

Subjects

The study included 141 patients with schizophrenia (76 males, 65 females), consecutively admitted to the Clinic of Psychiatry in Plovdiv and the District Psychiatry Dispensary in Plovdiv with mean age 32.09 years (SD = 9.73). All patients satisfied DSM-IV criteria for diagnosis of schizophrenia on the basis of case records review, a semi-structured interview based on a checklist of items from DSM-IV (performed by psychiatrists of the Department of Psychiatry and Medical Psychology at the Clinic of Psychiatry, Medical University – Plovdiv, Bulgaria) and information obtained from relatives to enhance the validity of the diagnosis. Potential subjects were excluded if they had any signs of mental retardation, a history of drug or alcohol abuse, an identifiable neurological disorder (seizure disorder, head injury, multiple sclerosis, etc.) or a general medical condition with direct effects on the central nervous system [2].

Exclusion criteria: a history of drug or alcohol abuse; an identifiable neurological disorder (seizure disorder, head injury, multiple sclerosis etc.); intellectual disability or a somatic disorder with neurological components; pathological conditions, associated with variation of dermatoglyphic patterns, e.g., psoriasis, congenital abnormalities, etc.

The normal comparison group comprised 120 mentally healthy subjects (54 males, 66 females) with a mean age of 39.65 years (SD =10.68), volunteers with socioeconomic background comparable to that of the patients. Normality was defined as the absence of a major axis I or axis II disorder according to DSM-IV based on a semi-structured interview performed by the authors with the collaboration of psychiatrists of the Department of Psychiatry and Medical Psychology at the Clinic of Psychiatry, Medical University – Plovdiv, Bulgaria [2]. The mean age of the control group was greater than that of the patient group to minimize the cumulative risk of developing future major psychiatric disorder. Normal controls satisfied exclusion criteria similar to those applied to patients. In addition, to distinguish better the control from the patient group potential controls were excluded if they had a first-degree relative with a history of a psychotic disorder, major affective disorder or suicide.

All patients and control subjects were of Bulgarian origin to avoid the potential confounding effects of racial and ethnic variations.

The study was approved by the local Ethics Committee at the St. George University Hospital. All subjects gave written informed consent to participate.

Experimental procedure

A set of dermatoglyphic patterns with low racial instability and high diagnostic value was examined [10]. Fingerprints and palmprints were obtained using an ink method and were read with light (6D) magnification in accordance with the methods

given by Cummins, Midlo [5]. Fingerprinting was carried out in a passive manner, using a rotary cone sample divider method. For greater reliability the scoring of the palmprints was done separately by two persons according to the rules in Memorandum on dermatoglyphic nomenclature [18].

Data analysis

Thirty – five dermatoglyphic patterns were analyzed, including ridge counts of the fingers of the right and left hands, total finger ridge count for the right and left hands, arches, ulnar and radial loops, whorls for the right and left hands, a-b, b-c, c-d and total ridge counts for the right and left hands, white lines on the right and left palms.

The data were analyzed with SPSS 28.0 using logistic regression. All statistical analyses were performed separately for males and females in view of the available evidence for significant gender differences in ectodermal derivatives [1]. The level of statistical significance was set at $P < 0.05$. Dermatoglyphic patterns were included in a logistic regression procedure using a forward stepwise selection algorithm. Through the stepwise (Forward Stepwise Selection) logistic approach, the characteristic with the most significant contribution in predicting the status of "schizophrenic patients - control subject" was first determined. When determining the contribution of each of the characteristics, its interrelationship with the analyzed previous characteristics was considered. In the presence of significant intercorrelation between certain traits, they were excluded to create the best final logistic regression model. In order to determine the reliability of the obtained regression models, the indicators Cox & Snell R Square and Nagelkerke R Square, as well as the Hosmer and Lemeshow test were applied. As a rule, the Cox & Snell R Square indicator shows in what percentage the variation of the dependent variable (in the present study, the belonging of individuals to a certain group) can be explained by the logistic model. Higher values of this indicator also reflect greater reliability of the regression model.

The Nagelkerke R Square modification ranges from 0 to 1 and is a more reliable indicator than the Cox & Snell R Square. As a rule, it is always higher than the Cox & Snell index. The Nagelkerke index determines in percentage the correlation between the predictors and the prediction. An alternative to the presented indicators is the Hosmer and Lemeshow test. The essence of this model is the division of the studied objects into 10 groups and the comparison of the actual number of objects belonging to each of these groups with the predicted number of objects belonging to the groups obtained by the regression model. The probability level P was calculated based on chi-square with 8 degrees of freedom to test the reliability of a logistic model. If the Hosmer and Lemeshow test statistic shows a score greater than 0.05, it is impossible to reject the null hypothesis that there is no difference between the observed and model-predicted values. This means that the model estimates match the actual observed data to an acceptable level. Well-overlapping models indicate a lack of significance in the Hosmer and Lemeshow test. This desired result of no statistical significance indicates that the predicted pattern is not significantly different from the observed pattern.

Results

The logistic regression model successfully distinguished between the two groups as 81.0% of the cases were correctly classified in males and 81.7% in females (**Table 1**).

Table 1. Classification table – percent schizophrenic patients correctly classified by the one-step logistic model in males and females.

	Predicted group affiliation		Correctly classified
Observed	**Controls**	**Schizophrenia**	**%**
Males			
Controls	29	12	**70.7%**
Schizophrenia	8	56	**87.5%**
Totally			**81.0%**
Females			
Controls	46	10	**82.1%**
Schizophrenia	9	39	**81.3%**
Totally			**81.7%**

Forward stepwise logistic regression analysis was applied in order to establish the predictor dermatoglyphic variables, which contributed independently to the prediction of the status "schizophrenia patients - control subjects" (**Table 2**). Totally 76.2% of the male and 60.6% of the female subjects were correctly classified by the analysis in predicted group affiliation.

Table 2. Classification table – percent schizophrenic patients correctly classified by the Forward Stepwise Selection model in males and females.

	Predicted group affiliation		Correctly classified
Observed	**Controls**	**Schizophrenia**	**%**
Males			
Controls	26	15	**63.4%**
Schizophrenia	10	54	**84.4%**
Totally			**76.2%**
Females			
Controls	42	14	**75.0%**
Schizophrenia	27	21	**43.8%**
Totally			**60.6%**

Cox & Snell and Nagelkerke indicators were taken into account in order to determine the reliability of the regression model (**Table 3**).

Table 3. Cox & Snell and Nagelkerke indicators summarizing the one-step logistic regression model for the predilection of the "schizophrenia – controls" status in males and females.

Model Summary

	Step	-2 Log likelihood	Cox & Snell R Square	Nagelkerke R Square
Males	1	81.269	0.431	0.584
Females	1	87.701	0.416	0.555

Hosmer and Lemeshow's test, with greater sensitivity in determining the reliability of the logistic model, showed a lack of statistical significance, which determined the regression analysis as sufficiently reliable to determine the group affiliation of males and females to the status of "patients with schizophrenia - controls" (**Table 4**).

Table 4. Hosmer and Lemeshow test of reliability of the one-step regression model in patients with schizophrenia and controls in males and females.

Hosmer and Lemeshow Test

	Step	χ^2	df	Sig.
Males	1	8.264	8	0.408
Females	1	3.045	8	0.931

The variables – dermatoglyphic features with statistically significant independent contribution to the prediction of the status "schizophrenia patients – control subjects" in males were disassociated white lines of the left hand, ulnar loops of the left hand and loops of the right hand, total a-b ridge count and the ridge count of L2 (**Table 5**).

Table 5. Logistic regression analysis (Forward Stepwise Selection) with independent variables dermatoglyphic features and dependent variable the status "schizophrenic patient – control subject" in males.

Step - entering the model variable	B	Wald	P	χ^2	Sig.	Correctly Classified %
Entering the model						
Constant	5.673	8.618	0.003			
1. Disassociated white lines on the left hand	-1.830	8.086	0.004	9.904	0.002	**61.0%**
2. Ulnar loops on the left hand	-0.759	9.143	0.002	15.824	0.000	**66.7%**
3. Loops on the right hand	0.787	8.542	0.003	20.914	0.000	**71.4%**
4. Total a-b ridge count	-0.058	6.649	0.010	26.417	0.000	**76.2%**
5. Ridge count of L2	0.090	4.135	0.042	30.843	0.000	**76.2%**

In females the dermatoglyphic features with statistically significant independent contribution to the prediction of the status "schizophrenia patients – control subjects" were: ulnar loops on the left hand and severe corrugations of white lines on the right hand (**Table 6**).

Table 6. Logistic regression analysis (Forward Stepwise Selection) with independent variables dermatoglyphic features and dependent variable the status "schizophrenic patient – control subject" in females.

Step – entering the model variable	B	Wald	P	χ^2	Sig.	Correctly classified %
Entering the model						
Constant	0.120	0.042	0.837			
1. Ulnar loops on the left hand	-0.301	3.772	0.052	14.268	0.003	**60.6%**
2. Severe corrugations of white lines on the right hand	2.503	8.398	0.015	10.310	0.006	**61.5%**

Discussion

The results of the present study in schizophrenia allow the identification of a set of dermatoglyphic features that could reveal early dysontogenic events associated with the subsequent development of the disease. Differences between the patients and control groups were statistically significant for five dermatoglyphic features in males and two in females (out of a total of 35 dermatoglyphic patterns examined) that made significant contribution to the prediction of the patient-control status in the regression model. These were disassociated white lines on the left hand, ulnar loops on the left hand, loops on the right hand, total a-b ridge count and ridge count of L2 in males, and ulnar loops on the left hand and severe corrugations of white lines on the right hand in females. The results that we obtained confirm similar studies of dermatoglyphic features and could be explained as follows [19]. On the one hand the change in the frequency of specific dermatoglyphic patterns or the deviation from the mean values of quantitative dermatoglyphic characteristics of individuals reveal disturbances in normal morphogenesis, even though they do not represent anomalies by themselves [17]. The individuality of papillary images, their unchanged structure after birth and the common ectodermal origin with the nervous system draw attention to genetic and epigenetic events occurring during the embryonic period, which can be considered biological markers of dysontogenesis affecting the development of dermatoglyphics [9]. This defines the period 6.5 to 16-18 gestational weeks as the most critical period in the development of dermatoglyphics and the nervous system and determines the research of causal relationships of dysontogenetic events in this period. Certain dermatoglyphic patterns in patients with schizophrenia could serve as chronomarkers for determining the duration of action of exogenous factors damaging ectodermal derivatives. In this sense, the processes of formation and differentiation of papillary images are of great

importance and depend on the size and shape of the dermal pads and some gender differences [4, 11, 14, 22].

Another significant point that could explain the obtained results is the pronounced sexual dimorphism in most of the dermatoglyphic traits. In general, male patients have more statistically significant features in ridge patterns than female patients. Regarding the disease, earlier onset of schizophrenia symptoms has been found in men, followed by a more severe course of the disease, while in women there is more favorable outcome of the disease, presented by milder course and better response to therapy [3, 6]. Given the multifactorial etiology in the development of schizophrenia, it is clear that males are more vulnerable and more sensitive to endogenous and exogenous influences than females, which explains the greater abnormal dermatoglyphic findings in males with schizophrenia [15, 16, 22]. This is probably due to the protective effect of neurohumoral regulatory mechanisms in females, as well as individual anatomical characteristics and differences between the genders. For example, the later onset of schizophrenia in females compared to males is probably due to the protective effect of estrogen. Gender differences successfully define the male sex as more susceptible to abnormalities in the development of ectodermal derivatives. This is well illustrated by the predictor patterns in male and female patients. In this sense, the stepwise logistic regression model identified a larger set of traits that successfully distinguished patients from controls better in males than in females [13, 22, 24].

Conclusions

As a whole, established by us the logistic regression model defines a set of dermatoglyphic features (five in males and two in females from the examined patterns) that distinguishes sufficiently well patients with schizophrenia from mentally healthy individuals and thereby contributes to the validation of dermatoglyphics as biological markers in the development of schizophrenia.

Acknowledgments: The research was possible due to the cooperation of the Department of Psychiatry and Medical Psychology at the Faculty of Medicine of Medical University – Plovdiv, Bulgaria.

References

1. Akabaliev, V. H., S. T. Sivkov. Sexual dimorphism in minor physical anomalies in schizophrenic patients and normal controls. – *Compr. Psychiatry,* **44**(4), 2003, 341-348.

2. American Psychiatric Association. *Diagnostic and statistical manual of mental disorders*, 4th Edition, Washington, DC, APA, 1994.

3. Canuso, C. M., G. Pandina. Gender and schizophrenia. – *Psychopharmacol. Bull.*, **40**(4), 2007, 178-190.

4.Chakraborty, R. Statistical interpretation of DNA typing data. – *Am. J. Hum. Genet.,* **49**, 1991, 895-897.

5.Cummins, H., C. Midlo. *Fingerprints, palms and soles.* – New York, Dover Publications, 1961.

6. Eranti, S. V., J. H. Maccabe, H. Bundy, R. M. Murray. Gender difference in age at onset of schizophrenia: a meta-analysis. – *Psychol. Med.*, **43**(1), 2012, 155-167.
7. Fatemi, S. H., T. D. Folsom. The neurodevelopmental hypothesis of schizophrenia, revisited. – *Schizophr. Bull*. **35**(3), 2009, 528-548.
8. Fatjó-Vilas, M., D. Gourion, S. Campanera, F. Mouaffak, M. Levy-Rueff, M. E. Navarro, et al. New evidence of gene and environment interactions affecting prenatal neurodevelopment in schizophrenia spectrum disorders: A family dermatoglyphic study. – *Schizophr. Res.,* **103**(1-3), 2008, 209-217.
9. Guardiola-Ripoll, M., A. Sotero-Moreno, B. Chaumette, O. Kebir, N. Hostalet, C. Almodóvar-Payá, M. Moreira, M. Giralt-López, M. Odile-Krebs, M. Fatjó-Vilas. Genetic and neurodevelopmental markers in schizophrenia-spectrum disorders: analysis of the 2 combined role of the cannabinoid receptor 1 gene (CNR1) and dermatoglyphics. – *Biomedicine*, **12**(10), 2024, 2270
10. Hit, G., N. Dolinova. *Racial differentiation of humanity (Dermatoglyphic data)*, Moscow: Science, 1990, 3-200. [in Russian].
11. Jamison, C. Dermatoglyphics and the geschwind hypothesis I: Theoretical background and palmar results of dyslexia II. Digital results of dyslexia and developmental implications. In: *Trends in Dermatoglyphic Research* (Eds. N. Durham, C. Plato), Kluwer Academic Press, Dordrecht, Netherlands, 1990, 99–135.
12. Majeed, N. S., B. Arko-Boham, D. K. Fiagbe, K. K. Adutwum-Ofosu, N. K. K. Koney, B. A. Hottor, R. M. Blay, M. Abdul-Rahman, J. Ahenkorah. Digital-palmar dermatoglyphics characteristics of patients living with schizophrenia in Ghana. – *All Life*, **16**(1), 2023, 2224937.
13. Mantarkov, M., P. Nonchev, D. Stoyanov. Sexual dimorphism and the correlation structure of the somatotype of mentally healthy persons. – *Psychiatr. Clin. Psychopharmacol*., **4**, 2013 [in Russian].
14. Mavalwala, J., P. Mavalwala, S. M. Kamali. Issues of sampling and of methodologies in dermatoglyphics. – *Birth Defects Orig. Artic. Ser.,* **27**, 1991, 291-303.
15. Miller, B. J., N. Culpepper, M. H. Rapaport, P. Buckley. Prenatal inflammation and neurodevelopment in schizophrenia: A review of human studies, *Prog. Neuro-psychopharmacol. Biol. Psychiatry*, **42**, 2013, 92-100.
16. Moore, S. J., B. L. Munger. The early ontogeny of the afferent nerves and papillary ridges in human digital glabrous skin. – *Dev. Brain Res.,* **48**, 1989, 119-141.
17. Oxundjonovich, D. A. Dermatoglyphics or skin pictures. – *IJIMM*, **2**(6), 2024, 393-396.
18. Penrose, L. Memorandum on dermatoglyphic nomenclature, *Birth Defects Orig. Artic. Ser.,* **4**(3), 1968, 1-12.
19. Salvador, R., M. Á. Ángeles García-León, I. Feria-Raposo, C. Botillo-Martín, C. Martín-Lorenzo, C. Corte-Souto, T. Aguilar-Valero, et al. Fingerprints as predictors of schizophrenia: A deep learning study. – *Schizophr. Bull.*, **49**(3), 2023, 738-745.
20. Sanches, M., M. S. Keshavan, P. Brambilla, J. C. Soares. Neurodevelopmental basis of bipolar disorder: A critical appraisal. – *Psychiatry*, **32**, 2008, 1617-1627.
21. Tornjova-Randelova, S., D. Paskova-Topalova, Y. Yordanov. *Dermatoglyphics in anthropology and medicine,* Sofia, Professor Marin Drinov Academic Publishing House, 2011, [in Bulgarian].
22. Umraniya, Y. N., H. H. Modi, H. K. Prajapati. Sexual dimorphism in dermatoglyphic pattern study. – *Medical Science,* **1**(1), 2013, 24-26.
23. Wertheim, K. Embryology and morphology of friction ridge skin, In: *Fingerprint Sourcebook* (Eds. E. K. Holder, L. O. Robinson, J. H. Laub), National Institute of Justice, 2011, 3-26.
24. Zaichenko, A. A., E. A. Lebedeva. Biometric predictors of constitutional risks for developing paranoid schizophrenia in men. – *Saratov J. Med. Sci. Res.,* **5**(3), 2009, 384-389.

Institute of Experimental Morphology, Pathology and Anthropology with Museum
Bulgarian Anatomical Society

Acta Morphologica et Anthropologica, 31 (3-4)
Sofia ● 2024

Unusual Burial and Violent Death of a Woman in the Beniamin Burial Ground, Armenia

(1st century BC – 3rd century AD, Shirak Province)

Anahit Yu. Khudaverdyan

Institute of Archaeology and Ethnography, National Academy of Science, Republic of Armenia, Yerevan, Armenia

*Corresponding author e-mail: ankhudaverdyan@gmail.com

The article is dedicated to the blessed memory of archaeologist Hamazasp Khachatryan

An individual whose skeleton was exhumed from the grave No. 2 of Beniamin Burial Ground exhibited healed trauma of the right midface, damage to the left parietal and temporal bones and on the left clavicle. The position of the bones in the burial suggests that the body was carried to the burial site in a sack. Such position is found rarely in burial rituals, but most often is characteristic for bodies, deposited in different circumstances, most often after a violent death, interpreted as criminal homicide, sacrifices, executions et cett. Her cause of death is likely severe trauma to the occipital bone.

Key words: Armenia, Beniamin, 1st century BC – 3rd century AD, violent trauma, hird occipital condyle, Kimmerle anomaly

Introduction

The Armenian Plateau was, in early history, a crossroad linking the worlds of East and West. Armenia has been rich and independent, particularly under the dynasties of the Ervandids, the Artashesians, the Arshakunis (since the third century BC to the fourth century AD) [38, 3, 58, 71: XI, V, 8]. The Armenian Plateau has been an area of frequent military conflicts, and its history was largely determined by external forces [3, 58]. Many nomad tribes and peoples pouring in from different parts of Eurasia brought considerable changes in the ethnic composition of the Armenian Plateau population, which was reflected in further cultural and ethnic processes in this area [58, 3]. The period 1st century BC – 3rd century AD characterizes by the interaction of various ethno-cultural groups – Iranic nomads (Scythians, Sarmatians, Sauromatians, Saka) and locals. Their presence in this region perhaps goes back to the 8th century

BC [58]. It is generally accepted that in the 7th century BC the Scythians mounted their incursions into the Ancient Near East through the Caucasus [58]. A statistical analysis of measurements of crania from the 1st century BC − 3rd century AD from the cemeteries at Armenia indicates considerable morphological heterogeneity [39].

Here we report the pattern of injuries in a skeleton from Beniamin, a cemetery dated in the 1st century BC − 3rd century AD. The ancient cemetery is located in the Akhuryanovsky district, near the village of Beniamin (**Fig. 1**). It is located in the Shirak region, 12 km from the regional centre of Gyumri. Excavations of burials from the 1st century BC – 3rd century AD show a great variety of burial types (1990-2005). The most common type of burial is a cist, made of stone slabs, but there are also burils in jug, pithoi and earth pits. Children and young women were more likely got buried in jars and pithoi [39, 82]. The orientation of the burials is quite stable: most of the burials are with the head facing north-east. The position of the buried is either on the back, right or left side. The analysis of the burial inventory of the Beniamin cemetery shows that most of them are ordinary burials of the residents of the settlement [82]. Archaeological rescue excavations in Beniamin at burial No. 2 were conducted on 19 July 2022. Several traumatic events have left their mark on the bones of the buried individual.

Fig. 1. Map of Armenia showing the location of Beniamin

We will evaluate the hypothesis – are the injuries related to violence (intentional injuries) or are they the result of a fall (unintentional injuries). Distinguishing between accidental and intentional injuries in individual cases is problematic in skeletal remains. A 2004 study of Judd showed that skeletal remains from the ancient city of Kerma showed fracture distribution patterns that differed drastically from the clinical cases of injury distributions in two modern samples, where falls were the primary mechanism of injury [30]. Accidental trauma includes injuries that occur as a result of an accident (dizziness, bad feeling, etc.) and often reflects the hazards of everyday life and the daily interactions between people and their physical environment [48, 45, 63].

Materials and Methods

During the excavations (1990-2005) led by Felix Ter-Martirosov (Institute of Archaeology and Ethnography, National Academy of Sciences, Republic of Armenia), Hamazasp Khachatryan and Larisa Eganyan (Shirak Regional Museum, Gyumri, Republic of Armenia) and Anahit Khudaverdyan (Institute of Archaeology and Ethnography, National Academy of Sciences, Republic of Armenia), a total of 235 burials were found in the Beniamin cemetery. We obtained a collection of 112 (65 female, 46 male) adult skulls (one subject sex undetermined) and 67 child skulls.

The article analyzes the bone remains of an individual from burial # 2 from excavations 2022. The excavations were carried out by the archaeologists Hamazasp Khachatryan and Levon Agikyan.

The individual (Burial 2/2022) was buried in a stone cist (dimensions 1.10×1.30m) oriented on an east-west axis (**Fig. 2**). Most of the postcranial skeleton (except a few cervical vertebrae) is in anatomical position. **Figure 2** shows strong flexion in the knee and hip joints, the thoracic cage, pelvis and limbs in anatomical position, with clear articulation in the limb joints, spine and thoracic cage. The position of bones could present a body carried in a sack to the place of deposition. Such position is found rarely in burial rituals with use of shroud, but most often is characteristic for bodies, deposited in different circumstances, most often after a violent death, interpreted as criminal homicide, sacrifices, executions et cett. Only the skull is in disarticulated position. However, there are no signs of decapitation on the skull or cervical vertebrae (C1-C5). The disarticulation of the lower jaw could be explained by a posthumous disturbance in the grave, or it could have occurred after the decomposition of the soft tissues in a stone case. Such a burial is first found in ancient Armenia and in particular in the Beniamin cemetery.

Fig. 2. Picture of the burial discussed in the text (photographs of Armen Shakparonyan)

The skeleton was analyzed in details, assessing preservation and completeness of bone material, as well as assessing age-at-death and sex of the individual. Morphological features of the pelvis and cranium were used for the sex identification [59, 9]. A combination of pubic symphysis [26, 32, 55], auricular

surface changes [50], degree of epiphyseal union [9], and cranial suture closure [55] were used for adult age-at-death estimation.

All bones were examined macroscopically and X-rayed for evidence of traumatic lesions. The location of fractures was described and measured. The scoring protocol followed the descriptive terms outlined in Lovell [48]. Ante mortem trauma was distinguished from perimortem trauma by the appearance of new bone deposits, resulting in callus formation or beveled edges [5]. Such evidence of healing is absent in both perimortem and postmortem fractures. A reliable distinction between perimortem trauma and postmortem damage is crucial, as the former may allow conclusions to be drawn about the circumstances of death. The term perimortem is used to describe all injuries to wet/fresh bone when the bone still contains its organic components, although somatic death may have occurred [73]. In contrast, post-mortem damage occurs when the bone has lost most of its organic elements and fractures occur on a dry bone. It implies the involvement of taphonomic factors such as geological, biological or (un)intentional human alteration [23, 73, 13, 12].

Several papers mention the hat brim line (HBL) rule as the most useful criterion for distinguishing falls from blows [69, 22, 28, 18]. Nowadays, the HBL is defined as the area above the Frankfurt horizontal plane, which is located between the line passing through the glabella (G-line) and the line passing through the centre of the external auditory meatus (EAM-line) [40] (**Fig. 3**). According to this rule, an injury at the level of the brim of a hat is more likely to be the result of a fall, whereas a blow would generally cause an injury above this line.

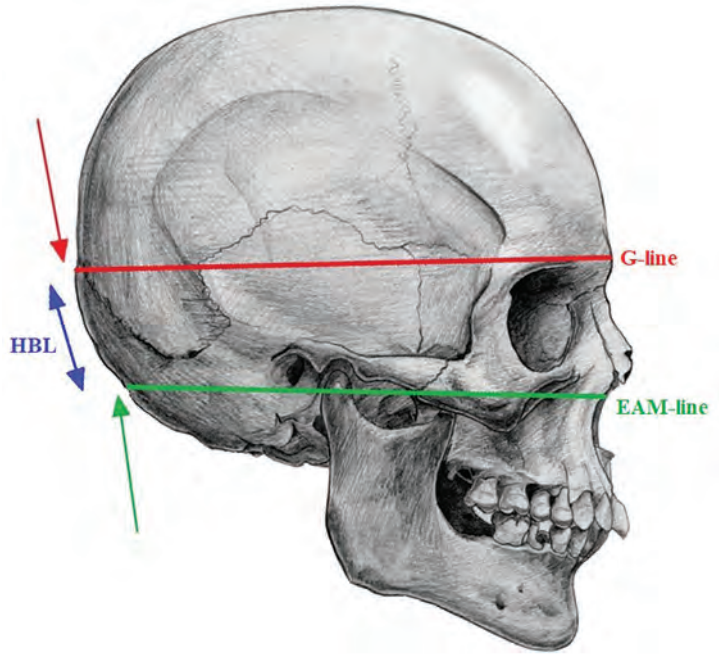

Fig. 3. The hat brim line (HBL), area located between the G-line (the superior margin) and EAM-line (the inferior margin)

Careful observation of the traumatic lesions, registered on the skull from grave # 2/2022 (with 4× or 10× magnification) was applied for assessing the degree of healing.

In assessing the anthropological features the inferior aspect of the basiocciput was examined for the presence of a precondylar tubercle. This consisted of bony elevations ranging from ridges near the anterior end of the occipital condyles to larger median or paramedian projections along the anterior margin of the foramen magnum. Their location, size, shape and presence of facets were noted.

Foramen transversarium is the special foramen located on the left and right transverse processes of the cervical vertebrae (C1 to C7) containing the vertebral vessels and sympathetic plexus. Variations of foramen transversarium could be associated with compression of vertebral vessels, resulting in blood flow disturbances, especially vertebrobasilar insufficiency [33, 44, 75], or it could modify the blood flow, due to a strong link between the diameter of the foramen transversarium and the blood flow of the vertebral artery [42, 27]. The variations in number and size of foramina transversaria of cervical spine may be one of the causes for complaints like headache, migraine, and fainting attacks and are due to the compression of the vertebral artery [81]. All cervical vertebrae were examined macroscopically for the existence of the double foramen transversarium on both sides.

The diagnostic criteria used for assessing characteristics of degenerative joint disease include marginal and surface osteophytes, porosity, and eburnation [65, 79, 21].

X-ray (Portable Digital X-ray Radiography System) was used at the Institute of Archaeology and Ethnography of NAS RA to assess the condition of the skeleton. This was done to provide detailed characterisation of the fracture edges. X-ray analysis allowed for high-resolution observation and analysis of antemortem and perimortem injuries.

Results

Individual identification

Skeletal material from burial No. 2 is well preserved allowing morphological determinations of age and sex (**Fig. 4**). Based on the obliteration of the coronal suture, the attrition of the masticatory surface of the tooth crowns, the changes in the auricular surface and the early degenerative-dystrophic changes in the articular surface, we can conclude that the biological age of the buried was 30 to 39 years. The results of the analysis indicate that this individual is likely female.

Trauma lesions

There is a defect, which we can interpret as an antemortem fracture on the maxilla, that extends to the lower edge of the right eye socket (length fracture of 23.2 mm) (**Fig. 5**). This type of fracture is characterized by a dissociation of the maxilla, the nasal bones, and the nasal septum from the cranial skull and from the lateral midface. The fracture line extends from the nasofrontal suture via the fronto-maxillary suture through the lacrimal bone to the floor of the orbit. From there, it extends through the infraorbital margin via the facial wall of the maxillary sinus to the zygomatico-alveolar crest.

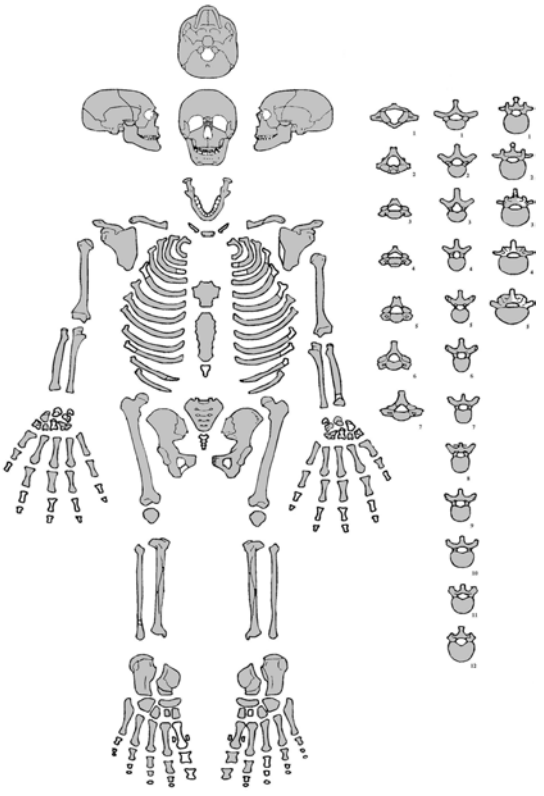

Fig. 4. Completeness of the human skeleton of Beniamin (grey colour – skeletal elements present, white – absent)

Fig. 5. Fracture of the midfacial.

Changes within the nasal are observed. In the studied individual registeres enlarged bulla ethmoidalis, enlarged pneumatised middle turbinate were the cause of violation of ventilation and drainage of paranasal sinuses and as a result - recurrence of sinusitis. Pneumatization of the middle turbinate is associated with a significant nasal septum deviation (**Fig. 6**).

Fig. 6. Bulla ethmoidalis and nasal septum deviation

The individual had a healed fracture in the region of the parieto-temporal bones, left side (dimensions 50mm×43.7mm), which originated from a massive depression fracture (**Fig. 7**). The zygomatic process of the temporal bone is fractured, and no signs of healing are observed in the zygomatic arch. In this case, both the compression trauma to the temporo-parietal region and the zygomatic fracture occurred in two different accidents.

Fig. 7. Fracture of the frontal, temporal and parietal bones

During the analysis, we noted more defects of injuries on the skull. Inspection of the fractures suggests peri-mortem injuries of the frontal bone between glabella and right superciliary arch (length crack of 64.5 mm), and occipital squamma (length crack of 104 mm) (**Figs. 2, 8**). The injuries appear perimortem and may have contributed to the death of the individual or occurred shortly after death while the bone was still retaining its organic component.

Fig. 8. Perimortem injuries frontal and occipital bones

The left clavicle displays a simple, well-healed, oblique fracture at its medial third (**Fig. 9**) and was notably shorter (120mm) than the unaffected right clavicle (132 mm). Due to a misaligned healed fracture the left clavicle is shorter and wider. The clavicle was fractured at the middle, and the medial part overlaps the lateral part. No signs of infection were observed.

Fig. 9. Fracture of the left clavicle.

Blunt force trauma was evident on the femur in the region of the right condyle (**Fig. 10**). There is a concave depression approximately 32 mm long and 12.5 mm wide, there appears to have been some healing of the area as the edges are slightly smooth rather than sharp.

Fig. 10. Fracture of the right condyle.

Anatomical features and variation

Anomalies found around the foramen magnum may be of clinical significance as it is closely associated with vascular and nervous structures. Beniamin's skull had a complete prebasioccipital arch. Position of this arch may be related to traumatic medullary lesions of the occipito-vertebral region. The prebasioccipital arch was conical in shape, measuring approximately 12 mm in length and 20.5 mm in width (**Fig. 11**). It was located at the anterior margin of the foramen magnum in the midline. The prebasioccipital arch did not project into the foramen magnum. Both occipital condyles were directed anteromedially and were constricted in the middle with a maximum length of 33 mm (right) and 27 mm (left).

Fig. 11. Skull showing tubercles at the anterior margin of foramen magnum

We will also mention some non-metric traits that have clinical symptoms and may be relevant to the topic of this article. The arcuate foramen is a potentially clinically/surgically significant anatomical variant of the atlas, leading to symptomatic entrapment. Additional compression of the vertebral artery by a lateral ponticle could very likely lead to stenosis of the vertebral artery [75]. We report a variant of unilateral left arteriae vertebral canal in atlas, connecting posterior part of superior articular process to the posterior arch of atlas (**Fig. 12**).

Fig. 12. Foramen arcuale of atlas

Out of 7 cervical vertebrae, only 2 vertebrae (C5, C6) showed the accessory foramina (**Fig. 13**). The transverse accessory foramina were smaller than the regular foramina in all cases. Under such circumstances, the course of the vertebral artery may be distorted. The variations in the number and size of the foramina transversaria of the cervical spine may be one of the causes of complaints such as headaches, migraines and fainting spells. They are due to compression of the vertebral artery [11].

Fig. 13. Accessory foramen transversarium on both sides of C5, C6 vertebrae

Discussion

The distinction between accidental falls and violence is an important one in bioarchaeology. One of the first authors to attempt to differentiate between falls and blows on the basis of skull lesions was Richter in 1905 [62]. In 1921, Kratter's researches showed falls can cause injuries to the vertex area and cranial vault when the fall was from a great height or if there was an impact with an obstacle during the fall [40, 41, 25]. In 1931, Walcher developed the HBL (hat brim line) rule, which states that fall-related injuries are not above the HBL if certain conditions are met (standing position of the person before the fall, flat floor without inclines or stairs, falling from one's own height, and absence of intermediate obstacles), but the rule does not apply to young children [25]. E. Ehrlich and H. Maxeiner [20, 53], C. Kremer and A. Sauvageau [40, 41] and P. Guyomarc'h et al. [28] carried out studies to distinguish between falls and blows in blunt head trauma. The study confirmed that injuries caused by blows are often located above the occipital bone, that a laceration within the occipital bone is more likely to be caused by a fall (66.7%), and that a skull fracture within the occipital bone is equally common in both aetiologies. Henriques et al. [18] find more fractures related to falls than to blows above this HBL. The focus of this study is the skeleton of Individual 2, which differs from the rest of the Beniamin sample in that it shows evidence of multiple injuries with significant sequelae. According to the definition of the "hat brim line" (HBL) representing an area defined by anthropometric landmarks, the G-line (glabella-line) and the EAM-line (external auditory meatus-horizontal line), previously provided by Kremer at al. [40], the present study revealed 2 injuries within the HBL. This is for wounds within the HBL that are associated with falls. In addition, a study [40, 41] showed that the majority of skull fractures caused by blows were on the left side, whereas the right side was predominant for fall fractures. In the case of the woman from tomb 2 (lower and upper edges of the right orbit, **Fig. 5**), can we say that an accident seems most likely? Injuries to the maxillofacial region are a serious problem because of its anatomical importance, i.e. the location of important organs and the fact that the digestive and respiratory systems originate from this area. Due to anatomical proximity together with maxillofacial injuries, damage to the central nervous system can occur and injuries to this region can result in serious dysfunction. The most common site of maxillary fracture was the Le Forte [24]. In some studies the sex ratio was 9:1, but in others it was 2:1. Males are more susceptible to trauma [24, 29, 6]. The most common age group involved was 21-30 years (37.66%), followed by 31-40 years (19.36%) [4, 1].

An enlarged nasal turbinate is also known as a concha bullosa [70]. Prevalence was found to vary between studies depending on definitions used (e.g. 44% in Stallman et al. [70], 68% in Smith et al. [68]). It is usually asymptomatic. However, it can sometimes cause problems if it is too large [14]. Some studies have found that enlarged turbinates are associated with deviated septum [70], but not with sinus disease [70, 68]. In the present study the Bulla ethmoidalis is found to coexist with a fracture. It is likely that the inflammation has penetrated through the orbit and/or through periodontal inflammatory lesions. These are usually associated with abnormal air flow and impaired patency of the openings of sinuses into the middle nasal passage, because the hypertrophy of the middle turbinate obstructs the ethmoidal infundibulum and leads to recurrent sinusitis.

Side lateralization of the fracture is another useful criterion for differentiation, as the injury in the Beniamin case is on the left side. Individual had a healed fracture on the region of the temporal and parietal bones that originated in a massive depression fracture (**Fig. 7**). When one falls on the side, the shoulders hit the surface first, followed by the parietal eminences. The problem, however, is to establish if the victim simply fell or was hit. In fact, most cranial injuries due to interpersonal violence are found on the left side, indicating an attack by a right-handed adversary [45]; it should be remembered that 90% of humans are right-handed [10]. Considering the violent history of the 1st century BC − 3rd century AD in the region [3, 39] and its hinterland, the osteological indicators of intentional violence in the cemetery of Beniamin [39] correlates well with this rule. As noted, during the Classical/Late Antiquity period, various ethno-cultural groups - Iranian nomads (Scythians, Sarmatians, Sauromatians, Saka) and indigenous people - interacted on the Armenian plateau. And, their interactions have not always been peaceful. The Beniamin sample (1990-2005) exhibits a relatively high frequency of craniofacial trauma (32.7 %). Males from Beniamin exhibit higher frequencies of craniofacial injuries compared to females. This, might be a result of division of labour and activities according to sex, where more difficult and hazardous activities are performed by males, as well as a cultural behaviour that associates virility with aggressiveness. Several authors [80, 2, 72, 31] point out that high frequencies of head and face trauma are conclusive proof of intentional violence. However, these areas are often vulnerable not only to violence. They are also prone to traumatic injuries from falls and accidents. Klotzbuecher et al. [37] found that if an individual sustains one fracture than they are at a greater risk of acquiring another. Although a previous maxillary fracture predisposes the investigated individual from Beniamin to double the likelihood of another fracture, we are inclined to believe that the injury was caused by violence.

We considered frontal and occipital linear fractures to be perimortem when there was no evidence of healing and the fracture characteristics were typical of fresh bone [54, 77]. Frontal and occipital linear fractures are usually caused by impacts, falls and accidents.

Clavicular fractures are usually the result of a direct blow to the shoulder [16, 57, 64], but a fall should not be ruled out either. The fracture to the left clavicle would have caused pain at the site of injury and may have been associated with bruising and swelling [36]. Complications with clavicular fractures are rare, but may occasionally include brachial plexus injury, resulting in peripheral neuropathy, or injury to the subclavian vessels, lung or pleura [36, 56, 60]. The clavicle would have taken between six to ten weeks to heal and during this time, the left arm may have been immobilizsed to reduce movement and aid healing [19, 35, 46, 64]. Following the initial healing process, it may have taken a further six to eight weeks to regain strength in the affected left upper limb and to return to pre-injury activity levels. A modern clinical study found that strength was regained 12–24 weeks after the initial injury [46]. Extensive lamellar remodelling in the left clavicle of Beniamin indicates that the fracture occurred some years before death and they are of accidental origin. Indeed, falling is believed to be one of the most frequent causes of clavicular fractures [48, 49].

Injuries to the distal femoral epiphysis are not common. Femur fracture is consistent with high-impact trauma [76]. A distal femur fracture can also be caused by a low-impact event, such as a fall from a standing position [51]. However, violence against this woman is the most likely scenario, given the burial of the deceased (**Fig. 2**).

In this paper we found some non-metric traits associated with skeletal anomalies. Non-metric traits are anomalies in the normal anatomy of the skeleton. For example, Kiel [34] considered the caroticoclinoid foramen to be a developmental anomaly of the embryonic chondrocranium, and Scheuer & Black [67] agreed with Kiel's proposal. Lang & Hetterich [43] suggested that the pterygospinous foramen is formed as a developmental anomaly similar to the caroticoclinoid foramen, rather than as a result of secondary ossification of the pterygospinous ligament.

An accessory foramen (foramen arcuale) of the atlas is formed from the vertebral artery groove. Foramen arcuale is a potential clinically significant anatomical variant of the atlas; leads to symptomatic entrapment, additional compression of the vertebral artery by a lateral ponticle could very likely result in stenosis of the vertebral artery [75]. Foramen arcuale is associated with Barre-Lieou syndrome, which represents symptoms of headache, retro-orbital pain, vasomotor disturbance of the face and recurrent disturbances of vision, swallowing and phonation due to alteration of blood flow within the vertebral arteries and an associated disturbance of periarterial disturbance of periarterial nerve plexus [47]. A head, clavicular or femoral epiphysis may have been injured when an individual with these symptoms fells to the ground.

A cervical vertebra can be distinguished from other vertebrae by the presence of a foramen transversarium in the transverse processes [66]. The foramen transversarium is a result of the special formation of the cervical transverse processes. It is formed by the vestigial costal element fused to the body and the true transverse process of the vertebra. The foramina transversaria, present on the transverse process of cervical vertebrae, are known to transmit the vertebral artery, vertebral veins and sympathetic nerves [15]. These foramina are known to exhibit variations with respect to the shape, size and sometimes are multiple or absent. Their etiology may be related to variations of the course of vertebral artery and is developmental [15]. An accessory transverse foramen, smaller and posterior to the primary foramen, may be found in the sixth vertebra, and less frequently in the adjacent vertebrae [7]. Under such circumstances, the course of the vertebral artery may be distorted. The variations in number and size of foramina transversaria of cervical spine may be one of the causes for complaints like headache, migraine, and fainting attacks and are due to the compression of vertebral artery [11]. However, the cervical vertebrae (C1-C5) do not show any pathological changes, such as proliferative porous bone accumulation, bone erosion, changes in the shape and dimensions of the lateral foramina, which occur in cases of advanced vascular pathologies in this area. The injuries found on an individual's skeleton could not be the result of a repetitive falls on hard surfaces with serious consequences. The individual had a complete prebasioccipital arch. Prebasioccipital arch also known as hypocondylar arch is a bony, bulging complete arch at the front rim of the occipital foramen magnum. Hyperostotic traits are believed to be as age- progressive changes and more frequently on left side and hypostatic traits are age-regressive changes [8]. The cranial bone variations could be due to the genetic variation or adaptation to environment including postnatal stress factors [17]. These enlarged paramedian bony masses ventral to the foramen may form a pseudojoint with the apical segment of the odontoid process or anterior arch of the atlas, thereby affecting the kinetic anatomy and integrity of the atlantooccipital articulation. Presence of this arch may lead to limitation in the range of motion of the CVJ [78].

Conclusion

Injury recurrence is a major topic of research in paleopathology and bioarchaeology, and studying trauma circumstances that combine antemortem healed, or perimortem elements provides a compelling assessment of the live experience of individuals suffering multiple traumatic events [52, 61]. The causes of maxillofacial injuries vary widely from one part of the world to another because of various factors including social, cultural, geographical and environmental factors [74]. A female from Beniamin accumulated multiple injuries in at least three incidents. There were no overlapping wounds, so it was not possible to establish a specific order of injury. The surviving trauma to the midface and left temporal region would have left the individual with visible scars and an unpleasant appearance with a crooked nose and uneven left profile. This could lead to social rejection in ancient society. Described hypothetical symptomatic, after anatomical variation in the cervical and basilar regions, could also be assessed negativlly in past societies as laziness and low socialization, which could also lead to rejection and aggression to the individual, who doesn't fit to the social model. The injuries found on an individual's skeleton could not be the result of a fall. Her cause of death is likely severe trauma to the occipital bone. The position of the bones in the burial suggests that the body was carried to the burial site in a sack. Such position is found rarely in burial rituals, but most often is characteristic for bodies, deposited in different circumstances, most often after a violent death, interpreted as criminal homicide, sacrifices, executions et cett.

Acknowledgements: I would like to thank Armen Shakparonyan of the Museum of Regional Studies in Gyumri for photographing the burial.

References

1. Adeyemo, W. L., A. L. Ladeinde, M. O. Ogunlewe, O. James. Trends and characteristics of oral and maxillofacial injuries in Nigeria: A review of the literature. – *Head Face Med*, **1**, 2005, 7.

2. Alvrus, A. Fracture patterns among the Nubians of Semna South, Sudanese Nubia. – *International Journal of Osteoarchaeology*, **9**, 1999, 417-429.

3. Arakelyan, V. N. *Outline of the history of ancient Armenian art, 6st century BC – 3rd century AD.* Yerevan, National Academy of Science of Armenia, 1976, 124 p.

4. Ahmed, H. E., M. A. Jaber, Abu, S. H. Fanas, M. Karas. The pattern of maxillofacial fractures in Sharjah, United Arab Emirates: A review of 230 cases. – *Oral Surg. Oral Med. Oral Pathol. Oral Radiol. Endod.,* **98**, 2004, 166-170.

5. Aufderheide, A. C., C. Rodriguez-Martin. *The Cambridge encyclopedia of human paleopathology*. Cambridge, Cambridge University Press, 1998, 496 p.

6. Back, C. P., N. R. McLean, P. J. Anderson, D. J. David. The conservative management of facial fractures: Indications and outcomes. – *J. Plast. Reconstr. Aesthet. Surg.*, **60**, 2007, 146-151.

7. Bergman, R. A., S. A. Thompson, A. K. Afifi, F. A. Saadeh. *Compendium of human anatomic variation*. Germany, Urban and Schwarzenberg, 1988, 197 p.

8. Berry, A. C. Factors affecting the incidence of non-metrical skeletal variants. – *Journal of Anatomy*, **120**, 1975, 519-535.

9. Buikstra, J., D. Ubelaker. *Standards for the data collection from human skeletal remains*. Fayette, Arkansas, Arkansas Archaeological Survey Research Series, 1994, 272 p.
10. Calvin, W. H. Did throwing stones shape hominid brain evolution? – *Ethology and Sociobiology,* **3**, 1982, 115-124.
11. Caovilla, H. H., M. M. Gananca, M. S. Munhoz, M. L. Silva, F. F. Gananca, M. L. Silva, M. S. Munhoz, M. M. Gananca, H. H. Caovilla. *Sindrome cervical, Quadros Clinicos Otoneurologicos Mais Comuns*. Sao Paulo, Atheneu, 2000, 252 p. [in Portuguese]
12. Cappella, A., A. Amadasi, E. Castoldi, D. Mazarelli, D. Gaudio, C. Cattaneo. The difcult task of assessing perimortem and postmortem fractures on the skeleton: a blind text on 210 fractures of known origin. – *J. Forensic. Sci.,* **59**, 2014, 1598–1601.
13. Christensen, A. M., N. V. Passalacqua, E. J. Bartelink. *Forensic anthropology: current methods and practice*. Oxford, Academic Press, 2014, 464p.
14. Cohen, S. D., B. L. Matthews. Large concha bullosa mucupyocele replacing the anterior ethmoid sinuses and contiguous with the frontal sinus. - *Annals of Otology, Rhinology and Laryngology*, **117**, 2008, 15-17.
15. Das, S., R. Suri, V. Kapur. Double foramen transversaria: An osteological study with clinical implications. – *Internal Medicine Journal*, **12**, 2005, 311-313.
16. Hamblen, D. L., A. H. R. W. Simpson. *Adam's outline of fractures including joint injuries* (twelfth edition). London, Churchill Livingstone Elsevier, 2007, 340 p.
17. Hanihara, T., H. Ishida. Frequency variations of discrete cranial traits in major human populations. III. Hyperostotic variations. – *Journal of Anatomy*, **199**, 2001, 251-272.
18. Henriques, M., B. Saliba-Serre, L. Martrille, A. Blum, K. Chaumoître, P. Donato, N. Campos, E. Cunha, P. Adalian. Discrimination between falls and blows from the localization and the number of fractures on computed tomography scans of the skull and the trunk. – *Forensic Sciences Research*, **8**, 2023, 30–40.
19. Hill, J. M., M. H. McGuire, L. Crosby. Closed treatment of displaced middle-third fractures of the clavicle gives poor results. – *Journal of Bone and Joint Surgery,* **79-B**, 1997, 537-539.
20. Ehrlich, E., H. Maxeiner. External injury marks (wounds) on the head in different types of blunt trauma in an autopsy series. – *Med. Law*, **21**, 2002, 77-782.
21. Faccia, K. J., R. C. Williams. Schmorl's nodes: clinical significance and implications for the bioarchaeological record. – *International Journal of Osteoarchaeology*, **18**, 2008, 28-44.
22. Galloway, A. The circumstances of blunt force trauma. – In: *Broken bones – anthropological analysis of blunt force trauma* (Ed. A. Galloway), Springfield, IL, Charles C. Thomas, 1999, 224-254.
23. Galloway, A., L. Zephro, V. L. Wedel. Diagnostic criteria for the determination of timing and fracture mechanism. In: *Broken bones: Anthropological analysis of blunt force trauma* (Eds. V. L. Wedel, A. Galloway). Springfeld, Charles C Thomas, 2014, 47-58**.**
24. Gassner, R., T. Tuli, O. Hächl, A. Rudisch, H. **Ulmer.** Cranio-maxillofacial trauma: A 10 year review of 9,543 cases with 21,067 injuries. – *J. Craniomaxillofac. Surg.*, **31**, 2003, 51-61.
25. Geserick, G., K. Krocker, I. Wirth. Walcher's hat brim line rule – a literature review. – *Arch. Kriminol.*, **234**, 2014, 73-90.
26. Gilbert, B. M., T. W. Mckern. A method for aging the female os pubis. – *American Journal of Physical Anthropology*, **38**, 1973, 31-38.
27. Guerra, M. M., P. R. Fuentes, I. Roa. Anatomical variations of the foramen transversarium in cervical vertebrae. – *Int. J. Morphol.*, **35**, 2017, 719-722.
28. Guyomarc'h, P., M. Campagna-Vaillancourt, C. Kremer et al. Discrimination of falls and blows in blunt head trauma: a multicriteria approach. – *J. Forensic Sci.*, **55**, 2010, 423-427.

29. Gupta, R., S. Suryanarayan, A. Sharma, V. Pandya, S. Sathaye. Traumatic mandibular fractures: Pendulum towards closed reduction. – *The World Articles in Ear, Nose and Throat,* **3**, 2010, 1-3.
30. Judd, M. A. Trauma in the city of Kerma: ancient versus modern injury patterns. – *International Journal of Osteoarchaeology*, **14**, 2004, 34-51.
31. Jurmain, R. *Stories from the skeleton: a behavioural reconstruction of human osteology.* Amsterdam, Gordon and Breach Science Publishers, 1999, 344 p.
32. Katz, D., J. M. Suchey. Age determination of the male os pubis. – *American Journal of Physical Anthropology*, **69**, 1986, 427-435.
33. Kaya, S., N. D. Yilmaz, S. Pusat, C. Kural, A. Kirik, Y. Izci. Double foramen transversarium variation in ancient Byzantine cervical vertebrae: Preliminary report of an anthropological study. – *Turk. Neurosurg.,* **21(4)**, 2011, 534-538.
34. Kiel, E. L. Embryology of the normal optic canal and its anomalies: an anatomic and roentgenographic study. – *Investigative Radiology*, **1**, 1966, 346-362.
35. Kihlström, C., Möller, M., Lönn, K., Wolf, O. Clavicle fractures: epidemiology, classification and treatment of 2422 fractures in the Swedish Fracture Register; an observational study. – *BMC Musculoskeletal Disorders,* **18 (1)**, 2017, 82.
36. Khan, L. A. K., T. J. Bradnock, C. Scott, C. M. Robinson. Fractures of the clavicle. – *Journal of Bone and Joint Surgery*, **91**, 2009, 447-460.
37. Klotzbuecher, C., P. D. Ross, P. B. Landsman, T. A. Abbott 3rd, M. Berger. Patients with prior fractures have an increased risk of future fractures: A summary of the literature and statistical synthesis. – *Journal of Bone and Mineral Research*, **15(4),** 2000, 721-739.
38. Khorenatsy, M. *History of Armenia*. Moscow, Gattsuk, 1893, 230 p.
39. Khudaverdyan, A. Yu. *The population of the Armenian uplands during Antiquity, based on data from the Beniamin cemetery*. Yerevan, Tigran Mec, 2000, 120 p.
40. Kremer, C., S. Racette, C.-A. Dionne, A. Sauvageau. Discrimination of falls and blows in blunt head trauma: systematic study of the hat brim line rule in relation to skull fractures. – *J. Forensic. Sci.,* **53(3)**, 2008, 716-719.
41. Kremer, C., A. Sauvageau. Discrimination of falls and blows in blunt head trauma: assessment of predictability through combined criteria. – *J. Forensic. Sci.,* **54(4)**, 2009, 923-926.
42. Kotil, K., C. Kilincer. Sizes of the transverse foramina correlate with blood flow and dominance of vertebral arteries. – *Spine J.*, **14(6)**, 2014, 933-937.
43. Lang J., A. Hetterich. Contribution on the postnatal development of the processus pterygoideus. – *Anatomischer Anzeiger*, **154**, 1983, 1-31.
44. Lamberty, B. G., S. Zivanovic. The retro-articular vertebral artery ring of the atlas and its significance. – *Acta Anat. (Basel),* **85**, 1973, 113-122.
45. Larsen, C. S. *Bioarchaeology: Interpreting behavior fromthe human skeleton*. Cambridge University Press, Cambridge, 1997, 461 p.
46. Lazarides, S., G. Zafiropoulos, M. Tydfil. Conservative treatment of fractures at the middle third of the clavicle: The relevance of shortening and clinical outcome. – *Journal of Shoulder and Elbow Surgery*, **15**, 2006, 191-194.
47. Limousin, C. A. Foramen arcuale and syndrome of Barre-Lieou. Its surgical treatment. *International Orthopaedics*, **4**, 1980, 19-23.
48. Lovell, N. C. Trauma analysis in paleopathology. – *Yearbook of Physical Anthropology,* **40**, 1997, 139-170.
49. Lovejoy, C. O., K. G. Heiple. The analysis of fractures in skeletal populations with an example from the Libben site, Ottowa County, Ohio. – *American Journal of Physical Anthropology,* **55 (4)**, 1981, 529-541.
50. Lovejoy, C.O., R. S. Meindl, T. R. Pryzbeck, R. P. Mensforth. Chronological metamorphosis of the auricular surface of the ilium: A new method for the determination

of adult skeletal age at death. – *American Journal of Physical Anthropology, **68**, 1985, 15-28.*
51. Lu, B., Sh. Zhao, Z. Luo, Z. Lin, Y. Zhu. Compression screws and buttress plate versus compression screws only for Hoffa fracture in Chinese patients; a comparative study. – *J. Int. Med. Res.*, **47**, 2019, 142-151.
52. Mant, M. Time after time: individuals with multiple fractures and injury recidivists in long eighteenth-century (c. 1666–1837) London. – *International Journal of Paleopathology*, **24**, 2019, 7-18.
53. Maxeiner, H., E. Ehrlich. Site, number and depth of wounds of the scalp in falls and blows – k a contribution to the validity of the socalled hat brim rule. – *Arch. Kriminol.,* **205**, 2000, 82–91.
54. McKinley, J. I. Compiling a skeletal inventory: disarticulated and co-mingled remains. In: *Guidelines to the Standards for Recording Human Remains* (Eds. M. Brickley, J. I. McKinley). Institute of Field Archaeologists Paper No 7, 2004, 14-17.
55. Meindl, R. S., C. O. Lovejoy, R. P. Mensforth, L. D. Carlos. Accuracy and direction of error in the sexing of the skeleton: Implications for paleodemography. – *American Journal of Physical Anthropology,* **68**, 1985, 79-85.
56. Mouzopoulos, G., E. Morakis, M. Stamatakos, M. Tzurbakis. Complications associated with clavicular fracture. – *Orthopaedic. Nursing.,* **28**, 2009, 217-224.
57. Nowak, J., H. Mallmin, S. Larsson. The aetiology and epidemiology of clavicular fractures. – *International Journal* of Integrated *Care*, **31**, 2000, 353-358.
58. Piotrovsky, B. B. *Vansky kingdom (Urartu)*. Moscow, East literature, 1959, 260 p.
59. Phenice, T.W. A newly developed visual method of sexing the os pubis. – *American Journal of Physical Anthropology*, **30**, 1969, 297-302.
60. Postacchini, F., S. Gumina, P. De Santis, F. Albo. Epidemiology of clavicle fractures. – *Journal of Shoulder and Elbow Surgery*, **11**, 2002, 452-456.
61. Redfern, R. C., M. A. Judd, S. N. DeWitte. Multiple injury and health in past societies: An analysis of concepts and approaches, and insights from a multi-period study. – *International Journal of Osteoarchaeology*, **27**, 2017, 418-429.
62. Richter, M. *Gerichtsärztliche diagnostik und technik*. Leipzig, Germany, Hirzel, 1905, 304p. [in German]
63. Robb, J. E. Violence and gender in early Italy. In: *Troubled Times: Osteological and archaeological evidence of violence*. (Eds. D. L. Martin, D. W. Frayer). New York, Gordon and Breach, 1997, 108-141.
64. Robinson, C. M. Fractures of the clavicle in the adult: epidemiology and classification. – *Journal of Bone and Joint Surgery*, **80-B**, 1998, 476-484.
65. Rogers J., T. Waldron. *A field guide to joint disease in archaeology*. New York, John Wiley, 1995, 119 p.
66. Rosse, C., P. Gaddum Rosse. *The vertebral column*. Hollinshead's text book of anatomy. Philadelphia, Lippincott-Raven, 1997, 902p.
67. Scheuer, L., S. Black. *Developmental juvenile osteology*. London, Academic Press, 2000, 587p.
68. Smith, K. D., P. C. Edwards, T. S. Saini, N. S. Norton. The prevalence of concha bullosa and nasal septal deviation and their relationship to maxillary sinusitis by volumetric tomography. – *International Journal of Dentistry*, 2010. Article ID 404982.
69. Spitz, W. U. Blunt force injury. In: *Spitz and Fisher's medicolegal investigation of death: guidelines for the application of pathology to crime investigation*. (Eds. W.U. Spitz, D.J. Spitz), 4th edn. Springfield, IL: Charles C. Thomas, 2006, 199-251.
70. Stallman, J. S., J. N. Lobo, P. M. Som. The incidence of concha bullosa and its relationship to nasal septal deviation and paranasal sinus disease. – *American Journal of Neuroradiology*, **25**, 2004, 1613-1618.

71. Strabo The *Geography* XI, IV. (Translation and Notes by G. Stratanowski). Moscow, Science, 1964, 944 p.
72. Standen, V. G., B. T. Arriaza. Trauma in the preceramic coastal populations of northern Chile: violence or occupational hazards? – *American Journal of Physical Anthropology,* **112**, 2000, 239-249.
73. Symes, S. A., E. N. L'Abbé, E. N. Chapman, I. Wolf, D. C. Dirkmaat. Interpreting traumatic injury to bone in medicolegal investigations. In: *A companion to forensic anthropology*. (Ed. D. C. Dirkmaat), Wiley-Blackwell, Oxford, 2012, 340-388.
74. Tadj, A., F. W. Kimble. Fractured zygomas. – *American Journal of Surgery*, **73**, 2003, 49-54.
75. Tubbs, S., M. M. Shoja, G. Shokouhi, R. M. Farahani, M. Loukas, J. W. Oakes. Simultaneous lateral and posterior ponticles resulting in the formation of a vertebral artery tunnel of the atlas: Case report and review of the literature. – *Folia Neuropathologica*, 45, 2007, 43-46.
76. Villa, P. E. A., T. R. Nunes, F. P. Gonçalves, J. S. Martins, G. S. P. de Lemos, F. B. de Moraes. Avaliação clínica de pacientes com osteomielite crônica após fraturas expostas tratados no hospital de Urgências de Goiânia, Goiás. *Revista Brasileira de Ortopedia*, **48**, 2013, 22-28. [in Portuguese]
77. Villa, P., E. Mahieu. Breakage patterns of human long bones. – *Journal of Human Evolution*, **21(1)**, 1991, 27-48.
78. Von Torklus, D., W. Gehle. *The upper cervical spine*. New York, Grune & Stratton, 1972, 259 p.
79. Waldron, T. *Paleopathology*. Cambridge, University Press, 2009, 298p.
80. Walker, P. L. Cranial injuries as evidence of violence in prehistoric Southern California. – *American Journal of Physical Anthropology,* **80**, 1989, 313-323.
81. Zibis, A., V. Mitrousias, N. Galanakis, N. Chalampalaki, D. Arvanitis, A. Karantanas. Variations of transverse foramina in cervical vertebrae: What happens to the vertebral artery? – *Eur. Spine. J.,* **27(6)**, 2018, 1278-1285.
82. Yeganyan, L. G. *Shiraki hnagitakan yev patma-azgagrakan usumnasirut'yuny [Archaeological and Historical-Ethnographic Study of Shirak]*. Vol. 1. Yerevan-Gyumri, Science and Shirak Centre for Armenological Studies, 2010, 280 p. [in Armenian]

Institute of Experimental Morphology, Pathology and Anthropology with Museum
Bulgarian Anatomical Society

Acta Morphologica et Anthropologica, 31 (3-4)
Sofia ● 2024

Review Articles

Medical Care in Late Antiquity and its Influence in the Middle Ages

Maria Christova-Penkova

Institute of Experimental Morphology, Pathology and Anthropology with Museum – Bulgarian Academy of Sciences

*Corresponding author email: mariachristova@abv.bg

In its ten-century history, Byzantium managed to preserve and systematize the ancient heritage, particularly medical knowledge. Based on it, Byzantium managed to develop a hospital model, which has two very important characteristics: firstly, the work in these establishments is carried out by trained and qualified staff, whose payment is provided by the community; secondly, the medical institution is accessible to everyone, regardless of their social status, ethnic or religious affiliation. The Byzantine hospital model is based on solid medical practice and knowledge, preserved in practice to accumulate medical expertise and experience to be systematized and recorded to serve in the training of the next generations, and some really impressive encyclopedic works have reached us in later copies among which it stands out the Alexander of Tralles's *Therapeutics* and Paul of Aegina's *Epitome medicae libri septem*.

Key words: Byzantine medicine, medieval hospital, Alexander of Tralles, Paul of Aegina

Introduction

Late Antiquity was a period of profound transformation, and the social, economic, political, demographic, and military processes that took place then were the subject of more than one or two studies. However some aspects of this transformation, such as the organization of medical care, reflecting the change towards the person as a whole as a result of the affirmation of new Christian values, have been undeservedly neglected. Various commentaries consider that during Cyprian's plague, Christians took care of the suffering, while the usual behavior of others was to hide. And although they were the main suspects in this disaster and officially accused, their way of acting reversed attitudes and was one of the many factors that led to the change of religion. This attitude

also reveals a potential to bring organized medical care in the upcoming centuries to a new level.

Medical Care in Ancient Societies

Christian communities began setting up special places to take care of the poor, the hungry and the sick. The first information about such "hospices" (in the Greek *ξενώνες*) comes from the Greek cities of the Eastern Mediterranean. The *Chronicon Paschale* (7th century) describes hostels founded by Leontius, Bishop of Antioch (344-358). The care of the poor and the foreigners was leading, but there is no evidence of specialized medical care provided by doctors [12]. The earliest evidence of such care is related to the work of St. Basil the Great, Bishop of Caesarea (370-379). A shelter for the poor, a leprosarium for lepers, an inn for foreigners, and separate buildings for the sick functioned in his complex, called *καταφύγιο, katagogia* (a shelter), as he described it in a letter to the Governor of Cappadocia [9]. To ensure the care for the sick, St. Basil personally selected trained staff - doctors and assistants; according to Sozomenos, the "shelter" fully performed the functions of a hospital [11]. The complex is known as *Basililiad* and is becoming a pattern for a charitable establishment. At the end of the 4th century, St. John Chrysostom established similar complexes in Constantinople. Palladium defines them as places of care for the needy and the sick, but the use of the word *nosokomeion* (from the Greek word for disease - *νόσος*) suggests that they served more for healing [12]. Additional light on the activities of the shelters of St. Basil the Great and St. John Chrysostom is shed by the metaphor used by St. Nilus of Sinai, which features the world as *nosokomeion* and Christ as a physician. Thus St. Nilus of Sinai implies that the doctors of the late 4th and early 5th centuries not only alleviated suffering until death, but sought to cure the sick. Finally, he states that the places where such care was provided were for the poor and the homeless [12]. In those first hospitals, the poor were given access to medical examinations, and the care needed for the treatment lay with the monks. The charitable initiatives of individual Christian communities led to the establishment of shelters/hospitals in several cities - in Jerusalem, founded by Emperor Anastasios (491-518) at the request of St. Sava; 5 km to the south of Jerusalem, the monk Theodore founded a dormitory for monks with three shelters for the sick, where medical care was provided; hospitals were also established in Ephesus, Bethlehem, central Syria, Alexandria [11].

To bring order to these charitable institutions, Emperor Justinian (527–565) issued certain regulations. This reform affects the specialization of the various establishments, the qualification of the medical staff, as well as the admission of patients. Each establishment is well defined according to the function it performs, and this is reflected in the terms used. Thus, in novellas, *nosocomae* or *xenones* are terms used for places where patients are treated; *Xenodochi*a are inns, i.e. places of shelter for foreigners; *Ptochei* are shelters for the poor and able-bodied beggars, while *gerontokomeia* is a term referring to nursing homes. There is also talk of orphanages (*orphanotropheia*), crèches (*brepotropheia*) and leprosoria (*ptochotropheia*). In the hospitals until the time of Justinian, patients were cared for by people of good will with some medical knowledge, but they did not necessarily have to be educated doctors. After the publication of Justinian's novellas, this role was assigned to the best practitioners of the Empire, the *archiatras*, the organization

of elite doctors created by Emperor Antoninus Pius (138-161). From that moment on, the place for practicing the profession of *archiatras* was the hospital. However, they no longer depended on the municipal administration, but on the bishops, because hospitals, as a charitable institutions, remained under the control of the Church. Justinian was not content only with putting the best doctors at the service of hospitalized patients but also provided them with competent staff. The *hypourgoi* (nurses) were in charge of administering the treatment; They should be able to carry out small interventions and take on duty, especially at night. *Hyperetai* or caregivers helped them in their work [11]. Thus, Justinian's large-scale reform allowed the poor, like the rich, to benefit from quality medicine. These medical institutions differed radically from the places associated with a saint-healer, where the sick were treated with prayer and chrismation, as well as from the well-known in Western Europe „houses of mercy", in which people were only cared for in purely everyday terms until death. These were institutions for „active treatment", in which the applied treatment fit into the great medical tradition inherited from Antiquity [2]. It was based on rational medicine, based on specific knowledge of the human body, etiology of diseases and remedies. Information about medical practice and organization of medical care is found in written sources. For example, in the work The *Miracles of St. Artemy* contains two stories that reveal some details in the organization of hospitals, patients and treatments. The first reveals the story of Stephan, a deacon in the church of *Hagia Sofia* in Constantinople. He suffered from groin pain (here I should add that St. Artemius is associated with the treatment of hernias, which gives us an indication of what deacon Stephan suffered from). After a long treatment at home, he was taken by his parents in the xenon of Samson to *Hagia Sofia*, where he was admitted. During his short stay there, Stephan was placed on a bed near the eye department. After a cold cauterization that lasted three days, he was operated on. Going through this painful therapy, Stephan was finally cured [1]. In addition to the applied treatment, this passage is interesting with two more facts – the information about Samson's xenon and the presence of an ophthalmological and surgical department in it. This hospital was founded by the physician Samson in his house at the end of the fourth century and was burned down during the Nika revolt (532). By order and with the financial support of Emperor Justinian, it was restored together with the hospital of Eubulos, located in the same area. Samson's xenon is located between the churches of *Hagia Sofia* and *Hagia Eirene* and was studied archaeologically. The seals kept in the Dumberton Oaks collection show that it functioned in the following centuries. In the following years, a number of hospitals were founded in Constantinople: at the monastery of St. Kozma and Damian outside the city walls, where surgery functioned; the hospital of Christodota near the church of St. Anastasia, where the medical teams worked every other month, etc. By order of Justinian, the hospital in Side was also built, preserved almost entirely; the hospital in Antioch, destroyed by Khuzro I (531–579) in 540, was also rebuilt; two xenons were built in Jerusalem, near the Church of the Virgin Mary [11]. In the 6th century in Thessaloniki, there was already a hospital at the church of St. Demetrios [2]. The second story in The *Miracles of St. Artemius* reveals the staff organization in Christodota's xenon. During his long stay there, the clergyman who was admitted for treatment was cared for by doctors (γιατρόι), assisted by their medical assistants (*ὑπουργοι*), who, in turn, had assistants in charge of non-medical care (*ὑπηρέτας*), i.e. the organization of medical care strictly followed Justinian's regulations [12].

Thus, the model established in Late Antiquity has two very important characteristics: first, the work in these establishments is carried out by trained and qualified personnel, whose payment is provided by the community; Secondly, the medical institution is accessible to everyone, regardless of their social status, ethnic or religious affiliation. And if the first of these characteristics can be found in the ancient period, when doctors from the community were also hired for a fee, then the wide access of those in need to medical care is a new element, previously unknown. In the following centuries, these institutions underwent their development in order to receive a complete form in the famous xenon at the Pantocrator Monastery in Constantinople. The Typicon of the Monastery of Christ the Savior and Pantocrator, was issued by John II Komnenos (1118-1143) and his spouse Irene and regulates all aspects of the functioning of the huge complex. The Typikon was issued in October 1136 and consisted of two parts: one regulating life in the monastery (the liturgical cycle, the life of the monks, their diet, administrative regulations, etc.), and the second concerning the number of hospital beds, number and nomenclature of the staff, remunerations, etc. [6]. The hospital beds were fifty in total; they were divided into five wards: two male wards - one for healing fractures and injuries (ten beds) and the second ward of ophthalmology and intestinal diseases (eight beds); two mixed wards for "ordinary" (probably chronic) diseases with ten beds each; one female ward with twelve beds. One extra bed was provided for each ward, as well as six more beds ("with a hole") for the seriously ill. The medical personnel were headed by two chief physicians (*πριμμικηριος*), who were responsible for the admission of patients, for the diagnosis, the appointment of treatment and the training of doctors (with the help of a specially appointed teacher, *διδάσκαλος*). Only they had the right to practice outside the hospital, but not in the months when they worked there. The staff worked every other month, and in their free month they did not have to leave the city ("to be available"). The scattered data in the Typikon on the organization of the work in the hospital reveal the following picture: two chief surgeons worked in the ward for healing fractures and injuries; two senior physicians (*πρωτομηνῖται*) in the ward for eye and intestinal diseases; four physicians (*γιατρόι*) took care of the patients suffering from "common" diseases in the two rooms [6]. Three doctors (two men and one woman) worked in the women's ward. Three more assistant-doctors and two trainee doctors worked in each man's ward, and in the women's ward there were four assistant-doctors and two trainees (all women). The duties of today's nurses were taken over by two assistants in each ward (women in the female ward), defined by the term *ύπουργοι*. The hospital had an outpatient clinic staffed with two surgeons and two general practitioners. They reported the severe cases to the chief physicians who decided to admit them to the hospital [6]. The hospital also had a pharmacy, served by one chief pharmacist, three pharmacists and two assistant pharmacists. Five more washermen took care of the normal functioning of the hospital; two firemen in the boiler room, who constantly ensured the availability of hot water; two bakers and one miller; one groom, one waste cleaner and security guard. Upon admission to the hospital, the sick received clothes, and it was the practice to give them to the poorest when they were discharged. The hospital provided each patient with utensils (ceramic bowl, cup and plate), as well as a place-bed (straw mattress and two blankets made of goat skin). Annual change of straws and blankets was required, and the better preserved were distributed to the poor. The monastery statute also provided for a portion of food, which was controlled

by the chief physician. According to the typikon approved by the ktetor, the hospital functioned as a financially autonomous unit under the control of a council headed by the hegoumenos. The expenses were covered by a fixed percentage of the monastery's revenues, namely from its lands, markets, handicrafts [6]. The xenon at the monastery of Christ Pantokrator features the most extensive system of hospital treatment and sets a model that was followed, to one degree or another, in other similar complexes. For example, in 1152 Sebastokrator Isaac Komnenos established the monastery of the Theotokos Kosmosoteira at the city of Bera (Greece), which had a hospital with thirty-six beds. The monastery typikon ordered the hegoumenos to hire a "*competent and proven doctor*" for "*appropriate remuneration and salary*" to care for the sick [15]. The Byzantine hospital model was also basic in the establishment of the hospital of St. John of Jerusalem after the establishment of the Latin Kingdom in the Holy Land, served by the Knights Hospitallers (Ioannite Knights). Elements such as the presence of various wards in the hospital and of separate beds, the hiring of specialists were unknown in Western Europe until then. The statutes of Roger de Moulin stipulate that four "wise" physicians should be hired to prescribe the therapy and determine the actions of other specialists. A letter from Pope Lucius III mentions four physicians and four surgeons working at the hospital [7].

The Byzantine hospital model is based on solid medical practice and knowledge, in which the ancient ideas about the structure of man and the nature of disease states are preserved and further developed. Here it should be noted the role of the schools in Athens and Alexandria, where medicine is studied on a par with the other sciences. St. Basil graduated from the school in Athens and is an educated doctor. His *Hexaemeron* known as *Sermons on the days of the Creation* (Genesis 1-24) reveal his extensive knowledge of the natural sciences, with his commentary on "*harmful plants*" being particularly impressive. He emphasizes that *"... nothing was created in vain and without benefit" and that "... with the help of medical science, it reveals itself to be fit for ourselves*". And he gives examples: *"Doctors use mandrake as a sleeping pill, and opium soothes severe pains in the body. And some with hemlock have pacified the rage of wishes, and with hellebore they have eradicated many chronic diseases"* [16]. We find the same passage almost literally translated in the John the Exarch' *Hexaemeron* from the 10th century [8]. In his sermons, St. Basil does not talk about the anatomical structure of man. This is what his brother, St. Gregory of Nyssa, who revealed anatomical knowledge in his treatise „*On the Structure of Man*", accepted as a continuation of „*Sermons on the days of the Creation"*. There, in the last, thirtieth chapter, entitled „*A Brief, rather Medical Examination of the Structure of Our Body*," extraordinary anatomical knowledge is revealed. The aspiration does not stop only at the topographical enumeration of the individual organs, but to arrange them hierarchically according to their function and role in the maintenance of life. The description of some details is downright stunning: the atria of the heart and its role in maintaining body temperature; the structure of the lungs; the role of the liver in blood formation; the description of the vena cava connecting the heart and liver (although it is incorrectly defined as carrying air); the skeleton and its mobility, provided with joint ligaments, tendons and muscle, as well as its importance for the preservation and protection of vital organs; and above all, the brain and spinal cord, giving „*impetus and strength to all the connections of bones and joints and the rudiments of muscles, with every movement and at every stop*" [17].

It should be emphasized that in medieval East Mediterranean lands there was a practice for the accumulated medical knowledge and experience to be systematized and recorded to serve in the training of the next generations, and some really impressive encyclopedic works have reached us in later copies. Among them, two stand out, which I would like to briefly present. The first is the treatise of 12 books with the general title „*Therapeutics*" by Alexander of Thralles. It includes descriptions of the etiology of a number of diseases, their exact symptoms and recommendations for treatment [13].

Alexander was born in Tralles, near Ephesus, around 525, his father was a doctor, and his eldest brother was none other than the famous architect Anthemius, who, together with Isidore of Miletus, built the majestic Basilica of Hagia Sophia in Constantinople for five years, at the request of Justinian. Alexander participated as a military doctor in almost all of Justinian's campaigns in the Mediterranean, which allowed him to gain vast experience. In his last years, he devoted himself to training young doctors and writing his treatise. He died approx. 605 A.D. In his *Therapeutics*, Alexander of Thrall systematized his knowledge in the following books: I. Diseases of the head (including alopecia, migraine, and „lethargy"); II. Eye diseases; III. Diseases of the mouth (including ulcers); IV. Heart disorders; V. Diseases of the lungs (in particular, various types of pneumonia); VI. Pleurisy; VII. Stomach problems; VIII. Intestinal diseases; IX. Liver disease; X. Disentery and dropsy; XI. Genital and urinary problems; XII. *Podagra* or gout, with numerous treatments [13; 14]. Already in the introductory part of his work, Alexander states that he relies above all on the accumulated knowledge acquired in contact with his patients and presents himself as a practicing physician, not a compiler of medical knowledge [10].

Alexander of Tralles is above all a remarkable clinician and therapist. Its distinguishing feature is the accurate diagnosis[1], and the effort to clarify the causes of the disease. Alexander sought to achieve an etiological cure and stated that „*the doctor's first goal is to eliminate the cause of the disease"* [10]. For each disease he supplies descriptions, stages of development, recommendations for treatments, whether the illness was chronic or acute, whether a krisis signaled a cure or the onset of death, or if the *kritis*[2] was but one of many in a chronic illness (quite characteristic of fevers). Alexander had mastered a phenomenal variety of drugs, both in their "simple" forms and in the compound formulas almost always typical of his treatments for diseases. The *Therapeutics* fairly bulge with formulas, recipes, and measures for the compounding of drugs [13]. In his therapeutic approach, Alexander pays special attention to pharmacology, which for him is the most dynamic branch of therapy. For example, in his *Therapeutics* he explains that he is not enthusiastic about the use of

[1] According to Nicholaos Myrepsos (13th century), it was Alexander of Tralles who developed the uroscopic diagnostic method, which was subsequently further developed by Theophilos Protospatharios and Myrepsos himself. According to the diagram developed, urine was divided depending on color (10 different), sediment (five different solid particles discriminated), and transparency. This method was inalienably present in Byzantine treatises until the 15th century and was later adopted in Western Europe. Today, Alexander of Tralles' authorship of the treatise dedicated to this method is a matter of dispute

[2] Patient condition involving unstable vital signs and a prognosis that predicts the condition could worsen; or, a patient condition that requires urgent treatment in an intensive care or critical care medical facility.

surgery: „*arteriotomy, trephination, cauterization and all other drugs ... become a punishment for many and are not a cure*“ [10].

The second major work is the emblematic medical encyclopedia *Epitomes iatrikes biblia hepta* (*Epitome medicae libri septem*) – the work of one of the most respected and revered Byzantine encyclopedists Paul of Aegina. His work consists of as many as 7 volumes. They are precious to historians and medics alike, as they summarize the best of two ancient medical systems – the ancient Greek and the Roman. His work was highly appreciated and became a cornerstone in Arabic medicine. In the 11th century, through the Arab tradition, it entered Western Europe, where future medics were trained in Epitome medicae until the dawn of the Renaissance. During the Renaissance, the University of Paris recommended that surgery be taught only from his books. Paul studied all sections of surgery, trauma, primarily such as sprains and fractures, amputations, cavity surgery, etc [1].

Information about Paul‘s life is scarce. It is certain that he was born on the island of Aegina, around 625 and died around 690. In an epigram reproduced in many manuscripts, he is defined as περιοδευτής, i.e. a traveling doctor. He became famous as a particularly good surgeon. *Epitomes iatrikes biblia hepta* includes the following seven books: I. Hygiene and dietetics; II. The different varieties of fever; III. Diseases are classified according to their location from head to toe; IV. Skin diseases and intestinal pathologies; V. Poisons; VI. Surgery; VII. Combination drugs.

His work provides original descriptions of procedures including lithotomy, trepanation, hernitomy, paracentesis, breast amputation, and tracheostomy. The doctor also participates in other surgical procedures, including eye surgeries, removal of nasal polyps, tooth extraction, tonsillectomy, removal of bladder stones. Again, according to experts, the most significant contribution from the work of Paul of Aegina is in the field of surgery [19]. It gives very clear and precise instructions for some interventions, such as the removal of tonsils, for example. The patient should sit in front of the sun, his mouth should be wide open, and his tongue should be pressed with a spatula. With a quick movement, the lymphatic organ is pulled forward (through a hook), and with a curved scalpel, the surgeon excises the tissue at the base of the tonsil. The patient, if he is still conscious, should gargle with cold water (according to the doctor‘s writing) after the procedure [18; 3]. One of the best surgical descriptions of Paul of Aegina is that of tracheostomy [19]. Today it is routine, but in the past, it was used as a last resort in saving the patient’s life. Turning to the historical aspects of tracheostomy, Paul of Aegina provides a detailed description of the operation in his Epitome. It is very similar to the modern procedure just described: *“... but in inflammations about the mouth and palate, and in cases of indurated tonsils which obstruct the mouth of the windpipe as the trachea is unaffected, it will be proper to have recourse to pharyngotomy, to avoid the risk of suffocation. When, therefore, we engage in the operation we slit open a part of the arteria aspera (for it is dangerous to divide the whole) below the top of the windpipe, about the third or fourth ring. This is a convenient situation, as being free of flesh, and because the vessels are placed at a distance from the part which is divided. Wherefore, bending the patient’s head backward, to bring the windpipe better into view, we are to make a transverse incision between two of the rings, so as that it may not be the cartilage that is divided, but the membrane connecting the cartilage. If one be more timid in operating, one may first stretch the skin with a hook and divide it, and then, removing the vessels aside, if they come in the way, make the incision.”* [14]. By

comparison, the first evidence of a successful tracheostomy in Western Europe was not officially published until 1546 by Antonio Brazavola, and the refusal to perform this „radical" manipulation on George Washington in 1799 by the two senior physicians in the trio of physicians caring for him led to his death.

In its ten-century history, Byzantium managed to preserve and systematize the ancient heritage, and medical knowledge in particular. Based on it, the Byzantine Empire managed to develop a hospital model, the modern analog of which can be found in the clinical medicine of revolutionary France which recentered medical research and instruction in the hospitals of Paris. In the early nineteenth century, this clinical movement made great progress in improving hospital care, in describing accurately the symptoms of diseases, in compiling statistical records of these symptoms, and in the outcome of similar cases. Careful consideration of Byzantine medical science is only beginning, and the study of medieval treatises will surely reveal more clearly the achievements and failings of Byzantine medicine and the contribution of hospitals to its development [12]. But in the history of science, the legacy of Byzantium is not the property of only one country - its vast territory and influence also covers the lands of today's Bulgaria, from where it spread to the rest of the Slavic world.

References

1. **Aledzhanov, N. Yu.** Phlebology in ancient Greece and Byzantium. – *The Greek E-Journal of Perioperative Medicine* **20**, 2021, 2-12.
2. **Bakirtzis, Ch.** Late Antiquity and Christianity in Thessaloniki: Aspects of a transformation. In: *From Roman to early Christian Thessaloniki: Studies in religion and archaeology* (Eds. L. Nasrallah, Ch. Bakirtzis, and S. J. Friesen), Harvard University Press, 2010, 397-426.
3. **Bishop, W. J.** *The early history of surgery*. New York, Barnes & Noble, First Edition 1995, pp. 192.
4. **Bolgova, A. M.** Aleksandr Trall'skij, vrach (525-605 gg.). In: *Klassicheskaja i vizantijskaja tradicija*. Sbornik materialov XI nauch. konf. / NIU BelGU. Belgorod, 2017, 353-361. [in Russian]
5. **Bouras-Vallianatos, P.** Clinical experience in Late Antiquity: Alexander of Tralles and the therapy of epilepsy. – *Medical History*, **58**(3), 2014, 37–353.
6. **Gautier, P.** Le typicon du Christ Sauveur Pantocrator. - *Revue des Etudes Byzantines*. **32**, 1974, 1-145. [in French]
7. **Greif, E.** The Byzantine hospital organization and the Knights of St. John in Jerusalem. – *Imago Temporis Medium Aevum*, XIV, 2020, 199-214.
8. **Joan Ekzarh.** *Shestodnev*, Sofia, Nauka i Izkustvo, 1981, pp. 376. [in Bulgarian]
9. **Kapsambelis, D.** Invention or evolution in the provision of health care in Late Antiquity in the Eastern Roman Empire. The case of the hospital. *Master thesis*, University of Wales, Trinity Sant David. 2011, pp. 87.
10. **Kostjuchenko Sv., L. Bolohovec** Razvitie mediciny v Vizantijskoj imperii - referat. Gomel State Medical College, Gomel, 2010. [in Russian]
11. **Le Coz, R.** La naissance de l'hôpital. – *Histoire des sciences médicales* T. XXII, №2, 1998, 139–145. [in French]
12. **Miller, T. S.** Byzantine hospitals. – *Dumborton Oaks Papers*, 1984, **38** 53-63.
13. **Scarbrough, J**. The life and times of Alexander of Tralles. – *Expedition Magazine*, **39**(2), 1997, 51-60.
14. **Serletis, D.** Paul of Aegina and tracheostomy. In: – *The Proceedings of the 10th Annual History of Medicine days*, Calgary, 2001, 26-29.

15. Ševčenko, N. P. Kosmosoteira: Typikon of the Sebastokrator Isaac Komnenos for the Monastery of the Mother of God Kosmosoteira near Bera. – In: *Byzantine Monastic Foundation Documents* (Eds. J. Thomas and A. C. Hero), Washington DC, Dumbarton Oaks Research Library and Collection, 2000, 782-858.
16. Sveti Vasiij Veliki. *Besedi varhu Shestodnev*. Sofia, Pravoslavno Otechestvo, 2018, pp. 175 [in Bulgarian]
17. Svjatoj Grigorij Nisskij. *Ob ustroenii cheloveka*. Sankt-Peterburg, Axioma, 2000, pp. 220. [in Russian]
18. Tsoukalas, G., L. Konstantinos, M. Sgantoz, G. Androutsos. Paul of Aegina (c. 7th Century AD): Introducing in the surgical operating theatre of the era an innovative tonsillectomy with forceps under the sunlight. – *History of Innovation*. *Surgical Innovation*, **23(**1), 2016, 102-103.
19. Walsh, J. Paul of Aegina. – In: *Old-time makers of medicine, the story of the students and teachers of the sciences related to the medicine during the Middle Ages,* California, US, Create Space Independent Publishing Platform, 2016, pp. 410

Institute of Experimental Morphology, Pathology and Anthropology with Museum
Bulgarian Anatomical Society

Acta Morphologica et Anthropologica, 31 (3-4)
Sofia ● 2024

Kamen Usunoff and His Scientific Contribution to Neuroscience: Scientific Rite of Passage

Enrico Marani [1], Wladimir Ovtscharoff [2], Nikolai Lazarov [2, 3]

[1] Tiboel Siegenbeekstraat 15, 2313HA Leiden, The Netherlands
[2] Department of Anatomy, Histology and Embryology, Medical University of Sofia, Sofia, Bulgaria
[3] Institute of Neurobiology, Bulgarian Academy of Sciences, Sofia, Bulgaria

*Corresponding author e-mail: enrico.marani@outlook.com

The current paper summarises the outstanding scientific contribution made by Professor Kamen Usunoff to the neuroscience and neuroanatomy. He contributed fundamentally to our knowledge of the (1941-2009) nervous system. He was one of the important anatomists that achieved remarkable success in brain research by understanding pathogenesis of neurodegenerative diseases. Some data about his scientific and academic career are also provided. Professor Usunoff is highly recognised as a leading scientist and teacher who has made significant contribution to the development of the Bulgarian morphological school.

Key words: neuroscience, basal ganglia, amygdala, pain

Introduction

A rite of passage marks an important stage after a person's death to place its definitive scientific identity. The young Bulgarian scientists hardly remember or know of Kamen Usunoff's scientific inheritance. Therefore, let's start with some remarkable moments in his life (don't expect a chronological overview). Kamen participated in a scientific exchange between Leiden's Neuroanatomy and Sofia's Anatomy (Prof. Wladimir Ovtscharoff) instigated by both governments, but without financial support in 1990. The 3th October is "Leidens Ontzet" (Leiden's relief (1574) of the Spanish occupation of Holland during 16th and 17th century). Walking back from the lab, we were stopped by the 3th October festival procession. In front of us an open trailer with women dressed as Wrens (Woman's Royal Navy Service) singing Second World War songs. To my surprise Kamen knew the songs by heart, he knew them all, the consequence of the free post-war time in Bulgaria? His memory of the songs was incomprehensibly good. Bulgarian radio refused to let Kamen participate any longer in the game "guess the song". He always won.

Kamen went with his father to London. His father, a well-known psychiatrist, was invited due to his excellent studies on alcoholic encephalopathies (a real pestilence around 1940-1955). Kamen noticed the underhand sniggering of his father's colleagues due to his bad English. Because of this he achieved excellent English by self-study.

During his military time in communist Bulgaria, Kamen had to do sports as all people in the military had to. He chose wrestling and boxing. His technique caused him to became a Bulgarian military wrestling champion. Although he had the possibility to participate in the international wrestling arena, it never happened.

Kamen started his medical studies in 1961 in Sofia and finished in 1967 and then became a member of the Anatomical Department of the Medical University, Sofia, in the same year. His further specialisation in 1972 occurred in Germany in Frankfurt am Main in the department of Prof. Dr Rolf Hassler (1914-1984; head of the Max Planck Institute), known for his substantia nigra studies and stereotactic treatment of Parkinson patients. A remnant of that time was Kamen's strong support of Hassler's subdivision of the human substantia nigra [14].

Fig. 1. Kamen Usunoff, "remember his piercing glance during straight forward discussion. Personally he was tough at the outside, but soft and very friendly in the inside" (photos 15-04-2005 and Chaldakov's obituary citation, 2010) [1].

Kamen Usunoff's Achievements in Neuroscience and Neuroanatomy

Kamen's interest was mainly putamen, globus pallidus, substantia nigra and the subthalamic nucleus (**Fig. 2**, basal ganglia and related nuclei). He contributed to all aspects of the basal ganglia, although other brain areas, such as the amygdala, were also frequently researched. His thesis (1990) concerned: "Cytoarchitectural, ultrastructural, and histochemical characterization of the substantia nigra"; it appeared in six volumes and only parts have been published in international journals [12]. Due to the Hassler time he had an incredible overview of all neurological related diseases.

Hidden in a large article on "Neuromelanin in the human brain" [4 also 19, 20], you will find descriptions of idiopathic Parkinson's disease, Parkinson-plus

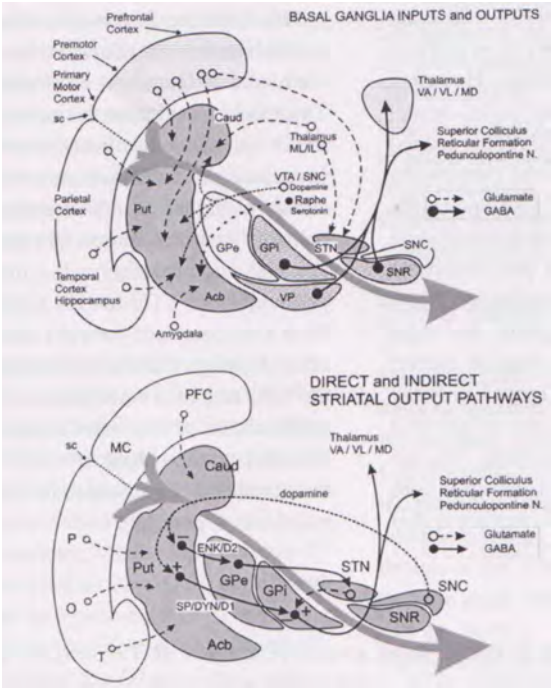

Fig. 2. Neuroanatomical schemes for basal ganglia input and output and the direct and indirect striatal output pathways, which were Kamen Usunoff's main research areas (courtesy H. J. Groenewegen, see Groenewegen and Van Dongen, 2008) [3].

syndromes (supranuclear palsy, dementia complex, cortico-basal degeneration, multiple system atrophy, and Pick's disease to name a few) and secondary parkinsonian syndromes. Notice has been given to etiology and pathogenesis of Parkinson's disease that treats topics, now in the midst of our attention: genetics, environment, cascade of multiple deleterious factors, role of iron, glutamate excitotoxicity, role of calcium, mitochondria, glia cells and necrosis. One has to read the text carefully and, often underestimated, you will find unexpected ideas on these diseases, ready for research. An effective network kept him up to date, also due to the students he had trained in neuroscience.

Kamen cooperated also with Andreas Wree, head of the Anatomy department in Rostock. Together they published in 2003 an overview on the pedunculopontine tegmental nucleus (a hardly known article) [13]. It was a forward-looking publication. The bulk of articles on this nucleus have been published between 2010-2023. It also contributed to the publication and thesis of Marcel Lourens (University Twente, 2009, 2011, 2013) [6, 7, 8] concerning the pedunculopontine nucleus as an alternative target for deep brain stimulation and added to the opening towards more computational modelling of this nucleus [8, 13, 22].

Kamen's Rostock cooperation was also based on his earlier amygdala studies and has been directed to this nucleus and its surrounding area. Orexinergic and nitric-oxid synthase distribution, efferent projections of the medial amygdala, parabigeminal nucleus projections and amygdala-trigeminal projections, showed his immunological and connectivity interest of this nucleus of "fear and threat" [15, 17]. Next to these studies, the Rostock connection extended to pain research. Together with Propatiloff, Schmitt and Andreas Wree a monograph "Functional neuroanatomy of pain" appeared (2006) [18].

Those who think that Kamen's interests belonged exclusively to neuroscience have to be disappointed. As a real anatomist he worked together with several scientists in the department. For example, with Krassimira Michailova he studied serosal membranes. Michailova published a series of articles from 1988 on till 2006, on stomata, milky spots, transport through serosal membranes, its secretory functions and healing and regeneration of these serosal membranes under the guidance of the former head of the department Vasil Vassilev (1928-2020). The milky spots attracted Kamen's special

neuroanatomical attention because bundles of thin unmyelinated or myelinated fibers are occasionally present in the vincinity of the milky spot vessels [10]. If you have ever worked with serosal membranes one appreciates Michailova's electron microscopic pictures that are of a high quality. This cooperation produced a monograph [11] exclusively on serosal membranes of nearly all organs.

Jaap Schoen, a Dutch neurologist, who worked on the human brain at the Leiden Department of Neuroanatomy under WJC Verhaart and J Voogd, left, by his sudden death, an enormous amount of human series on brain damage, prepared with Nauta and Fink Heimer silver impregnations. Kamen, during his visits at the Leiden department, started organising the results that brought a monograph on the human trigeminal nucleus in the series of Advances in Anatomy, Embryology and Cell Biology. Subdivisions of the human descending trigeminus and the small trigeminal related nuclei all are given attention [16], resulting in citations in the large neuroanatomical handbooks. The human mesencephalic part of the trigeminal system was larger than anticipated in other publications. Its nearly hundred citations for a well-known human brain area, of which one should expect that everything is known, shows its importance. Incidentally trigeminal studies centered also in the rest of Bulgaria performed by Nikolai Lazarov [4, 5] and sometimes co-supported by Kamen Usunoff. The human trigeminal study posed two questions: are interneurons present in the trigeminal motor nucleus and is the cortical input mono-synaptically transferred to the trigeminal motor neurons? Its clinical consequences are clear.

In 1998 the first National congress of the Bulgarian Society for Neuroscience took place. Over 80 abstracts were present in the congress booklet. In it a series of foreign participations and of course a large in-put by Wladimir Ovtscharoff, Kamen Usunoff and Nikolai Lazarov, showing the strong activity and high quality of the Bulgarian neuroscientists, not least by Kamen's contributions.

Fig. 3. The Bulgarian neuroanatomist crew (Nikolai Lazarov, Enrico Marani, Wladimir Ovtscharoff and Kamen Usunoff) at the appointment of E.Marani's professorship in Neurophysiology (1998) at the Twente University. Kamen Usunoff at the Leiden groups outing. He was a very good story teller. The 5th December photos of Kamen with Saint Nicolas are renounced of!

In 1998 a cooperative project also started between Leiden Neuroanatomy, Sofia Anatomy and Twente's department of Biomedical Signals and Systems (**Fig. 3**). The project originated from the deep brain stimulation of the subthalamic nucleus in Parkinson's disease. The two monographs (Part I Marani et al., 2008 and Part II T. Heida et al, 2008, both together with Kamen Usunoff) [2, 9] on subthalamic's development,

topography, connections modelling and simulation of activity reached their targets: Springer sold over 5000 monographs in 2017. Since several species beside Man are used in studies on deep brain stimulation, the topography of rat, cat and baboon were included [19, 20, 21]. These distributions of the subthalamic nucleus originated from Kamen's thesis (**Fig. 4**). His critical reading of the neuroanatomical text increased its quality enormously and to our surprise Kamen was not unknown with subthalamic nucleus physiological activity. Note in **Fig. 4** Kamen's topographic naming, while normally one encircles areas in its abstracts of figures, Kamen had an inborn overview and memory of its sections, look for example at the thalamus.

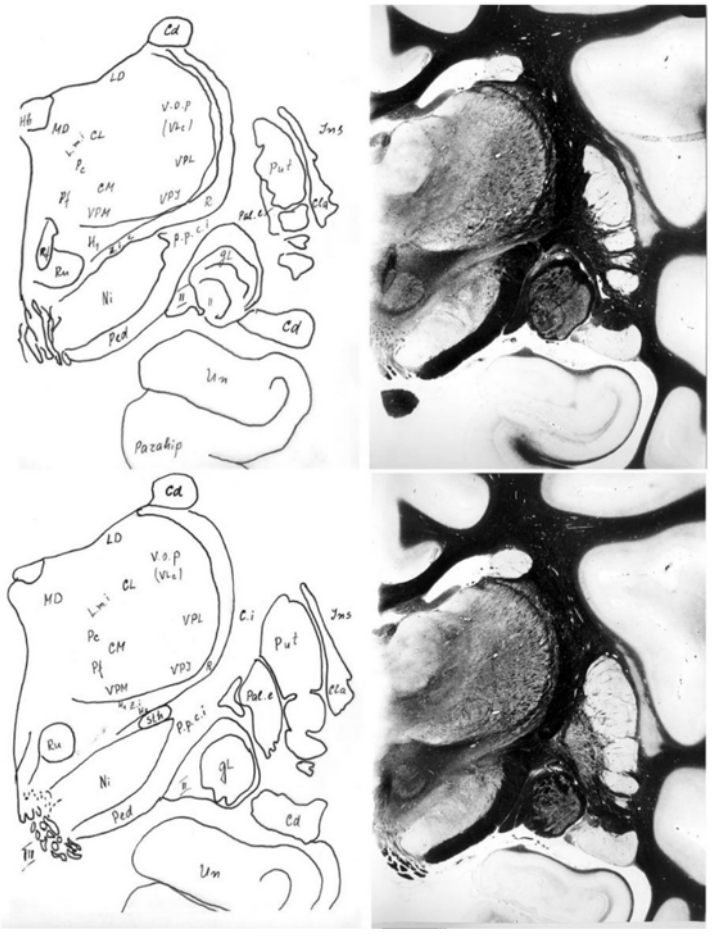

Fig. 4. Figures from Kamen's thesis and Fig. 11, in The Subthalamic nucleus part I: Transverse Woelcke and Nissl sections of the baboon's mesencephalon. Main abbreviations: cd , nucleus caudatus; ci , capsula interna; cla , claustrum; H , H1 , H2 , fields of Forel; Ni , Nic , Nir , substantia nigra, pars compacta, pars reticulata; pale , pali , globus pallidus externus and internus, respectively; ppci , pars peduncularis of the capsula interna; put , putamen; Ru , nucleus ruber; STH , nucleus subthalamicus; TcTT(R) , tractus corticotegmentothalamicus (Rinviki); VPM , VPI and VPL , nucleus ventralis posterior, intermediate and lateralis thalami; Zi , zona incerta; II , optic tract [12].

You cannot do research without assistance. At the lab the analytical women and men are of the utmost importance, as the digital supporters are (both often underestimated). Whether in Leiden, Twente or Sofia his friendly character with co-operaters made working for Kamen a nice job. He sometimes had to support sad members and he was always there for them. Could he be serious on the work quality, you bet.

Kamen Usunoff contributed fundamentally to our knowledge of the nervous system (six monographs have been published, besides over 115 publications, with nearly 1600 citations and 5000 reads). Not only by his results, but also by his scientific personality, which still is expressed in a series of students he educated and who are widespread over the world. To those who worked with Kamen, his friendly, but sometimes strict attitude, showed his involvement in you.

"*The past is gone, invisible, but in various aspects still with us", which also holds for Kamen Usunoff's scientific contributions.*

References

1. Chaldakov, G. In Memoriam Kamen G Usunoff (1941-2009) Great in triplicate – scientist, scholar, friend. – *Biomed. Rev.*, **21**, 2010**.**

2. Heida, T., E. Marani, K. G. Usunoff. The subthalamic nucleus. Part II, modelling and simulation of activity. – *Adv. Anat. Embryol. Cell Biol.,* **199**, 2008, 1-85.

3. Groenewegen, H. J., Y. C. Van Dongen. Role of the basal ganglia. In: *Parkinsonism and related disorders* (Eds. E. C. Wolters, T. Van Laar, H. W. Berendse), VU Univ. Press, Amsterdam, 2008.

4. Lazarov, N. Neurobiology of orofacial proprioception. – *Brain Res. Rev.*, **56**, 2007, 362-383.

5. Lazarov, N. The mesencephalic trigeminal nucleus in the cat. – *Adv. Anat. Embryol. Cell Biol.*, **153**, 2012, 1-102.

6. Lourens, M. Neural network dynamics in Parkinson's disease. *PhD Thesis*, University Twente, 2013.

7. Lourens, M. A. J., G. H. Meijer, T. Heida, S. A. Van Gils. The pedunculopontine nucleus as alternative target for deep brain stimulation. – In: *Proc 4th Ann Sympos IEE-EMBS Chap 9-10*, Twente Univ. Press, 2009.

8. Lourens, M. A. J., G. H. Meijer, T. Heida, E. Marani, S. A. Van Gils. The pedunculopontine nucleus as an additional target for deep brain stimulation. – *Neural Networks*, **24**, 2011, 617-630.

9. Marani, E., T. Heida, E. A. J. F. Lakke, K. G. Usunoff. The subthalamic nucleus Part I, development, topography and connections. – *Adv. Anat. Embryol. Cell Biol.*, **198**, 2008, 1-113.

10. Michailova, K. N., K. G. Usunoff. The "milky spots" of the peritoneum and pleura: normal, structure, development and pathology. – *Biomed. Rev.*, **15**, 2004, 47-66.

11. Michailova, K. N., K. G. Usunoff. Serosal membranes (pleura, pericardium, peritoneum): normal structure, development and experimental pathology. – *Adv. Anat. Embryol. Cell Biol.*, **183**, 2006, 1-144.

12. Usunoff, K. G. Cytoarchitectural, ultrastructural and histochemical characteristics of the substantia nigra. *Doctor of Medical Sciences Thesis*, Sofia, 1990.

13. Usunoff, K. G,. D. E. Itzev, S. R. Lolov, A. Wree. Pedunculopontine tegmental nucleus. Part I: cytoarchitecture, transmitters, development and connections. – *Biomed. Rev.*, **14**, 2003, 95-120.

14. Usunoff, K. G., D. E. Itzev, W. A. Ovtscharoff, E. Marani. Neuromelanin in the human brain: A review and atlas of pigmented cells in the substantia nigra. – *Arch. Physiol. Biochem.*, **110**, 2002, 257-369.

15. Usunoff, K. G., D. E. Itzev, A. Rolfs, O. Schmitt, A. Were. Brain stem afferent connections of the amygdala in the rat with special references to a projection from the parabigeminal nucleus: a fluorescent retrograde tracing study. – *Anat. Embryol.*, **211**, 2006, 475-496.

16. Usunoff, K. G., E. Marani, J. H. R. Schoen. The trigeminal system in man. – *Adv.Anat. Embryol. Cell Biol.*, **136**, 1997, 1-126.

17. Usunoff, K. G., O. Schmitt, D. E. Itzev, S. J-P. Haas, N. E. Lazarov, A. Rolfs, A. Wree. Efferent projections of the anterior and posterodorsal regions of the medial nucleus of the amygdala in the mouse. – *Cells Tissues Organs*, **190**, 2009, 256–285.

18. Usunoff, K. G., A. Propatiloff, O. Schmitt, A. Wree. Functional neuroanatomy of pain. – *Adv. Anat. Embryol. Cell Biol.*, **184**, 2006, 1-119.

19. Usunoff, K. G. Tegmentonigral projection in the cat. Electron microscopic observations. – In: *Parkinson-specific motor and mental disorders,* Advances in Neurology (Eds. R. G. Hassler, J. F. Christ), New York, Raven Press, 1984, 55-61.

20. Usunoff, K. G., R. Hassler, K. Romansky, P. Usunova, A. Wagner. The nigrostriatal projection in the cat. I. Silver impregnation study. – *J. Neurol. Sci.*, **28,** 1976, 265–288.

21. Usunoff, K. G., R. Hassler, K. V. Romansky, A. Wagner, J. F. Christ. Electron microscopy of the subthalamic nucleus in the baboon. II. Experimental demonstration of pallidosubthalamic synapses. – *J. Hirnforsch*, **23**, 1982a, 613–625.

22. Usunoff, K. G., D. P. Ivanov, Z. A. Blagov, K. V. Romansky, G. B. Malinov, D. V. Hinova-Palova, A. U. Paloff. Axonal degeneration following destruction of the mesencephalic reticular formation. III. Pathways arising in nucleus tegmenti pedunculopontinus and terminating in the monoaminergic neuronal groups of the midbrain, and in the basal ganglia. – *Med. Biol. Probl. (Sofia)*, **10**, 1982b, 27-42.

Institute of Experimental Morphology, Pathology and Anthropology with Museum
Bulgarian Anatomical Society

Acta Morphologica et Anthropologica, 31 (3-4)
Sofia ● 2024

IN MEMORIAM

Professor Michail Slavchev Davidoff (18.07.1940 – 19.06.2024)
Corresponding member of the Bulgarian Academy of Sciences
Academician of the German National Academy of Sciences Leopoldina

On 19th of June 2024 Professor Michail Davidoff passed away in Hamburg.
Michail Davidoff was born into a German-Bulgarian family on July 18th, 1940 in Sofia. His father was Slavtscho M. Davidoff, Professor of Dental, Oral and Maxillofacial Surgery, and his mother Irmgard was German. The Bulgarian revolutionary hero Vasil Levski was born on the same date July 18th in 1837 and Prof. George Chaldakov exclaimed "A coincidence and/or a touch by God's finger".

In 1966 Michail Davidoff graduated in medicine as a distinguished student at Higher Medical Institute in Sofia (now Medical University-Sofia). Soon after he stated his research and academic career. Thanks to his nice personality devoted to do science and teaching, he quickly found a mentor in Prof. Dr. Georgi P. Galabov, the head of the Department of Anatomy in Sofia, who supported him and let him qualify. As a

student he had already been allowed to work in research laboratories. After completing his medical studies he obtained the position of a research assistant at the Central Laboratory of Regeneration (CLR) at the Bulgarian Academy of Sciences. At the same time he became an assistant lecturer at the Department of Anatomy, Histology and Embryology at the Medical University of Sofia.

In 1969, Michail Davidoff started his advanced training with Prof. Theodor-Heinrich Schiebler, Director of the Institute of Anatomy at the University of Würzburg, Germany. This stay was a great pleasure for him since he was familiar with the German language and culture through his parents. Hence, Michail Davidoff had no difficulty to settle in Germany and to deliver his anatomy teaching in German.

In 1970 Michail Davidoff defended PhD thesis „Electron microscopical characteristics and histochemistry of the developing and differentiated guinea pig placenta". In 1974 he was promoted in Assoc. Professor in Anatomy, Histology and Embryology in the CLR and in 1977 he defended dissertation for Doctor of Medical Sciences on "Lysosomes of the Central Nervous System". Michail Davidoff was invited many times as Visiting Professor in the Institute of Anatomy, at Würzburg University (1975-1983). His first time in Würzburg was such a stunning success and it prompted Michail Davidoff to be invited 5 times for a total of 5 years to Würzburg as a guest scientist, lecturer and professor. In 1982 he was promoted in Professor in Anatomy, Histology and Embryology in the CLR and later he was Visiting Professor at the Institute of Anatomy at University of Hamburg, Germany (1985-1989). Michail Davidoff was very happy to work and settle in Hamburg as his mother was born in Hamburg. In 1985 he was elected as a member (Academician) of the German National Academy of Sciences Leopoldina and three years later in 1989 he was elected as a Corresponding member of the Bulgarian Academy of Science.

Michail Davidoff worked as a Professor and he was Deputy Director of the Institute of Cell Biology and Morphology (now Experimental Morphology, Pathology and Anthropology with Museum) at the Bulgarian Academy of Sciences (1989-1991). Later he moved to Germany as Visiting Professor in the Institute of Anatomy at University of Hamburg (1990-1993). After several terms as a guest scientist Michail Davidoff had the opportunity to take up a permanent position in Hamburg. In 1993, he was appointed C3 professor for anatomy and Deputy Chair of the Department of Microscopic Anatomy at the Institute of Anatomy, University of Hamburg. Prof. Michail Davidoff taught many students in Hamburg in lectures and courses on macroscopic anatomy, cytology, histology, microscopic anatomy, embryology and neuroanatomy. All his colleagues and students were impressed by his knowledge and diligence in presenting. He trained young scientists and doctoral students and they achieve scientific success under his supervision. Prof. Davidoff was Acting Director of the Department of Microscopic Anatomy of the Institute of Anatomy, University of Hamburg (2001-2005).

Prof. Michail Davidoff retired in 2005, but continued to work on stem cell topics, out of office, at the Medical History Museum Hamburg at the University Hospital Hamburg-Eppendorf. But even after his retirement, he was actively involved at the University of Hamburg, including the Board of the Friends and Sponsors of the UKE-Hamburg. He was able to complete the monograph "The Neuroendocrine Leydig Cells and their Stem Cell Progenitors, the Pericytes" with co-authors Dieter Müller, Ralf Middendorff and Adolf-Friedrich Holstein. Prof. Michail Davidoff published more

than 200 publications in prestigious international journals that were cited more than 3500 times.

Two years after his graduation in medicine Michail Davidoff became a member of the Bulgarian Society of Anatomy, Histology and Embryology (now Bulgarian Anatomical Society) in 1968. Since 1969 he was a member of the Society for Histochemistry, Germany. For a long time he was a member of the Board of the Bulgarian Anatomical Society (1971–1989) - Treasurer and Secretary and he was also President of the Histochemical Section of the Bulgarian Society of Anatomy, Histology and Embryology (1982-1989). Prof. Michail Davidoff was Member of the board (1998 – 2002) and President (2001) of the Anatomische Gesellschaft. He was also a member of Editorial Boards of scientific journals – "Anatomisher Anzeiger", "Histochemistry", "Zeitschrift für mikroskopisch – anatomische Forschung", "Biomedical Reviews", "Acta Morphologica et Anthropologica"

The major scientific contributions by Prof. Michail Davidoff can be summarised in the following topics:

- **Morphology of the central and peripheral nervous system** that involved characterisation of the vegetative centres of the hypothalamus and spinal cord, vegetative network of the thoracic spinal cord of the Guinea pig and the rat. Prof. Michail Davidoff found out coexistence of neuroactive substances in different structures of the central nervous system as well as regeneration capacity of the damaged spinal cord.

- **Structure and function of parenchymal organs.** Prof. Michail Davidoff established regional differences and functional characteristics of the placental syncytiotrophoblast, the kidney, the liver, the adrenal gland and other organs.

- **Morphology, function and origin of neuroendocrine cell system.** Prof. Davidoff discovered neuroendocrine nature of the testicular Leydig cells. Similarities between the Leydig cells and neural crest cells were found out.

- **Adult Leydig cells.** For the first time Prof. Michail Davidoff reported that Leydig cells of the testis originate by trans-differentiation from pericytes of the micro vessel wall. Pericytes of the testis are progenitors of adult Leydig cells. He considered pericytes as ubiquitous adult stem cells.

Pericyte hypothesis was his great inspiration until end of his life. Prof. Michail Davidoff received highest recognition by Anatomical Institute in Hamburg for expanding and strengthening of research on reproductive medicine. Leaving and working in Germany he maintained his close relationship and collaboration with Bulgarian colleagues. In his fine responsible manner Prof. Davidoff always supported and encouraged them to pursue their own research promoting scientific achievements of the Bulgarian cellular anatomy and morphology. He was always concerned to share his latest findings with his colleagues in Bulgaria and to let them partake in his successes. Prof. Michail Davidoff was highly respected and recognised as a one of the greatest anatomist and morphologist in Bulgarian scientific societies. Being elected as a member of the German National Academy of Sciences Leopoldina, he represented Bulgaria and ultimately followed the steps of his famous predecessor Prof. Dr. Dimitri Kadanoff. Over decades, Prof. Michail Davidoff's talks at national Bulgarian scientific meetings were highly appreciated.

Prof. Michail Davidoff was one of the greatest scientists, with bright mind and personality, beloved teacher, colleague and true friend. He was a universe in science, and a universe in personality with enormous, humanity, generosity and high moral. With his refine manner in communicating, working and leading people Prof. Michail Davidoff will remain unreplaceable and remembered forever.

Nina Atanassova and Adolf-Friedrich Holstein

Prof. Michail Davidoff at National Congress
of the Bulgarian Anatomical Society in 2007 in Stara Zagora.

Fig. 1. Prof. Michail Davidoff (in the centre) with Prof. Wladimir Ovtscharoff (on the left) and Prof. Enrico Marani (on the right).

Fig. 2. Prof. Michail Davidoff with Prof. Vasil Vassilev (on the left) and Prof. Yordan Yordanov (on the right).

Fig. 3. Prof. Michail Davidoff presenting a lecture on his pericyte hypothesis of Leydig cell origin.

Institute of Experimental Morphology, Pathology and Anthropology with Museum
Bulgarian Anatomical Society

Acta Morphologica et Anthropologica, 31 (3-4)
Sofia ● 2024

IN MEMORIAM

Assoc. Prof. Elissaveta Borisova Zvetkova, MD, PhD
(05.07.1940 – 19.05.2024)

Elissaveta Zvetkova passed away on May 19th, 2024.
Elissaveta Zvetkova was born on July 5th 1940 in Veliko Tarnovo in a family of a military doctor and a pharmacist. She graduated Higher Medical Institute in Sofia in 1964. Dr. Zvetkova worked as a paediatrician in the District hospital in town Svishtov. In 1966 she became a PhD student at the Institute of Morphology, Bulgarian Academy of Sciences where she defended her doctoral thesis under the supervision of Acad. Assen I. Hadjioloff. With her supervisor Dr. Zvetkova published a monograph on the fluorescent properties of cells and tissues in vertabrates and human. With her colleagues she developed and published an original method for visualization of cytoplasmic RNP proteins in hemopoietic colonies in agar cultures. The method was later modified for simultaneous and differential staining of nucleoproteids and some cathionic proteins for quantitative analysis of blood and exfoliated cells.

Elissaveta Zvetkova has specialized in France, Russia and Germany. She was an expert in histology, embryology, fluorescent histochemistry, bone marrow hematopoiesis, etc. Dr. Zvetkova was promoted to Associated Professor in 1982.

Assoc. Prof. Zvetkova was Head of Department of Cell Differentiation in the Institute of Experimental Morphology and Anthropology (1995-2005). From 1976 to 1995 she was a part-time assistant at the Medical University-Sofia and Faculty of

Biology in Sofia University “St. Kliment Ohridski” where Dr. Zvetkova had seminars in histology and embryology.

Assoc. Prof. Zvetkova’s major scientific contributions are in the field of general and local regulatory mechanisms of bone marrow hematopoiesis in normal and pathological conditions. She studied the *in vitro* effect of neopterin and other pteridines on the proliferation, differentiation and colony formation of bone marrow hematopoietic granulocyte-macrophage progenitors. Of great interest to her was also the *in vitro* influence of growth factors on the hemorheological properties and cell-to-cell interactions of hematopoietic and endothelial cells. The obtained results were published in more than 120 scientific papers.

She supervised students in their master degree thesis as well as PhD students. Even after her retirement in 2006, Dr. Zvetkova continued to work and support young scientists in their scientific career and was an active and valuable member of Scientific juries. Dr. Zvetkova was a coordinator and/or participant in national and international research projects.

Due to her outstanding writing talent Elissaveta Zvetkova was a member of the Editorial board of several prestigious scientific journals. She was also a member of the Union of Scientists in Bulgaria, Bulgarian Anatomical Society, Bulgarian Society of Biorheology and the International society of Pteridines.

For her scientific achievements Assoc. Prof. Elissaveta Zvetkova obtained many national and international awards.

In her spare time she enjoyed playing music, drawing and writing poetry. Elissaveta Zvetkova loved to travel and to get acquainted with other cultures.

Assoc. Prof. Elissaveta Zvetkova dedicated her life to science and research and to her last breath she worked on review papers in the fields of cell biology, hematology and hemorheology. She will leave an everlasting trace in our hearts with her exquisite style, encyclopedic knowledge and generosity.

Yordanka Gluhcheva

Fig. 1. Assoc. Prof. Elissaveta Zvetkova with her INSO award in 2022.

Author Guidelines

Acta Morphologica et Anthropologica is an open access peer review journal published by Bulgarian Academy of Sciences, Prof. Marin Drinov Publishing House.
Corporate contributors are Bulgarian Academy of Sciences, Institute of Experimental Morphology, Pathology and Anthropology with Museum and Bulgarian Anatomical Society.

Acta Morphologica et Anthropologica is published in English, 4 issues per year.

The journal accepts manuscripts in the following **fields**: experimental morphology, cell biology and pathology, anatomy and anthropology.

Publication types: original articles, short communications, case reports, reviews, Editorial, letters to the Editors.

Acta Morphologica et Anthropologica is the continuation of Acta cytobiologica et morphologica

The **aim** of the Journal is to disseminate current interdisciplinary biomedical research and to provide a forum for sharing new scientific knowledge and methodology. The general editorial policy is to optimize the process of issuing and distribution of *Acta Morphologica et Anthropologica* in line with modern standards for scientific periodicals focusing on content, form, and function.

Scope – experimental morphology, cell biology and pathology (neurobiology, immunobiology, tumor biology, environmental biology, reproductive biology, etc.), new methods, anatomy and pathological anatomy, anthropology and paleoanthropology, medical anthropology and physical development.

Acta Morphologica et Anthropologica is published twice a year as one volume with 4 issues. For the first two issues (1-2) the deadline for manuscript submission is March 15th and for the next two issues (3-4), the deadline is September 15th. Electronic version for issues 1-2 is uploaded on the website till June 30th and for issues 3-4 – till December 30th.

Contact details and submission

Manuscript submission is electronical only. The manuscripts should be sent to the Managing Editor's e-mail address ygluhcheva@hotmail.com with copy to iempam@bas.bg and ama.journal@iempam.bas.bg

All correspondence, including notification for Editor's decision, requests for revision, is sent by e-mail.

Article structure

Manuscripts should be in English with total length not exceeding 10 standard pages, line-spacing 1.5, justified with 2.5 cm margins. The authors are advised to use Microsoft Word 97-2003, Times New Roman, 12 pt throughout the text. Pages should be numbered at the bottom right corner of the page.

The article should be arranged under the following headings: Introduction, Material and Methods, Results, Discussion, Conclusion, Acknowledgements and References.

Title page – includes:

- **Title** – concise and informative;
- **Author(s)' names and affiliations** – indicate the given name(s) and family name(s) of all authors. Present the authors' affiliation addresses below the names. Indicate all affiliations with a lower-case superscript after the author's name and in front of the appropriate address. Provide the full postal address information for each affiliation, including the country name.
- **Corresponding author** – clearly indicate who will handle the correspondence for refereeing, publication and post-publication. An e-mail should be provided.
- **Abstract** – state briefly the aim of the work, the principal results and major conclusions and should not exceed 150 words. References and uncommon, or non-standard abbreviations should be avoided.
- **Key words** – provide up to 5 key words. Avoid general, plural and multiple concepts. The key words will be used for indexing purposes.

Introduction – state the objectives of the work and provide an adequate background, avoiding a detailed literature survey or summary of the results.

Material and Methods – provide sufficient detail to allow the work to be reproduced. Methods already published should be indicated as a reference: only relevant modifications should be described.

Results – results should be clear and concise.

Discussion – should explore the significance of the results in the work, not repeat them. A combined *Results and Discussion* section is often appropriate. Avoid extensive citation and discussion of published literature.

Conclusions – the main conclusions of the study should be presented in a short section.

Acknowledgements – list here those individuals who provided help during the research and the funding sources.

Units – please use the International System of Units (SI).

Math formulae – please submit math equations as editable text, not as images.

Electronic artwork – number the tables and illustrations according to their sequence in the text. Provide captions for them on a separate page at the end of the manuscript. The proper place of each figure in the text should be indicated in the left margin of the corresponding page. **All illustrations (photos, graphs and diagrams)** should be referred to as "figures" and given in abbreviation "Fig.", and numbered in Arabic numerals in order of its mentioning in the manuscript. They should be provided in grayscale as JPEG or TIFF format, minimum 300 dpi. The illustrations should be submitted as separate files.

References – they should be listed in alphabetical order, indicated in the text by giving the corresponding numbers in parentheses. The "References" should be typed on a separate sheet. The names of authors should be arranged alphabetically according to family names. In the reference list titles of works, published in languages other than English, should be translated,

original language must be indicated at the end of reference (e.g., [in Bulgarian]). Articles should include the name(s) of author(s), followed by the full title of the article or book cited, the standard abbreviation of the journal (according to British Union Catalogue), the volume number, the year of publication and the pages cited, for books – the city of publication and publisher. In case of more than one author, the initials of the second, third, etc. authors precede their family names. Ideally, the names of all authors should be provided, but the usage of "et al" after the fifth author in long author lists will also be accepted.

For articles: **Davidoff, M. S., R. Middendorff, G. Enikolopov, D. Riethmacher, A. F. Holstein, D. Muller**. Progenitor cells of the testosterone-producing Leydig cells revealed. – *J. Cell Biol.,* **167**, 2004, 935-944.

Book article or chapter: **Rodriguez, C. M., J. L. Kirby, B. T. Hinton. The development of the epididymis.** - In: *The Epididymis - from molecules to clinical practice* (Eds. B. Robaire, B. T. Hinton), New York, Kluwer Academic Plenum Publisher, 2002, 251-269.

Electronic books: **Gray, H.** *Anatomy of the human body* (Ed. W.H.Lewis), 20th edition, NY, 2000. Available at http://www.Bartleby.com.

PhD thesis: **Padberg, G**. Facioscapulohumeral diseases. *PhD thesis*, Leiden University, 1982, 130 p.

Website: National survey schoolchildren report. National Centre of Public Health and Analyses, 2014. Available at http://ncphp.government.bg/files

Page charges
Manuscript publication is free of charges.

Ethics in publishing
Before sending the manuscript the authors must make sure that it meets the Ethical guidelines for journal publication of Acta Morphologica et Anthropologica.

Human and animal rights

If the work involves the use of human subjects, the authors should ensure that work has been carried out in accordance with *The Code of Ethics of the World Medical Association* (Declaration of Helsinski). The authors should include a statement in the manuscript that informed consent was obtained for experimentation with human subjects. The privacy rights of human subjects must always be observed.
All animal experiments should comply with the *ARRIVE guidelines* and should be carried out in accordance with the U.K. Animals (Scientific procedures) Act, 1986 and the associated guidelines *EU Directive 2010/63/EU* for animal experiments, or the National Institutes of Health guide for the care and use of Laboratory animals (NIH Publications No. 8023, revised 1978) and the authors should clearly indicate in the manuscript that such guidelines have been followed.

Submission Details

Acta morphologica et anthropologica is published twice a year as one volume with 4 issues. For the first two issues (1-2) the deadline for manuscript submission is March 15th and for the next two issues (3-4), the deadline is September 15th. Electronic version for issues 1-2 is uploaded on the website till June 30th and for issues 3-4 – till December 30th.

Manuscript submission is electronical only.

The manuscripts should be sent to the Managing Editor email address ygluhcheva@hotmail.com with copy to iempam@bas.bg

All correspondence, including notification for Editor's decision, requests for revision, is sent by e-mail.

Submission declaration

Submission of the manuscript implies that the work described has not been published previously, is not considered under publication elsewhere, that its publication is approved by all authors, and that if accepted, it will not be published elsewhere in the same form, in English or in any other language, including electronically, without the informed consent of the copyright-holder.

Contributors

The statement that all authors approve the final article should be included in the disclosure.

Copyright

http://www.iempam.bas.bg/journals/acta/Author%20Copyright%20Agreement_last.pdf

Upon acceptance of an article, the authors will be asked to complete a "**Copyright Transfer Agreement**".
http://www.iempam.bas.bg/journals/acta/Copyright_Transfer_Agreement_Form_AMA.doc

Peer review

Once a manuscript is submitted, the Managing Editor (or the Editor-in-Chief) briefly checks the manuscript for conformance with the journal's Focus, Scope, Policies and style requirements and decide whether it is potentially suitable for publication and can be processed for review, or rejected immediately, or returned to the author for improvement and re-submission.
Manuscripts are peer-reviewed by the Editors, Editorial Board members, and/or external experts before final decisions regarding publication are made. The entire editorial workflow is performed in the following steps:

1. The submitted manuscript is checked in the editorial office whether it is suitable to go through the normal peer review process.
2. If deemed suitable, the manuscript is sent to 2 reviewers for peer-review. The choice of reviewers depends on the subject of the manuscript, the areas of expertise of the reviewers, and their availability.
3. Each reviewer will have 2 weeks to provide evaluation of the manuscript. The Editor may recommend publication, request minor, moderate or major revision, or provide a written critique of why the manuscript should not be published (rejected).
4. In case only one reviewer suggests rejection of the manuscript, the latter is subjected to additional evaluation by a third reviewer.
5. The manuscript will be published in a revised form provided that the authors successfully answer the critics received. The Editor-in-Chief is the final authority on all editorial decisions.

Open Access

This journal provides immediate open access to its content on the principle that making research freely available to the public supports a greater global exchange of knowledge.

After acceptance

Proof correction

The corresponding author will receive proofs by e-mail in PDF format and will be requested to return it with any corrections within two weeks.

ISSN 1311-8773 (print)
ISSN 2535-0811 (online)